INORGANIC CHEMISTRY FRONTIERS

REVIEW

View Article Online
View Journal | View Issue

Cite this: *Inorg. Chem. Front.*, 2020, **7**, 3837

Noble-metal-free nanocatalysts for hydrogen generation from boron- and nitrogen-based hydrides

Qilu Yao, Yiyue Ding and Zhang-Hui Lu *

Received 28th June 2020,
Accepted 13th August 2020

DOI: 10.1039/d0qi00766h

rsc.li/frontiers-inorganic

Hydrogen has attracted much attention as a globally accepted clean energy carrier. Currently, the search for safe and efficient hydrogen storage materials is one of the most difficult challenges for the upcoming hydrogen economy. Boron- and nitrogen-based hydrides, such as metal borohydrides (*e.g.* $NaBH_4$), ammonia borane (NH_3BH_3), ammonia (NH_3), hydrous hydrazine ($N_2H_4{\cdot}H_2O$), and hydrazine borane ($N_2H_4BH_3$), have received much attention as potential chemical hydrogen storage materials because of their high hydrogen contents and the advantage of CO-free H_2 produced. In recent years, substantial efforts have been devoted to research highly efficient catalysts to significantly improve the kinetic properties for hydrogen evolution from the hydrolysis of sodium borohydride and ammonia borane, and selective decomposition of ammonia, hydrous hydrazine and hydrazine borane. Among them, non-noble metal catalysts have been widely considered as potential candidates due to their low cost, abundant reserves, and relatively high catalytic activities. In this review, we focus on the recent advances in non-noble metal catalyst design, synthesis and applications in hydrogen generation from boron- and nitrogen-based hydrides.

1. Introduction

The advancement of industrialization and economic growth means that human society is more heavily dependent on energy than ever before. The currently used fossil fuels (coal, crude oil, natural gas, *etc.*) are considered to be non-renewable energy and have limited reserves. In addition, the extraction, transport, and consumption of fossil fuels can also cause environmental pollution problems. Thus, it is urgent to find a clean and renewable alternative to fossil fuels. Hydrogen has been identified as a potential alternative energy carrier for future energy supplies because it is clean, renewable, and environment friendly, and has high energy density.[1–4] The use of hydrogen fuel cells in portable electronic devices or vehicles requires lightweight hydrogen storage or on-board hydrogen evolution. In particular, for vehicular applications, the most important requirements are safety, ease of control and fast reaction kinetics as well as high hydrogen content. To this

Institute of Advanced Materials (IAM), College of Chemistry and Chemical Engineering, Jiangxi Normal University, Nanchang, 330022, P.R. China.
E-mail: luzh@jxnu.edu.cn

Qilu Yao

Qilu Yao received her PhD (2017) degree in chemistry from Jiangxi Normal University under the supervision of Prof. Zhang-Hui Lu. Since 2017, she has been working as a research associate at the Institute of Advanced Materials, Jiangxi Normal University. Her research is centered on the design and preparation of nanostructured materials and their applications in energy-/environment-related catalysis.

Yiyue Ding

Yiyue Ding was born in Hunan, P. R. China in 1999. She received her bachelor's degree in Chemistry from Changchun Normal University (2019), China. She is currently studying for her master's degree at Jiangxi Normal University under the supervision of Prof. Zhang-Hui Lu. Her research is mainly focused on the design and synthesis of nanocatalysts for hydrogen production from chemical hydrogen storage materials.

end, the search for secure and efficient hydrogen storage materials has become extremely important.

In the last decades, several materials for hydrogen storage such as metal hydrides,[5] carbonaceous materials,[6] zeolites,[7] metal organic frameworks,[8] and organic hydrides,[9,10] have been extensively investigated, while big challenges still remain. Chemical hydrogen storage materials have high hydrogen contents and store hydrogen in the form of chemical bonds, and they are considered as highly promising hydrogen sources for fuel cells.[11–14] Among them, boron- and nitrogen-based hydrides, such as metal borohydrides (*e.g.* $NaBH_4$, 10.8 wt%), ammonia borane (NH_3BH_3, 19.6 wt%), ammonia (NH_3, 17.7 wt%), hydrous hydrazine ($N_2H_4{\cdot}H_2O$, 8.0 wt%), and hydrazine borane ($N_2H_4BH_3$, 15.4 wt%), have received much attention in recent years.[15–21] These materials are not only high in hydrogen content, but are also easy to store and transport under mild conditions, making them highly potential hydrogen storage materials.

In order to achieve effective hydrogen evolution from boron- and nitrogen-based hydrides under ambient conditions, it is highly desired to develop economical, highly efficient and stable catalysts. To date, a lot of noble/non-noble metals and their composites have been developed as catalysts for hydrogen evolution from boron- and nitrogen-based hydrides.[21–26] Among them, noble metal-based catalysts exhibit excellent catalytic activity, but they are unsuitable for large scale practical applications due to their high cost and insufficient reserves in the Earth's crust.[27–30] Therefore, the development of cost-effective catalysts is of great importance for practical applications. Non-noble metal (*e.g.* Fe, Co, Ni, *etc.*) catalysts have been considered as potential candidates due to their low cost, abundant reserves, and relatively high catalytic performances.[24,31,32] In this review, we summarize the recent developments in non-noble catalysts for hydrogen generation from these boron- and nitrogen-based chemical hydrogen storage materials.

Zhang-Hui Lu

Zhang-Hui Lu is currently a professor at Jiangxi Normal University. He received his PhD degree in Chemical Science and Engineering in 2011 from Kobe University (Japan) under the supervision of Prof. Qiang Xu. He is the winner of the First Prize in the Natural Science Award of Jiangxi Province in 2019 and has published more than 100 papers with citations >4000. His current research interest is mainly focused on synthesizing micro/nanostructured materials and exploring their applications in the area of heterogeneous catalysis and electro-catalysis for clean energy and environmental clean-up.

2. Metal borohydrides

Metal borohydrides, such as $LiBH_4$, $NaBH_4$, KBH_4 and $Mg(BH_4)_2$, have received considerable interest as promising hydrogen storage materials due to their high gravimetric hydrogen capacities.[33–43] Compared to $LiBH_4$, KBH_4 and $Mg(BH_4)_2$, $NaBH_4$ is more widely studied because it provides a safe and low-cost route to produce hydrogen.[16,21,33] Thus, $NaBH_4$ is taken as a representative for discussion.

Hydrogen stored in $NaBH_4$ can be released by either thermolysis or hydrolysis.[33,44–48] However, the thermolysis of $NaBH_4$ is not conceivable because it requires high temperature (>500 °C), and it inevitably produces toxic species. Alternatively, hydrolysis can be used to release H_2 from $NaBH_4$ easily and in a controllable way under friendly conditions.[33,47,48] As shown in eqn (1), half of the hydrogen produced originates from water, which is also an advantage of this reaction. In addition, the byproduct of this hydrolysis reaction ($NaBO_2$) is nontoxic and can be recycled for regeneration, which facilitates its use in fuel cells. In general, $NaBH_4$ is not stable in aqueous solution and can spontaneously release H_2 without catalysts. However, the self-hydrolysis is too slow and uncontrollable, and only 7–8% of $NaBH_4$ can be converted. In order to suppress the self-hydrolysis, NaOH is often added into the $NaBH_4$ solution as a stabilizer. The alkaline $NaBH_4$ solution can only be hydrolyzed by using suitable catalysts.

$$NaBH_4 + 2H_2O \rightarrow NaBO_2 + 4H_2 \quad (1)$$

Unlike the simple hydrolysis reaction formula shown in eqn (1), the detailed mechanism of the hydrolysis of $NaBH_4$ over transition metal catalysts is complicated and not fully understood.[49–53] As early as in 1971, Holbrook and Twist proposed a plausible mechanism for metal (M) catalyzed hydrolysis of $NaBH_4$.[49] Firstly, BH_4^- ions are chemisorbed on a metal active site surface, forming M–BH_3^- and M–H intermediate species. Subsequently, M–BH_3^- reacts with OH^- and H_2O, possibly *via* a BH_3 intermediate, to form $BH_3(OH)^-$ and M–H intermediate species. Then, the intermediate $BH_3(OH)^-$ finally converts into $B(OH)_4^-$ by the replacement of B–H bonds with B–OH^- bonds. Meanwhile, the intermediate M–H reacts with another M–H to generate H_2 and to regenerate the metal active sites. Peña-Alonso *et al.* suggested that the intermediate M–H directly reacts with H_2O to generate H_2.[50] Guella *et al.* proposed a mechanism based on ^{11}B NMR measurements, and suggested that the rate-controlling step of the metal catalyzed hydrolysis of $NaBH_4$ is the cleavage of the O–H bond in water.[51,52] It is worth noting that the catalytic hydrolysis of $NaBH_4$ is closely related to the metal active sites, as there is a charge transfer between the metal active sites and $NaBH_4$ or intermediates. Therefore, the development of efficient metal catalysts is very important.

Schlesinger and coworker first found that adding an acid into aqueous $NaBH_4$ solution can significantly accelerate the hydrolysis reaction.[54] Since then, a number of catalysts have been investigated to accelerate the $NaBH_4$ hydrolysis. Noble-

Table 1 Catalytic activities for hydrogen evolution from the hydrolysis of $NaBH_4$ by different catalysts

Catalyst	Synthetic method	Temp. (K)	Activity (mL min^{-1} g^{-1})	E_a (kJ mol^{-1})	Ref.
Intrazeolite Co nanoclusters	Ion-exchange and chemical reduction	298	—	34	62
Co/CCs	Hydrothermal and impregnation–reduction	293	10 400	24.04	66
Co/ACs	Hydrothermal and impregnation–reduction	298	11 220	38.4	67
Co@C-700	Pyrolysis	303	—	56.9	68
Co@NMGC	Pyrolysis	298	3575	35.2	69
Co/IR-120	Wet-chemical reduction	308	200	66.67	70
Co/Fe_3O_4@C	Impregnation–reduction	298	1403	49.2	71
Fe_3O_4@C–Co	Solvothermal and impregnation–reduction	298	1746	47.3	72
Co/SiO_2	Impregnation–reduction	313	8701	59	32
Cryogel p(AAm)–Co	*In situ* chemical reduction	303	1130.2	39.7	73
Cryogel p(AAm)–Ni	*In situ* chemical reduction	303	579.4	—	73
Ni/graphitic layer	Chemical vapor deposition	298	600	—	74
CoB	Chemical reduction and post-annealing	288	2970	—	77
Co–B thin films	Pulsed laser deposition	298	3300	—	78
Co–B hollow spheres	Chemical reduction and post-annealing	298	2720	45.5	79
CoB/SiO_2	Impregnation–reduction	298	10 586	—	80
Mesoporous Co–B	Chemical reduction	303	3350	40	81
Co–Cr–B	Chemical reduction	298	3400	37	85
Co–Mo–B	Chemical reduction	298	2875	39	86
Co–Mo–B/carbon cloth	Two-step electrodeposition	303	1280.9	51	91
Co–Mn–B	Chemical reduction and post-annealing	293	1440	52.1	92
Co–Ti–B	Chemical reduction	323	7760	49.88	93
Co–Ce–B	Chemical reduction and carbonization	303	4760	33.1	94
Co–Zn–B	*In situ* chemical reduction	303	2180	35.92	95
Co–B/carbon	Impregnation–reduction	298	1127.2	57.8	96
CoB/o-CNTs	Impregnation–reduction	298	3041	37.63	98
CoB/TiO_2	Impregnation–reduction	293	6738	51	99
Co–B/nickel foam	Electroless plating	298	111	33	103
Ni–B–silica nanocomposite	*In situ* chemical reduction	298	1916	60.7	104
Ni–B/Ni foam	Dipping–chemical reduction	303	—	61.841	105
Multi-shaped Ni–B	Complexing–reduction	303	—	64.9	106
$NiB/NiFe_2O_4$	Impregnation–reduction	298	299.88	72.52	107
Fe–B/C cloth	Adsorption–chemical reduction	298	813	—	108
Fe–B/Ni foam	Chemical reduction	323	5487	64.26	109
Cu–B	Complexing–reduction preparation	303	6500	23.79	110
Co–P/Cu substrate	Electroplating	303	954	—	111
Co–P	Electroless deposition	303	3300	60.2	112
Co–P/Cu sheet	Electroless deposition	303	1846	48.1	113
Co–P/Cu sheet	Electroless plating	323	2275.1	27.9	114
CoP/Ti mesh	Phosphidation	298	6100	42.01	115
CoP nanowire array/Ti	Phosphidation	293	6500	41	116
Co–W–P/Cu sheet	Electroless deposition	303	5000	22.8	117
Co–W–P/γ-Al_2O_3	Electroless deposition	318	11 820	49.58	118
Co–W–P/carbon cloth	Electroless deposition	303	4379	27.18	119
Co–Ni–P/Cu substrates	Electroless deposition	303	2479	—	120
Co–Ni–P/Cu sheet	Electroless plating	303	2172.4	53.5	121
Cu–Co–P/γ-Al_2O_3	Electroless deposition	298	1115	47.8	122
Fe–CoP/Ti	Phosphidation	298	6060	39.6	123

metal-based catalysts such as Ru, Rh, Pt, Pd and relevant alloys display excellent catalytic performances, but the high cost and scarcity of noble metals limit their industrial applications.[51,55–58] Low-cost and Earth-abundant transition metal (Co, Ni, and Fe), metal boride and metal phosphide catalysts are viable alternatives.[31,32] Among them, Co-based catalysts have been proven to be highly effective at catalyzing $NaBH_4$ hydrolysis (Table 1).[31,59–61]

2.1. Metal catalysts

Cobalt catalysts have been reported to be effective in catalytic hydrolysis of $NaBH_4$.[31,59] These are usually deposited on a support material in the form of Co^{2+} ions and then reduced to metal Co. Microporous and mesoporous materials are considered as suitable support materials because it can effectively limit the growth or sintering of metal nanoparticles (NPs). Özkar and coworkers reported the synthesis of intrazeolite Co nanoclusters by using ion-exchange of Co^{2+} ions with the extra-framework Na^+ ions in zeolite-Y followed by reduction with $NaBH_4$.[62] The obtained intrazeolite Co nanoclusters provided 36 000 turnovers in the hydrolysis of $NaBH_4$ and retained 59% of their initial catalytic activity after the fifth run. Later on, Kwon and coworkers developed a hydroxyapatite-supported Co (Co/HAP) pre-catalyst, which showed long-term stability, retaining 75% of its initial catalytic activity over 20 days of use.[63] Auroux and coworkers chose various materials with different acid/base surface properties as supports (hydrotalcites, KF/Al_2O_3, and heteropolyanions) to immobilize Co NPs.[64] Among them, a heteropolyanion supported Co pre-catalyst showed the highest hydrogen generation rate in $NaBH_4$ hydrolysis.

Various carbon supported Co catalysts have been reported, which have the advantages of relatively low cost and excellent catalytic hydrogen production performance.[65–69] Gou and co-worker found that Co supported on colloidal carbon spheres (Co/CCS) obtained from glucose exhibited a high HGR (10 400 mL min^{-1} g^{-1}) for $NaBH_4$ hydrolysis at 293 K, whereas Co supported on carbon aerogels (Co/ACs) showed a higher HGR of 11 220 mL min^{-1} g^{-1}.[66,67] Zhang *et al.* fabricated a Co@C pre-catalyst by using Co-MOF as the starting precursor.[68] The Co@C-700 pre-catalyst exhibited higher catalytic activity than Co@C-600 and retained 93.1% of its initial catalytic activity after five cycles in $NaBH_4$ hydrolysis. Recently, Li *et al.* synthesized nitrogen-doped mesoporous graphitic carbon encapsulated Co NPs (Co@NMGC) by a simple one-step pyrolysis of a complex of $Co(NO_3)_2{\cdot}6H_2O$ and ethylenediaminetetraacetic acid (EDTA).[69] Co@NMGC annealed at 773 K showed high catalytic activity and remarkable durability, retaining 82.5% of its initial catalytic activity after 20 hydrolysis cycles.

Magnetic catalysts can be easily recycled with a permanent magnet from a spent $NaBH_4$ system after hydrogen production.[70–72] Chen *et al.* synthesized a magnetic Co/IR-120 pre-catalyst by a combination of ion-exchange and reduction methods.[70] A stable generation rate of highly pure hydrogen near 200 mL min^{-1} g^{-1} was achieved over the Co/IR-120 pre-catalyst in 100 mL of 5 wt% $NaBH_4$ solution. Kim and co-workers reported novel Co NPs supported on magnetic carbon (Co/Fe_3O_4@C) *via* a modified wetness impregnation–chemical reduction method.[71] The abundant oxygen-containing-groups on the surface of the carbon layer can effectively immobilize and stabilize the Co NPs, thereby enhancing their catalytic activity for the hydrolysis of $NaBH_4$. Ferromagnetic metals Co, Ni, and Fe were supported on porous SiO_2 *via* an incipient wetness impregnation method.[32] The catalytic activities of ferromagnetic metal/SiO_2 followed the order Co/SiO_2 > Ni/SiO_2 > Fe/SiO_2. Furthermore, various other Ni-based catalysts have been reported, but Co-based catalysts have been found to be the most superior in terms of the maximum hydrogen generation rate.[73–75]

2.2. Metal boride catalysts

Schlesinger and co-workers first found that Co_2B was active for hydrogen evolution from the hydrolysis of $NaBH_4$.[54] Afterwards, there have been many reports on the preparation and catalytic activity of Co–B catalysts.[60,61,76–81] It has been reported that the structure and catalytic activity of Co–B catalysts were sensitive to their preparation conditions. Jeong and coworkers prepared a Co–B pre-catalyst by the chemical reduction method using $NaBH_4$ as a reductant.[76] The obtained Co–B catalyst was amorphous and showed excellent catalytic performance for hydrogen generation from an aqueous alkaline $NaBH_4$ solution, which was comparable to that of a Ru catalyst. Wu and coworker found that amorphous Co–B after heat treatment showed much higher catalytic activity than the untreated sample, which is attributed to the formation of the crystalline state of Co–B.[77] In addition, the Co–B catalyst treated at 500 °C exhibited the best crystallization and showed the highest hydrogen generation performances. When the Co–B catalyst was heated at 700 °C, the catalytic activity of the catalyst drastically decreased due to the decomposition of Co–B to form metal Co.

To further obtain efficient Co–B catalysts, the synthesis parameters such the cobalt salt, ratio of $NaBH_4/Co^{2+}$, calcination temperature and solvent type are investigated. Kim and coworkers examined the catalytic activity of a Co–B catalyst prepared by using different Co precursors ($CoCl_2$ and $CoSO_4$) and $NaBH_4/Co^{2+}$ molar ratios (0.67, 1.5, and 3) at different calcination temperatures (130, 250 and 450 °C).[82] With $CoCl_2$ as the precursor, a $NaBH_4/Co^{2+}$ molar ratio of 1.5, and a calcination temperature of 250 °C, the hydrogen evolution rate of the Co–B catalyst was the highest. Demirci and coworkers further confirmed that $CoCl_2$ is the best precursor, which showed a four times higher hydrogen generation rate than those of other Co salts ($Co(CH_3COO)_2$, $CoSO_4$, CoF_2, and $Co(NO_3)_2$).[83] The sizes, morphologies, and properties of the Co–B catalyst are also greatly influenced by the solvents used. Zhao and coworkers found that the Co–B catalyst was more likely to agglomerate as the viscosity of the solvent increased.[84] The catalytic activities of Co–B catalysts prepared in different solvents are in the order of MeOH > H_2O > EtOH > PrOH.

Although optimization of the synthesis parameters can improve the catalytic properties, the exothermic nature of the reduction reaction involves high surface energy and is easily prone to aggregation, leading to deteriorated activity. An efficient route to avoid agglomeration and increase the active surface area of Co–B particles is by doping with transition metals (Cr, Mo, W, *etc.*).[85–91] These dopant metals, mainly in the form of oxides, act as atomic barriers that are able to significantly increase the surface area of the catalyst by avoiding agglomeration. Additionally, these dopant metals can also act as electron donors to increase the electron density on the active metal, which can further improve the catalytic activity of the Co–B catalyst. For instance, Patel *et al.* conducted a systematic and comparative study on transition metal (Cr, Mo, W, Cu, Ni and Fe) doped Co–B catalysts for hydrogen generation by hydrolysis of $NaBH_4$.[86] They found that the hydrogen generation rate of Co–B catalysts doped with Cr, W, Mo, and Cu is about 3–4 times higher than that of the undoped catalysts. Ni and Fe are only able to slightly enhance the catalytic activity of the Co–B catalyst. In recent years, Co–B catalysts doped with Mn,[92] Ti,[93] Ce[94] and Zn[95] have been investigated and they also showed positive promotion effects on the hydrogen evolution of $NaBH_4$ hydrolysis. Another efficient route to enhance the catalytic performance is by supporting Co–B NPs in a support material, such as carbon,[96–98] Al_2O_3,[99] CeO_2,[99] TiO_2,[99–101] and Ni foam.[102,103] The above supports can effectively inhibit the agglomeration of metal NPs and increase the active sites of the catalysts, and therefore can effectively improve the catalytic activity of the catalysts.

Other metal boride catalysts such as Ni–B, Cu–B, and Fe–B are also investigated for hydrogen evolution from the hydrolysis of $NaBH_4$. Kim and co-workers reported a Ni–B–silica

nanocomposite pre-catalyst *via* an *in situ* reduction method.[104] The obtained amorphous pre-catalyst was active, providing a hydrogen generation of 1916 mL min^{-1} g^{-1}. Later on, a stable and physically adhesive Ni–B on Ni foam was prepared by Lee and coworkers *via* a dipping-chemical reduction process and it exhibited high catalytic activity towards the hydrolysis of $NaBH_4$.[105] Zhang and coworkers prepared an amorphous Ni–B pre-catalyst *via* an ultrasonic complexing reduction route.[106] They found that the chemical composition and phase state of the Ni–B pre-catalyst were greatly influenced by its complexing ability. The stronger the complexing ability of the complex, the smaller the size and the higher the dispersibility of the formed Ni–B, resulting in a higher catalytic activity of Ni–B. Recently, a Ni–B/$NiFe_2O_4$ magnetic pre-catalyst with a metal loading of 10 wt% retained 85% of its initial activity after the fifth run, and the Ni–B/$NiFe_2O_4$ can be easily separated from the reaction solution using an external magnet.[107]

Lee reported a Fe–B/C cloth pre-catalyst by electrochemical adsorption techniques.[108] The hydrogen generation rate using the Fe–B/C cloth pre-catalyst can achieve 813 mL min^{-1} g^{-1} at room temperature. The Fe–B/Ni foam catalyst was also prepared by the same group for hydrogen generation from $NaBH_4$ in a mixture solution of H_2O and CH_3OH.[109] They found that using methanol as an additive to water can increase and stabilize the rate of hydrogen generation, but with lower gravimetric capacity. Bekirogullari compared the catalytic activities of Cu–B, Fe–B, and Ni–B pre-catalysts for hydrogen evolution from $NaBH_4$.[110] The results reveal that the catalytic activities of these metal borides followed an order of Cu–B > Ni–B > Fe–B.

2.3. Metal phosphide catalysts

Like Co–B, the other counterpart Co–P catalysts were also able to produce hydrogen from hydrolysis of $NaBH_4$.[111,112] Kwon and co-workers first reported a Co–P pre-catalyst electrodeposited on a Cu substrate in a sulfate based solution containing $H_2PO_2^-$ ions.[111] They found that the amorphous Co–P pre-catalyst with 13 at% P showed the best hydrogen generation rate of 954 mL min^{-1} g^{-1} in a solution of 1 wt% NaOH and 10 wt% $NaBH_4$ at 303 K, which is 18 times higher than that of a pure Co pre-catalyst. To further obtain efficient Co–P catalysts, the synthesis parameters such as the pH value, reactant concentration and deposition time are investigated.[113,114] Chen's group found that the Co–P pre-catalyst formed at a pH value of 12.5, a NaH_2PO_2 concentration of 0.8 M, and a deposition time no more than 6 min showed the highest catalytic activity for the hydrolysis of $NaBH_4$ solution.[113] By tuning the deposition temperature, nanostructured Co–P/Cu sheets with different morphologies (nanoplatelets, nanospheres, pores and nanoclews) were selectively obtained.[114] Notably, the nanostructured Co–P pre-catalyst deposited at 50 °C displayed novel hierarchical architectures and exhibited the highest catalytic properties with a high hydrogen release rate of 2275.1 mL min^{-1} g^{-1} and a low apparent activation energy of 27.9 kJ mol^{-1}.

The Co–P based catalysts prepared by chemical and electrodeposition methods are usually formed in powder form. Compared to nanoparticle catalysts, monolithic catalysts have obvious advantages such as no aggregation, easy separation and reuse, and they can be utilized as an on/off switch for on-demand hydrogen generation.[115,116] Sun's group designed 3D cobalt phosphide nanosheet arrays on Ti mesh (CoP/Ti mesh) *via* a topotactical conversion reaction.[115] The obtained 3D monolithic pre-catalyst showed high catalytic activity, providing a maximum hydrogen generation rate of 6100 mL min^{-1} g^{-1} for $NaBH_4$ hydrolysis in alkaline media and an activation energy of 42.01 kJ mol^{-1}. Similarly, Liu and coworkers reported the synthesis of a CoP nanowire array integrated on a Ti mesh (CoP NA/Ti) for hydrolytic dehydrogenation of $NaBH_4$ in basic solutions.[116]

Not only binary Co–P but also ternary Co–M–P (M = W, Ni, Cu, Fe, *etc.*) catalysts have been developed as robust catalysts for hydrogen generation from the hydrolysis of $NaBH_4$ alkaline solution.[117–123] Ma and coworkers found that the catalytic activity of the amorphous Co–P pre-catalyst could be markedly improved by incorporating W.[117] However, the hydrogen generation rate of the Co–W–P pre-catalyst lost 49% of its activity after 5 cycles. Furthermore, by depositing Co–W–P on γ-Al_2O_3 and carbon cloth, the catalytic activity and stability of the pre-catalyst can be significantly improved.[118,119] Kim *et al.* synthesized porous Co–Ni–P on Cu substrates by electrodeposition.[120] The three-dimensional Co–Ni–P pre-catalyst formed at a high cathodic current density (>0.5 A cm^{-2}) had a larger surface area than the two-dimensional pre-catalyst formed at a low cathodic current density (0.01 A cm^{-2}), which significantly increased the rate of hydrogen generation in the alkaline $NaBH_4$ solution. Diverse nanostructures of Co–Ni–P pre-catalysts have been prepared on Cu sheets *via* the electroless plating method by tuning the depositional pH value.[121] Compared with football-, granular-, and shuttle-like Co–Ni–P, mockstrawberry-like Co–Ni–P exhibited the highest catalytic properties. It has been reported that the alloying of Cu into Co–Cu–P was also able to improve their catalytic activity in hydrogen production *via* $NaBH_4$ hydrolysis.[122] Lately, Fe-doped CoP nanoarrays on Ti foil (Fe-CoP/Ti) have been investigated by Sun's group as a robust catalyst for $NaBH_4$ hydrolysis, resulting in a hydrogen generation rate of 6060 mL min^{-1} g^{-1} and an activation energy of about 39.6 kJ mol^{-1}.[123]

Overall, Co-based catalysts are demonstrated to be cost-effective, active and stable catalysts for hydrogen generation from the hydrolysis of $NaBH_4$. In addition, most of the reported metal borides/phosphides are in an amorphous state.[61,124] The materials in the amorphous state have great structural distortion and high concentrations of unsaturated coordination sites, which make them show high catalytic activity. After heat treatment, the amorphous metal borides can be transformed into a crystalline state, because of which they usually exhibit higher catalytic performance. However, the material after heat treatment is often a mixture of the metal, borides and/or oxides. Thus, its composition and surface structures are complex, and it is difficult to identify the real active sites. Furthermore, the mechanism of their catalytic hydrogen production is not clear. Particularly, what is the exact active

composition of Co and B or P to achieve high catalytic activity? Therefore, future research can be focused on mechanistic studies of the hydrolysis reaction at the surface of the Co-based catalysts.

3. Ammonia borane

Ammonia borane (NH_3BH_3, AB) is a stable solid at room temperature with a density of 0.780 g cm^{-3} and a melting point of 112–114 °C.[125] Owing to its high hydrogen content (19.6 wt%), low molecular weight (30.9 g mol^{-1}), and nontoxic and environmentally friendly nature, NH_3BH_3 has been considered as a promising hydrogen storage material.[126–133] Hydrogen stored in NH_3BH_3 can be released by either thermal decomposition in the solid phase or catalytic solvolysis (hydrolysis and methanolysis) under mild conditions.[126,134–138] There are considerable works involving hydrogen release from the thermal decomposition of NH_3BH_3.[134–137] Although pure NH_3BH_3 possesses 3 equivalents of H_2, only 2 equivalents could be released at a temperature of 200 °C. In order to maximize the efficacy of NH_3BH_3, higher temperatures are needed, which also results in the release of the by-product borazine. To decrease the thermolysis temperature and suppress the volatile byproducts, various approaches have been achieved, including nano-confinement, catalysis, dispersion in ionic liquids and organic liquids, and the synthesis of derivatives (*e.g.*, metal amidoboranes).[139–142] Generally speaking, thermal decomposition of NH_3BH_3 requires high temperature and the reaction is relatively difficult to control. In contrast, the hydrolytic (eqn (2)) or methanolytic (eqn (3)) dehydrogenation of NH_3BH_3 can be conducted at room temperature with a stoichiometric hydrogen release in the presence of suitable catalysts.[25,126,138] The effective gravimetric hydrogen storage capacity (GHSC) of an NH_3BH_3 hydrolysis system ($NH_3BH_3{\cdot}2H_2O$) is about 8.9 wt%, which is higher than that from NH_3BH_3 methanolysis ($NH_3BH_3{\cdot}4MeOH$, 3.9 wt%).

$$NH_3BH_3 + 2H_2O \rightarrow NH_4BO_2 + 3H_2 \quad (2)$$

$$NH_3BH_3 + 4MeOH \rightarrow NH_4B(OMe)_4 + 3H_2 \quad (3)$$

In 2006, Xu's research group firstly found that a stoichiometric amount of hydrogen could be released from the hydrolysis of NH_3BH_3 by using noble metal-based (Pt, Ru, and Pd) catalysts.[126] Since then, numerous studies have been reported on hydrogen generation from the hydrolysis of NH_3BH_3.[143–148] Also, several reviews have been reported on the research progress on the hydrolysis of NH_3BH_3.[21,25,127,149–153] Here, we have mainly summarized the most active noble-metal-free nanocatalysts for the hydrolytic (Table 2) or methanolytic (Table 3) dehydrogenation of NH_3BH_3.

3.1. Monometallic catalysts

Xu's research group reported that non-noble-metals Co, Ni and Cu supported on different supports (Al_2O_3, SiO_2 and C) were catalytically active, whereas supported Fe was inactive in hydrolytic dehydrogenation of NH_3BH_3 at room temperature.[154] Unexpectedly, amorphous Fe NPs synthesized by *in situ* reduction (Fe/NH_3BH_3 = 0.12) with NH_3BH_3 and $NaBH_4$ exhibited noble metal-like catalytic activity in the hydrolysis of AB (Fig. 1).[155] The high activity of the amorphous metal NPs could be attributed to their amorphous structure, which has a much greater structural distortion and therefore a much higher concentration of active sites for the reaction than its crystalline counterpart. Then, the amorphous Co and Ni NPs were also found to exhibit enhanced catalytic performance in comparison with their crystalline counterparts.[156,157] In particular, the amorphous Co NPs showed the highest catalytic activity with a TOF of 44.1 min^{-1} for hydrogen production from the hydrolysis of NH_3BH_3, which is the highest among the non-noble metal catalysts ever reported.[156]

Co-Based catalysts have been widely studied in recent years due to their relatively higher catalytic activity and low cost.[158–165] Xu's research group synthesized dendrimer-encapsulated Co NPs (G6-OH(Co_{60})) through the complexation of Co^{2+} cations with the internal tertiary amine of sixth-generation hydroxyl-terminated poly(amidoamine) dendrimers followed by reduction with NH_3BH_3 and $NaBH_4$.[158] The synthesized (G6-OH(Co_{60})) was highly dispersed (1.6 nm) and active for the hydrolysis of NH_3BH_3. Duan *et al.* constructed a Co@g-C_3N_4 core–shell nanostructure anchored onto the surface of rGO sheets (Co@g-C_3N_4-rGO), where g-C_3N_4 shells could protect Co cores from aggregating or leaching and rGO sheets could strengthen the magnetic momentum transfer of Co NPs from the external magnetic field.[159] The self-stirring mode in the batch reactor and the magnetic fixing, stirring, and separating mode in the continuous-flow slurry-bed reactor provided an excellent catalytic process with Co@g-C_3N_4-rGO as the pre-catalyst. To further improve the activity of Co-based catalysts for NH_3BH_3 hydrolysis, post-modified supports have been used. Lu and coworkers reported well-dispersed Co NPs with an average size of 2.6 nm on PEI-decorated GO, and the resultant Co/PEI-GO nanocomposites showed excellent activity (39.9 min^{-1}) due to the chelation effect of PEI with precursor metal ions.[160]

Due to their tunable porous structures, metal–organic frameworks (MOFs) have been used as supports to control the sizes of metal NPs.[166–168] Gu and coworkers reported amorphous Co NPs with small particle size (1.6–2.6 nm) immobilized by MIL-101 through an ultrasound-assisted *in situ* method. The obtained Co/MIL-101 pre-catalyst showed excellent catalytic activity (51.4 min^{-1}) for hydrogen evolution from the hydrolysis of NH_3BH_3.[167] Chen and coworkers adopted a covalent triazine framework (CTF) as a support with the merits of high surface area, a well-defined porous structure and high nitrogen content (~17%).[169] Specifically, the Co/CTF with 3 wt% Co loading showed the highest activity towards NH_3BH_3 hydrolysis, providing a TOF value of 42.3 min^{-1} at room temperature. Zhou and coworkers developed a new type of metal–organic hybrid material, the porous coordination cage (PCC), which is efficient at stabilizing Co nanoclusters.[170] The obtained Co@PCC-2a exhibited extraordinary catalytic activity (90.1 min^{-1}) in the hydrolysis of NH_3BH_3 (Fig. 2).

Table 2 Catalytic activities for hydrogen evolution from the hydrolysis of NH_3BH_3 by different catalysts

Catalyst	Temp. (K)	n_{metal}/n_{AB}	TOF (mol_{H_2} mol_{metal}^{-1} min^{-1})	E_a (kJ mol^{-1})	Ref.
In situ Fe NPs	RT	0.12	3.12	—	155
Co/γ-Al_2O_3	RT	0.018	2.27	62	154
In situ Co NPs	RT	0.04	44.1	—	156
G6-OH(Co_{60})	298	0.013	10	50.2	158
Co/PEI-GO	298	0.11	39.9	28.2	160
Co/MIL-101	298	0.02	51.4	31.3	167
Co/CTF	298	0.05	42.3	42.7	169
Co NCs@PCC-2a	298	0.07	90.1	—	170
Co@N–C-700	298	0.057	5.6	31	171
Co/NPCNW	298	0.075	7.29	25.4	172
Co/HPC	323	0.11	2.94	32.8	174
Co-$(CeO_x)_{0.91}$/NGH	298	0.04	79.5	31.82	161
Co@C–N@SiO_2-800	298	—	8.4	36.1	162
Ni/γ-Al_2O_3	RT	0.018	2.5	—	154
Ni/C	298	0.0425	8.8	28	175
Ni/SiO_2	298	0.0225	13.2	34	180
Ni@MSC-30	RT	0.016	30.7	—	181
Ni/ZIF-8	RT	0.016	14.2	—	182
Ni NPs/ZIF-8[a]	298	0.03	85	42.7	183
Ni/CNT ALD	298	—	26.2	32.3	185
Ni@3D-(N)GFs	RT	0.009	41.7	—	186
NiMo/graphene	298	0.05	66.7	21.8	188
Ni-CeO_x/graphene	298	0.08	68.2	28.9	194
Ni/PDA-$CoFe_2O_4$	298	0.017	7.6	50.8	178
Ni/Ketjenblack	298	0.13	7.5	66.6	179
Cu/γ-Al_2O_3	RT	0.018	0.23	—	154
p(AMPS)-Cu	303	0.069	0.72	48.8	197
Zeolite confined Cu	298	0.013	1.25	51.8	201
Cu/$CoFe_2O_4$@SiO_2	298	0.0031	40	—	202
Cu/RGO	298	0.1	3.61	38.2	203
Cu@SiO_2	298	0.08	3.24	36	204
$Fe_{0.5}Ni_{0.5}$ alloy	293	0.12	11.1	—	210
$Fe_{0.3}Co_{0.7}$ alloy	293	0.12	13.9	16.3	216
$Cu_{0.33}Fe_{0.67}$	298	0.04	13.95	43.2	219
CuCo/graphene	293	0.02	9.18	—	220
$Cu_{0.2}Co_{0.8}$/PDA-rGO	303	0.05	51.5	54.9	221
$Cu_{0.2}Co_{0.8}$/PDA-HNTs	298	0.09	30.8	35.15	222
CuCo/C	298	0.033	45	51.9	223
$Cu_{0.5}Co_{0.5}$@SiO_2	298	0.08	4.26	24	230
$Cu_{0.3}Co_{0.7}$@MIL-101	RT	0.034	19.6	—	231
$Cu_{0.72}Co_{0.18}Mo_{0.1}$	298	0.04	46.0	45	190
$Cu_{0.72}Co_{0.18}Mo_{0.1}$[a]	298	0.04	119.0	—	190
CuNi/CMK-1	298	0.072	54.8	—	224
$Cu_{0.2}Ni_{0.8}$/MCM-41	298	0.05	10.7	38	228
CuNi/47-SiO_2	298	0.165	23.5	34.2	229
$Cu_{0.8}Co_{0.2}O$/GO	298	0.024	70	45.5	243
Ni_2P	298	0.12	40.4	44.6	255
CoP[a]	298	0.043	72.2	46.7	262
$Ni_{0.7}Co_{1.3}P$/GO[a]	298	0.026	109.4	—	263

[a] The reaction was promoted with the addition of NaOH.

Table 3 Catalytic activities for hydrogen evolution from the methanolysis of NH_3BH_3 by different catalysts

Catalyst	Temp. (K)	n_{metal}/n_{AB}	TOF (mol_{H_2} mol_{metal}^{-1} min^{-1})	E_a (kJ mol^{-1})	Ref.
Cu_2O	298	0.15	0.16	—	198
Nano-Cu@Cu_2O	298	0.15	0.12	—	198
Nano-Cu	298	0.15	0.08	—	198
PVP-stabilized Ni	298	0.005	12.1	62	267
Co–Ni–B	RT	0.2	10	—	276
Co–Co_2B	RT	0.2	6	—	276
Ni-Ni_3B	RT	0.2	3.6	—	276
Flower-like Cu	298	0.15	2.41	34.2	277
Cu–Cu_2O–CuO/C	298	0.04	24	67.9	278
b-CuO NA/CF	298	0.018	13.3	34.7	279
CuNi/graphene	298	0.03	49.1	24.4	280
Cu/$Co(OH)_2$	298	0.129	61.63	37.6	281

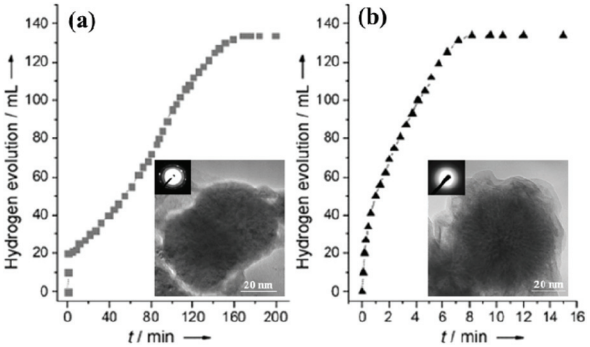

Fig. 1 Hydrogen generation by hydrolysis of aqueous AB (0.16 m, 10 mL) in the presence of (a) the pre-synthesized and (b) *in situ* synthesized Fe catalysts (Fe/AB = 0.12) at room temperature under argon. The inset shows the corresponding TEM images and SAED patterns of the as-synthesized catalysts. Reprinted with permission from ref. 155. Copyright (2008) Wiley-VCH.

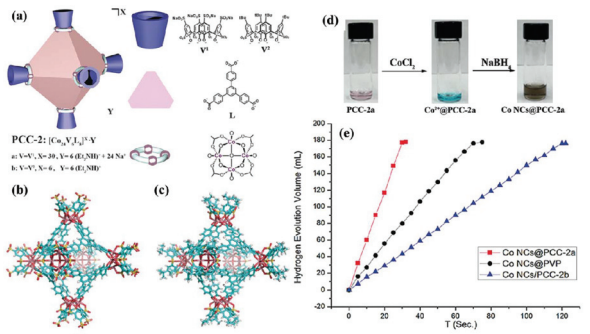

Fig. 2 (a) Cartoon of octahedron cage PCC-2 and the cage components, (b) the crystal structure of PCC-2, and (c) the crystal structure of PCC-2b. (d) The preparation of Co NCs with PCC-2a. (e) Time course plots of H_2 generation for the hydrolysis of AB by Co NCs@PCC-2a, Co NCs/PCC-2b, and Co NCs@PVP. Reprinted with permission from ref. 170. Copyright (2018) Wiley-VCH.

Recently, carbonization of inorganic/organic composites has been developed to prepared catalysts for the AB hydrolysis reaction due to their excellent chemical and mechanical stabilities, large specific surface areas and various functionalities.[163,171–174] Chen and coworkers reported the preparation of Co@N–C pre-catalysts through one-step thermolysis of Co (salen, *N*,*N*′-bis(salicylidene)ethylenediamine) at selected temperatures (600–800 °C) under an Ar atmosphere.[171] They found that Co@N–C obtained at 700 °C (Co@N–C-700) shows superior catalytic performance (5.6 min^{-1}) and high sustainability among the synthesized pre-catalysts. After that, they also synthesized Co NPs (~3.5 nm) supported on nitrogen-doped porous carbon nanowires (Co/NPCNW) by carbonization of a Co–metal organic framework (Co-MOF), which show a TOF of 7.29 min^{-1} and a relatively low activation energy of 25.4 kJ mol^{-1}.[172] Later on, Zhang *et al.* reported a series of highly active and stable nitrogen-doped mesoporous carbon embedded-Co NP pre-catalysts through a thermolysis and etching combined strategy.[173] More recently, Yang and coworkers employed a selective atom evaporation-isolation strategy with bimetal Co/Zn-MOF-74 as a sacrificial template to obtain a metallic Co/HPC pre-catalyst by direct carbonization and *in situ* reduction under an Ar atmosphere.[174] The as-synthesized Co/HPC pre-catalyst exerted higher catalytic activity and showed excellent reusability as compared to the Co/HPC derived from pure Co-MOF-74. The excellent catalytic performance can be attributed to the uniform dispersion and small particle size of metallic Co obtained under the assistance of the dopant Zn.

Ni catalysts are also widely studied as low cost non-noble metal catalysts owing to their exceptional activity in catalytic dehydrogenation of aqueous AB (Table 2).[175–179] Monodisperse Ni NPs (3.2 nm) supported on Ketjen carbon black (Ni/C) showed high catalytic activity for the hydrolysis of AB with a TOF of 8.8 min^{-1}.[175] However, Ni/C was not stable during the reusability test due to the agglomeration of Ni NPs on the carbon support. In order to improve the stability of Ni NPs, they used various oxides including SiO_2, Al_2O_3, and CeO_2 as support materials.[180] They found that 3.2 nm Ni NPs supported on SiO_2 showed the highest activity (13.2 min^{-1}) and durability. Subsequently, the Ni NPs (6.3 ± 1.7 nm) deposited into the nanoporous carbon (MSC-30) synthesized by Xu's research group showed excellent catalytic activity with a TOF value as high as 30.7 min^{-1}, which is the highest one among all of the Ni catalysts ever reported for this hydrolysis reaction at room temperature.[181] They also reported the synthesis of highly dispersed Ni NPs immobilized on the zeolitic metal–organic framework ZIF-8 (Ni/ZIF-8), which showed high catalytic activity and durability.[182] They pointed out that this is the first example of water-stable MOF-supported metal NPs for hydrogen generation from hydrolysis of NH_3BH_3. Using the zeolitic metal–organic framework ZIF-8 as the support, Astruc and coworkers further developed highly dispersed Fe, Co, Ni and Cu NPs, and the highest catalytic performance with a TOF value of 85 min^{-1} was achieved in the presence of Ni/ZIF-8 with the assistance of an additive (NaOH).[183]

Zhong and coworkers reported a Ni/CNT hybrid pre-catalyst for the hydrolysis of NH_3BH_3.[184] Combined with identical high-resolution TEM images, scanning transmission X-ray microscopy (STXM) clearly revealed the existence of a strong interaction between Ni NPs and thin CNTs (C–O–Ni bonds), which favored the tunable electronic structure of Ni NPs and facilitated the catalytic hydrolysis process. Later on, Qin and coworkers presented a facile atomic layer deposition approach (ALD) to synthesize highly dispersed Ni NPs on CNTs.[185] The resultant Ni/CNT pre-catalyst produced with 200 ALD cycles showed the best catalytic activity (26.2 min^{-1}) among all the Ni/CNT pre-catalysts. Mahyari *et al.* employed a three-dimensional nitrogen-doped graphene-based framework (3D-(N)GF) as a support to immobilized Ni NPs, which showed excellent catalytic activity (41.7 min^{-1}) and high stability in NH_3BH_3 hydrolysis.[186]

Recently, our group reported a facile chemical reduction method to incorporate a small amount of inactive metals (Mo,

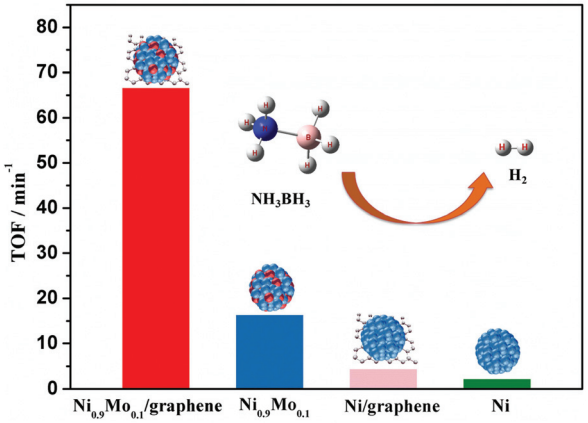

Fig. 3 Catalytic activities for hydrogen generation from AB aqueous solution (5 mL, 0.2 M) over $Ni_{0.9}Mo_{0.1}$/graphene, $Ni_{0.9}Mo_{0.1}$, Ni/graphene, and Ni at 298 K (metal/AB = 0.05). Reprinted with permission from ref. 188. Copyright (2016) Royal Society of Chemistry.

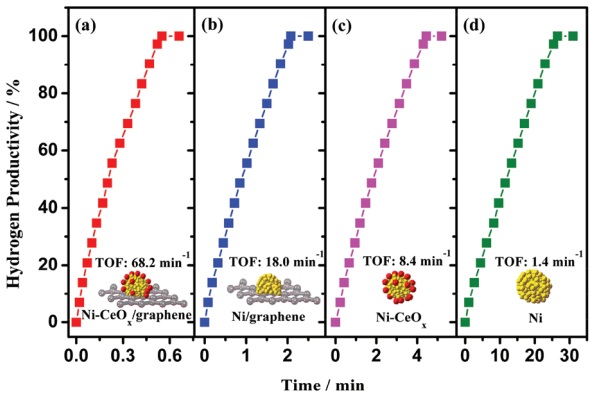

Fig. 4 Hydrogen productivity *vs.* reaction time for hydrogen release from an aqueous AB solution (200 mM, 5 mL) catalyzed by (a) Ni-CeO_x/graphene, (b) Ni/graphene, (c) Ni-CeO_x, and (d) Ni at 298 K (*n*Ni/*n*AB = 0.08). Reprinted with the permission from ref. 194. Copyright (2018) Springer Nature.

Cr, and W) into Ni NPs.[187] The characterization results revealed that the incorporation of Mo (mainly in the oxidation state) can not only reduce the metal particle size and crystallinity of the metal NPs, but also increase the electron density on the metal surface, which can effectively improve the catalytic activity of the catalysts. To further improve the dispersion and activity of the catalyst, Ni NPs modified with a Mo dopant have been synthesized on graphene (Ni–Mo/graphene), and they exhibit a high Pt-like catalytic activity (66.7 min^{-1}) and robust durability in the hydrolysis of NH_3BH_3 at room temperature (Fig. 3).[188] In addition, our synthesis is not limited only to Ni–M (M = Mo, Cr, W), but can also be extended to other transition metal systems (Cu–M, Co–W, *etc.*), providing a general method for the synthesis of highly efficient catalysts for the hydrogen evolution reaction.[189–193]

Ni doped with CeO_x and supported on graphene (Ni-CeO_x/graphene) was also fabricated by our research group *via* a facile chemical reduction route.[194] The combination of CeO_x, metal, and graphene of the Ni-CeO_x/graphene pre-catalyst confers remarkably enhanced catalytic activity (68.2 min^{-1}) for the hydrolytic dehydrogenation of NH_3BH_3 (Fig. 4), as well as high stability. In addition, some other rare-earth metal oxide (ReOx, Re = La, Dy, Er, Yb, Gd, and Tb) doped Ni/graphene (Ni-ReO_x/graphene) were also prepared and all showed higher catalytic activities than pure Ni/graphene. The excellent catalytic activities of Ni-ReO_x/graphene might be attributed to the similar physical and chemical properties of the ReO_x species, all of which promote the active sites of Ni to electron-rich states that are beneficial for the catalytic reaction. By using a similar approach, Co-CeO_x/NGH and CuNi-CeO_x/rGO were prepared and they showed synergistic and superior catalytic activities.[161,195]

Comparing Co- and Ni-based catalysts, Cu-based catalysts have been reported to show a lower catalytic activity (Table 2).[196,197] In 2006, Xu and coworkers found that Cu/γ-Al_2O_3 was catalytically active in NH_3BH_3 hydrolysis (0.78 min^{-1}), but it takes nearly 600 minutes to release 2.83 equivalents of hydrogen (*n*Cu/*n*AB = 0.018).[154] Subsequently, nanostructured Cu, Cu_2O, and Cu@Cu_2O NPs were synthesized by Kalidindi and co-workers *via* the solvated metal atom dispersion (SMAD) method.[198] They found that core–shell Cu@Cu_2O and Cu_2O NPs are more active than pure Cu NPs for this hydrolysis reaction. After that, Fukuzumi and co-worker synthesized a series of Cu/Co_3O_4 composite pre-catalysts by a conventional impregnation method.[199] The catalytic activities of Cu/Co_3O_4 were significantly dependent on the shape and size of nanosized Co_3O_4, and it was found that Co_3O_4 with a hexagonal sheet shape showed better catalytic activity than that with a cube or uncontrolled shape. They also found that capping of Cu_2O with Co_3O_4 NPs was an effective way to suppress agglomerate formation, which made the Cu_2O–Co_3O_4 composites exhibit high catalytic reactivity in hydrolytic dehydrogenation of NH_3BH_3.[200]

Özkar and co-worker synthesized zeolite confined Cu NPs by ion-exchange of Cu^{2+} with the extra framework Na^+ in zeolite-Y followed by the reduction of the Cu^{2+} ions with $NaBH_4$.[201] The zeolite confined Cu NPs were found to be active in the hydrolysis of NH_3BH_3 with a TOF value of 0.78 min^{-1}. Cu NPs supported on magnetic SiO_2/$CoFe_2O_4$ (CuNPs@SCF) were reported to have an initial TOF of 40 min^{-1} for hydrolysis of NH_3BH_3 at 298 K.[202] The authors claimed that this TOF value was higher than those of all the reported non-noble metal catalysts for the same hydrolysis reaction. It should be noted that the support of $CoFe_2O_4$ was not considered in the TOF calculation. The oxides of Fe and Co are difficult to be reduced by NH_3BH_3; however, they might be reduced by the Cu–H active species or hydrogen released in the hydrolysis reaction.

Our group reported the synthesis of reduced graphene oxide supported Cu NPs (Cu/RGO) *via* a facile *in situ* procedure using NH_3BH_3 as a reductant.[203] The obtained Cu/RGO showed a higher catalytic activity than Cu/graphite powder, Cu/activated carbon and free Cu NPs, over which the NH_3BH_3

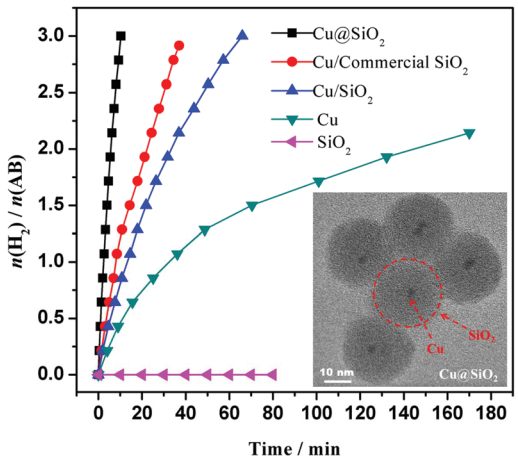

Fig. 5 Hydrogen generation from the hydrolysis of AB (0.2 M, 5 mL) in the presence of different catalysts at 298 K (Cu/AB = 0.09). The inset shows the TEM image of the $Cu@SiO_2$ catalyst. Reprinted with permission from ref. 204. Copyright (2014) Springer Nature.

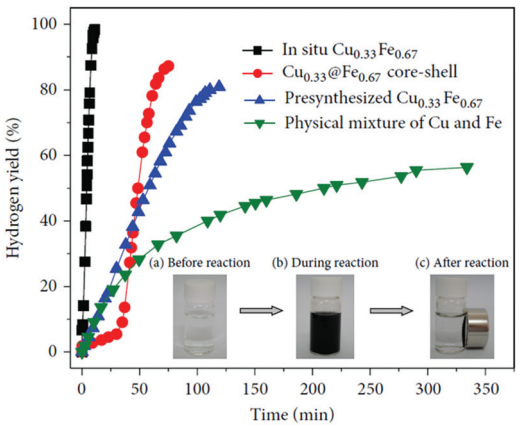

Fig. 6 Hydrogen generation from the hydrolysis of AB in the presence of different catalysts (metal/AB = 0.04). The inset shows photographs of the catalytic hydrolysis of AB *via in situ* synthesized $Cu_{0.33}Fe_{0.67}$ alloys. Reprinted with permission from Ref. 219. Copyright (2013) Elsevier.

hydrolysis reaction is completed in 8.3 min, giving a TOF value of 3.61 min^{-1} at 298 K. We also found that the ultrafine Cu NPs (~2 nm) encapsulated in porous silica nanospheres can be simply fabricated *via* a one-pot synthetic route in a reverse micelle system.[204] The outer shell of silica can effectively prevent the Cu NPs from aggregation. The $Cu@SiO_2$ core–shell nanospheres showed superior activity as compared to Cu/commercial SiO_2, Cu/SiO_2 and free Cu NPs for hydrolysis of NH_3BH_3 (Fig. 5). Furthermore, the $Cu@SiO_2$ core–shell nanospheres showed long-term stability, retaining 90% of their initial catalytic activity even after 10 runs. Recently, Zhang and coworkers fabricated Cu nanocrystals with different nanostructures (nanocubes, nanowires, nanotetrahedra, *etc.*) *via* simply adjusting the addition proportion of the reductant and orientation agent.[205] In comparison with the ordinary Cu NPs with extremely low or hardly any catalytic performance activity, all of the regularly shaped Cu nanocrystals showed high catalytic activity, among which the nanocubed Cu nanocrystals exerted the best catalytic performance for hydrolyzing NH_3BH_3 with 3 equiv. of H_2 extracted within 28 min at 298 K. However, the productivity of the hydrolysis reaction over a nanocubed Cu catalyst showed an obvious decrease after 5 runs.

3.2. Heterometallic catalysts

Heterometallic catalysts, including bi-metallic and multi-metallic catalysts, with unique structures may show higher catalytic performance than their monometallic counterparts due to the strong synergistic effects/electronic effects between the metals.[23,206–209] A number of heterometallic catalysts, such as Fe–Ni,[210–213] Fe–Co,[214–216] Ni–Co,[217,218] Cu–Fe,[219] Cu–Co,[220–223] and Cu–Ni,[224–228] have been reported toward the hydrolysis of NH_3BH_3. For example, our group prepared a series of $Cu_{1-x}Fe_x$ alloy NPs by a very simple *in situ* reduction method, and the optimal $Cu_{0.33}Fe_{0.67}$ alloy NPs exhibited superior catalytic activity with a TOF value of 13.95 min^{-1} (Fig. 6).[219] Moreover, these *in situ* synthesized CuFe alloy NPs can be easily separated from the solution with an external magnet, and they showed good recycling stability.

In subsequent research, various distinct support materials, such as carbon materials, nanotubes, nanofibers, silica spheres, metal–organic frameworks (MOFs), and so on, have been used to fabricate well-dispersed and stable bimetallic NP nanocatalysts.[220–224,229–231] Co decorated Cu NPs on graphene (graphene–CuCo) have been synthesized by Yan *et al. via* a one-step self-catalytic method, which showed high efficiency toward the hydrolytic dehydrogenation of NH_3BH_3.[220] Xu's research group employed diamine-functionalized reduced graphene oxide as a support for CuCo NPs (CuCo/PDA-rGO), which showed higher catalytic performance (41 min^{-1}) as compared to CuCo/rGO (20.6 min^{-1}).[221] Later on, Zhang and coworkers prepared poly(diallyldimethylammonium chloride) functionalized halloysite nanotube supported Cu–Co NPs (CuCo/PDDA-HNTs), in which CuCo NPs were highly dispersed on the surface of halloysite nanotubes and they showed an extraordinary catalytic property (30.8 min^{-1}) in NH_3BH_3 hydrolysis reaction.[222] Zahmakiran and coworkers reported copper–cobalt alloy NPs supported on activated carbon (CuCo/C) by a surfactant-free deposition–reduction technique. The obtained CuCo/C showed excellent catalytic performance with an initial TOF of 45 min^{-1}.[223]

Kleitz and coworkers selected mesoporous carbons (CMK-1 and MCNS) and mesoporous silica (MCM-48) as supports for CuNi alloy NPs.[224] The catalytic performances of carbon-supported $Cu_{0.5}Ni_{0.5}$/CMK-1 and $Cu_{0.5}Ni_{0.5}$/MCNS are comparable in the hydrolysis of NH_3BH_3 and are 3-fold higher than that of silica-supported $Cu_{0.5}Ni_{0.5}$/MCM-48. Yu and coworkers successfully immobilized CuNi NPs on six differently sized SiO_2 spheres (47, 97, 195, 333, 391 and 485 nm).[229] The results showed that the catalytic activity of CuNi/SiO_2 increases with the decrease of SiO_2 particle size, due to which the CuNi NPs supported on the smallest SiO_2 (CuNi/47-SiO_2) exhibit the

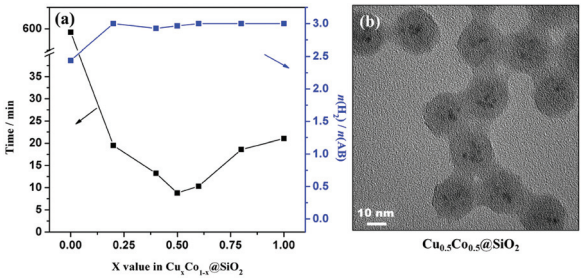

Fig. 7 (a) $Cu_xCo_{1-x}@SiO_2$ core–shell nanospheres with different x values under an ambient atmosphere at 298 K; (b) TEM image of $Cu_{0.5}Co_{0.5}@SiO_2$. Reprinted with permission from Ref. 209. Copyright (2015) American Chemical Society.

highest catalytic activity in the hydrolysis of NH_3BH_3 at 298 K. However, the stability of CuNi/47-SiO_2 showed obvious degradation after seven cycles. Our group successfully encapsulated ultrafine Cu–Co NPs (~2 nm) inside SiO_2 nanospheres (CuCo@SiO_2) (Fig. 7), which can effectively prevent metal NP aggregation and enhance the pre-catalyst stability.[230] The optimized $Cu_{0.5}Co_{0.5}@SiO_2$ pre-catalyst showed excellent catalytic activity in the hydrolysis of NH_3BH_3 and preserved 93% of its initial catalytic activity even after 10 runs. CuCo alloy NPs confined in the pores of MIL-101 (CuCo@MIL-101) *via* a double-solvent method combined with the excellent reduction approach also showed high activity and long durability for hydrolysis of NH_3BH_3.[231]

Trimetallic CuCoMo NPs without any surfactant or support have been fabricated by our group through a facile co-reduction method.[190] Compared to their bi-/monometallic counterparts, the obtained optimized trimetallic $Cu_{0.72}Co_{0.18}Mo_{0.1}$ pre-catalyst exhibits the highest catalytic activity for AB hydrolysis with a TOF value of 46.0 min^{-1} at 298 K (Fig. 8). Moreover, the catalytic performance of

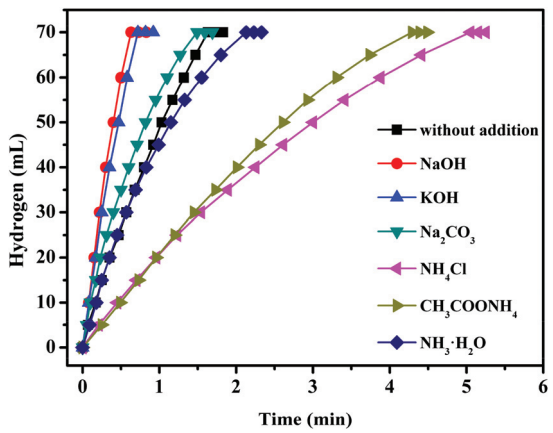

Fig. 8 Hydrogen generation from the hydrolysis of AB (0.20 M, 5 mL) with the addition of 1 M NaOH, KOH, Na_2CO_3, NH_4Cl, CH_3COONH_4 and $NH_3·H_2O$ (2 mL) catalyzed by $Cu_{0.72}Co_{0.18}Mo_{0.1}$ NPs at 298 K (n_{metal} = 0.04 mmol). Reprinted with permission from ref. 190. Copyright (2018) Royal Society of Chemistry.

$Cu_{0.72}Co_{0.18}Mo_{0.1}$ can be further significantly improved by introducing NaOH as a promoter, providing a TOF value as high as 119.0 min^{-1} at 298 K, which is among the highest values of all the reported non-noble metal catalysts (Table 2) and even higher than that of the commercial Pt/C pre-catalyst for the same reaction.[126] However, introducing the NH_4^+ species (*e.g.*, $NH_3·H_2O$, NH_4Cl, *etc.*) into the reaction system is unfavorable for the hydrolysis of AB.

In addition to alloy NPs, core–shell NPs have also attracted considerable attention due to their unique physical and chemical properties, and they exhibited excellent catalytic performance in hydrolytic dehydrogenation of NH_3BH_3.[232–238] Among them, catalysts with a Cu core are the most attractive. In 2011, Xu's research group first reported the synthesis of Cu@M (M = Co, Fe, Ni) NPs *via* a simple one-step seeding-growth route using NH_3BH_3 as a weak reducing agent, which could selectively reduce Cu^{2+} first to form the core, and successively reduce M^{2+} (M = Co, Fe, Ni) to form the shell.[233] A relatively stronger reductant $NaBH_4$, instead of NH_3BH_3, resulted in the formation of CuM alloys. Compared to monometallic and alloy counterparts, the core–shell Cu@M (M = Co, Fe, Ni) NPs showed synergistic and superior catalytic activity for hydrogen evolution from the hydrolysis of NH_3BH_3. In addition, H_2 generation over $Cu_1@Co_4$ NPs is the most active among that over all the Cu@M (M = Co, Fe, Ni) NPs, with which the hydrolysis reaction is completed within 10 min at room temperature. By following a similar approach, various core–shell catalysts based on Cu as a core, such as bimetallic Cu@Co,[234] trimetallic Cu@FeNi,[236] Cu@FeCo,[237] Cu@CoNi,[238,239] Cu@CoMo[240] and even tetrametallic Cu@FeCoNi,[225] have been synthesized and they showed higher activities than the corresponding monometallic and alloy counterparts toward the hydrolysis of ammonia borane for hydrogen production.

3.3. Other catalysts

Since non-noble metal NPs are very easy to oxidize, the direct use of non-noble metal oxides as catalysts for hydrolytic dehydrogenation of NH_3BH_3 has attracted much attention in recent years.[241–244] Li and coworkers prepared $CuCo_2O_4$ pre-catalysts with different shapes (nanoplates, nanosheets, and nanoparticles).[241] Among them, the nanoplate-shaped $CuCo_2O_4$ pre-catalyst showed the best catalytic activity for hydrogen production from the hydrolysis of NH_3BH_3, giving a TOF value of 44 min^{-1} at room temperature. Moreover, the $CuCo_2O_4$ nanoplate pre-catalyst almost retained its initial catalytic activity after eight cycles, indicative of its excellent durability and stability. Later on, they developed a series of non-noble metal oxides such as $NiCo_2O_4$,[242] $MnCo_2O_4$,[245] $CuCoMoO_4$,[246] $CuNiCo_2O_4$,[247] $Co_3O_4/CuMoO_4$,[248] CuO–NiO/Co_3O_4[249] and $Co_xCu_{1-x}Co_2O_4$@ $Co_yCu_{1-y}Co_2O_4$,[250] which are active in NH_3BH_3 hydrolysis reaction. Zhong and coworker reported the synthesis of bimetallic oxide NPs $Cu_xCo_{1-x}O$ deposited on graphene oxide (GO) *via* a facile route.[243] The obtained $Cu_{0.8}Co_{0.2}O$/GO pre-catalyst exhibits an initial TOF value as high as 70.0 min^{-1} for the hydrolysis of NH_3BH_3, owing to the interfacial interaction between CuCoO NPs and GO. Moreover,

they performed the first *in situ* XAS experiments to study the electronic structure changes of the pre-catalyst during hydrolysis. Recently, Liu and coworkers reported a graphene oxide supported Cu@$CuCoO_x$ pre-catalyst, with which superior catalytic activity was achieved toward the hydrolysis of NH_3BH_3 with a TOF of 44.6 min^{-1} at room temperature.[244] With a metal oxide as a pre-catalyst, the catalytically active component of the catalyst is the zero-valent metal because a part of the metal oxide can be reduced by NH_3BH_3. Therefore, such metal oxide catalysts are mainly Cu-based oxides, because Cu oxides can be easily reduced to Cu(0) by NH_3BH_3 at room temperature.

Non-noble-metal catalysts are also easily prone to aggregation in air and under the catalytic reaction conditions, resulting in loss or deactivation of catalytic activity. Recent studies have shown that the catalytic activity and stability of non-noble-metal catalysts could be improved by the introduction of metalloid elements (*e.g.* B and P).[60,61,116,251–257] A series of Co–B catalysts have been reported to show high catalytic activity and durability for hydrogen generation from NH_3BH_3.[251,252,258–261] For example, Figen and Coşkuner synthesized a Co–B pre-catalyst by the sol–gel reaction of boron oxide with cobalt chloride hexahydrate in the presence of citric acid.[252] The obtained amorphous Co–B pre-catalyst showed higher catalytic activity than a crystalline Co–B catalyst due to its high specific surface area and it retained 90% of its initial activity after 4 runs. They also found that Co–B supported on mesoporous silica (SBA-15) and a Co–B thin film pre-catalyst deposited by Pulsed Laser Deposition (PLD) were able to decrease the activation energy, thus improving the catalytic activity in NH_3BH_3 hydrolysis.[258,259]

Fu and coworkers reported the synthesis of Ni_2P NPs by reacting $Ni(OH)_2$ with solid NaH_2PO_2 in argon at 543 K.[254] The obtained Ni_2P NPs (<12 nm) showed excellent catalytic activity and high sustainability toward hydrogen evolution from the hydrolysis of NH_3BH_3 with an initial TOF of 40.4 min^{-1} at 298 K. In addition, they investigated the reaction mechanism *via* DFT calculations (Fig. 9), suggesting that the combination of the Ni_2P surface and substrate molecules significantly enhances the hydrolytic dehydrogenation activity by reducing the reaction barrier, making it easy to overcome at room temperature. They also found that the introduction of anions (OH^-, F^-, and Cl^-) during NH_3BH_3 hydrolysis could significantly promote the catalytic activity in NH_3BH_3 hydrolysis reaction over a Co–P pre-catalyst at room temperature.[262] Moreover, the effect of OH^- was higher than that of F^- and Cl^- on the TOF, and a high TOF of 72.2 min^{-1} was achieved at a CoP/NH_3BH_3 molar ratio of 0.041 at 298 K. Recently, a series of Co-doped Ni_2P NPs and their nanohybrid with graphene oxide were also fabricated by Fu and coworkers.[263] The optimal $Ni_{0.7}Co_{1.3}P$/GO pre-catalyst shows a high initial TOF of up to 109.4 min^{-1} in the presence of NaOH at 298 K. The incorporation of Co into Ni_2P can effectively optimize the electronic structures of $Ni_{2-x}Co_xP$ pre-catalysts, enhance their interaction with NH_3BH_3, and facilitate the hydroxyl activation of NH_3BH_3, thus resulting in a decrease of the reaction energy barrier and improvement of the hydrogen generation rate.

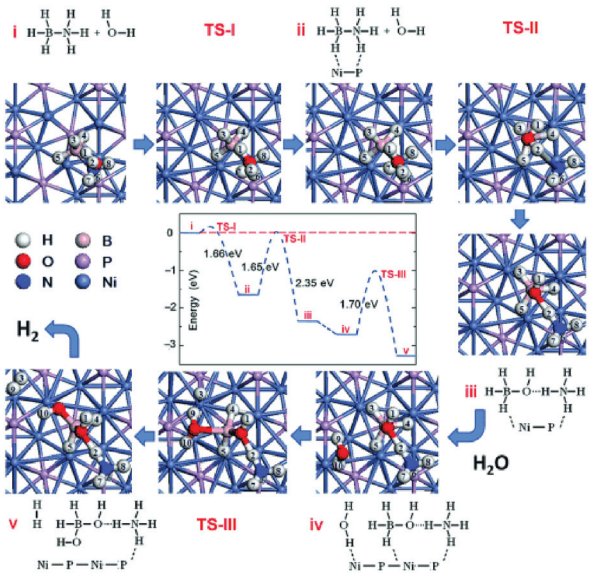

Fig. 9 Plot of energy changes *versus* reaction coordinates calculated for Ni_2P-catalyzed hydrolysis of AB. Reprinted with permission from ref. 254. Copyright (2016) Wiley-VCH.

For the transition metal catalyzed hydrolysis of NH_3BH_3, some plausible mechanisms have been proposed. In 2006, Xu's research group suggested that the formation of an activated complex species between a metal surface and NH_3BH_3 molecules is the rate-determining step.[154] Then, the activated complex species is attacked by H_2O, leading to concerted dissociation of the B–N bond and hydrolysis of the resulting BH_3 intermediate to produce the borate ion along with H_2 release. Jagirdar and Chen assumed that the release of H_2 is due to the attack of H_2O on a transient M–H.[198,264] Fu *et al.* proposed an almost self-powered process based on DFT calculations, which involves the formation of BH_3OH^- and NH_4^+ species, and then attacking adjacent H_2O to produce H_2.[254] Recently, He and Duan proposed that the rate-determining step for NH_3BH_3 is the breaking of the O–H bond in H_2O based on the kinetic isotopic effect measurements.[169,265]

3.4. Catalysts for NH_3BH_3 methanolysis

As for NH_3BH_3 methanolysis, despite the GHSC of the NH_3BH_3–4MeOH system (3.9 wt%) being much lower than that from the hydrolysis system, NH_3BH_3 methanolysis has some advantages that merit its potential applications as a portable hydrogen source.[25,138,266–273] Firstly, addition of suitable catalysts can initiate the NH_3BH_3 methanolysis reaction below 0 °C, thereby satisfying the applications in cold weather. Secondly, pure H_2 can be released by methanolysis of NH_3BH_3 without the production of NH_3. More importantly, the byproduct of NH_3BH_3 methanolysis (*i.e.*, $NH_4B(OMe)_4$) can be easily reconverted back to NH_3BH_3 by reaction with NH_4Cl and $LiAlH_4$ at room temperature.[138]

Compared with the extensive studies of NH_3BH_3 hydrolysis, there are only a few studies regarding NH_3BH_3 methanolysis (Table 3).[138,267,274–276] In 2007, $RuCl_3$, $RhCl_3$, $PdCl_2$, $CoCl_2$,

$NiCl_2$, Pd/C, and RANEY® Ni were firstly reported for the methanolysis of NH_3BH_3.[138] Since then, non-noble metal pre-catalysts such as PVP-stabilized Ni, Co-Co_2B, Ni-Ni_3B, Co–Ni–B, and Co–Ni–P pre-catalysts have been reported for dehydrogenation of NH_3BH_3 in methanol.[276] Later on, mesoporous Cu with diverse morphologies (flower-, nanosheet-, bundle- and dandelion-like) have been prepared by our group *via* a simple wet-chemical method combined with a reduction strategy.[277] Among the four Cu nanostructures, the flower-like Cu nanostructure was the most active with a TOF of 2.41 min^{-1} toward the methanolysis of NH_3BH_3. Moreover, the flower-like Cu nanostructures also showed excellent recyclability in the methanolysis of NH_3BH_3. Subsequently, Zahmakiran and co-workers reported Cu–Cu_2O–CuO/C composites to catalyze hydrogen generation from the methanolysis of NH_3BH_3, which showed high activity (24 min^{-1}) in this methanolysis reaction.[278] After that, bunch-like copper oxide nanowire arrays on copper foam (b-CuO NA/CF) were prepared *via* a simple oxidation process and they behaved as efficient pre-catalysts (13.3 min^{-1}) for methanolytic dehydrogenation of NH_3BH_3.[279] Recently, Sun's research group found that CuNi alloy NPs deposited on graphene (CuNi/G) showed excellent catalytic activity (49.1 min^{-1}) and recyclability toward the methanolysis of NH_3BH_3.[280] More recently, a noble-metal-free Cu/$Co(OH)_2$ nanohybrid pre-catalyst was fabricated by Chen and coworkers *via* a feasible *in situ* method.[281] By varying the metal/support ratio, a highly efficient catalytic performance (61.63 min^{-1}) for the methanolysis of NH_3BH_3 and long-term stability at ambient temperature were observed. By DFT calculations, they revealed the role of charge transfer in promoting the methanolysis reactions and the metal/support ratio in manipulating the catalytic activity *via* tuning electrostatic interactions.

In short, tremendous progress has been achieved in catalytic dehydrogenation of NH_3BH_3 by noble-metal-free catalysts (Table 2). However, further efforts are still needed to develop efficient and stable catalysts or some new methods (*e.g.* photocatalytic assisted technology) to promote the hydrolysis of NH_3BH_3. It is worth noting that the convenience of conducting AB hydrolysis reaction enables its use not only in chemical storage/hydrogen production, but also as a model reaction (similar to the CO oxidation reaction) for testing the activity of new catalysts, which will attract the attention of more and more researchers.

4. Ammonia

Ammonia is a second largest chemical in the world (after sulphuric acid) with over 170 megatonne per year being synthesized *via* the Haber–Bosch process, bulk of which is used as fertilizers.[282] Ammonia is also considered as a potential hydrogen carrier because of its high gravimetric capacity (17.7 wt% H), low price, and production of inherently CO_x-free H_2.[24,26,283–286] In particular, it can be readily liquefied under mild conditions (−33.4 °C at 1 atm or 20 °C at 8.46 atm), which makes its storage and delivery relatively easy.[287–289] NH_3 can be decomposed to release H_2 along with N_2 by the following reaction (eqn (4)):

$$2NH_3 \rightarrow N_2 + 3H_2 \quad (4)$$

The NH_3 decomposition is an endothermic reaction (ΔH = 92 kJ mol^{-1}) and a high temperature is required for efficient hydrogen generation.[290] Thermal decomposition of NH_3 into H_2 and N_2 has been extensively studied in the past decades.[24,26,284,286] The works before the 1990s on NH_3 decomposition were mainly studied to gain insight into the reaction kinetics of NH_3 synthesis.[291] Nowadays, the research on NH_3 decomposition is mainly focused on the generation of high quality H_2. Generally, N_2 adsorption is thought to be rate-limiting in NH_3 synthesis, while the rate determining step for NH_3 decomposition varies. For noble metal (*e.g.* Ru, Rh, Ir, Pt, or Pd) catalysts, N–H cleavage is the rate-determining step, while, for non-noble metal (*e.g.* Fe, Co, Ni, *etc.*) catalysts, N_2 desorption is the rate-determining step.[24,26,292,293]

Up to now, Ru-based catalysts are known to be the most active in catalytic decomposition of NH_3.[294–298] However, the high cost and limited availability inhibit the wide scale use of these catalysts. Therefore, much attention has been recently been paid to non-noble metal catalysts, such as Fe, Co, and Ni as well as a series of bimetallic systems, metal carbides, and metal nitrides.[24]

4.1. Monometallic catalysts

Fe-Based catalysts have been extensively studied in the NH_3 decomposition reaction owing to its industrial use in the NH_3 synthesis reaction.[299–304] Fe promoted by K_2O, CaO, SiO_2 and Al_2O_3 is active for NH_3 synthesis at temperatures above 400 °C and was initially considered as a potential pre-catalyst for NH_3 decomposition.[299] The overall activity of Fe-based pre-catalysts toward NH_3 decomposition is relatively low. Great efforts have been made to enhance the catalytic performances of Fe-based catalysts by depositing Fe onto supports such as carbon nanotubes, zeolites, and metal oxides, since their properties such as reducibility, particle size and dispersion, thermal stability and electronic structures would be improved after Fe particles are supported.[301–303,305] For example, Duan *et al.* synthesized a novel Fe-CNF/mica pre-catalyst *via* a catalytic CVD method and it showed excellent catalytic activity for NH_3 decomposition.[305] They also found that the size and shape of Fe particles on the top of CNFs depended on the Fe particle reconstruction and CNF morphology. In addition, the pre-catalyst of Fe–CNFs/mica showed a higher catalytic activity and stability than the Fe/CNF pre-catalyst, which could be attributed to the Fe particles isolated by mica and CNFs and the higher degree of graphitization of CNFs. Recently, a series of Fe-based catalysts supported on two-dimensional mica nanosheets (Fe/MS) were synthesized by Yuan and coworkers *via* three different methods namely homogeneous precipitation (HP), impregnation (IM), and deposition precipitation (DP) methods.[306] The catalytic results show that the Fe/MS prepared by the HP method showed the highest catalytic performance among all the synthesized pre-catalysts with different methods. The excel-

lent catalytic performance of the Fe/MS-HP pre-catalyst is attributed to the highly dispersed Fe species, layered structure of mica, and strong metal–support interactions between Fe and mica.

High temperatures easily lead to Fe sintering, but that can be prevented by confining Fe in porous materials or forming a core–shell structure.[307–309] Highly dispersed γ-Fe_2O_3 NPs (~6 nm) confined within the porous systems of CMK-5 carbons and a carbon-SBA-15 composite were synthesized by Lu and coworker *via* a facile wet impregnation method.[307] The obtained γ-Fe_2O_3/CMK-5 pre-catalyst showed the high catalytic activity toward the decomposition of NH_3 at 600 °C. The Fe_2O_3/carbon-SBA-15 pre-catalysts were much more stable over a long reaction time. The excellent catalytic performance is attributed to the space limitation in the pores and the strong interaction with the composite support, thus preventing the migration and subsequent sintering of nanoparticles. The group of Ji and Au has embedded Fe NPs in microporous and mesoporous silica shells *via* a sonication-assisted Stöber process.[308] The core–shell structure of Fe NPs showed higher catalytic activity and more stability than that of naked Fe NPs owing to the stable silica shells that effectively prevent aggregation of Fe NPs. Recently, Varisli *et al.* synthesized a robust Fe@mesoporous carbon pre-catalyst by a traditional impregnation procedure, which was very active for microwave-assisted NH_3 decomposition.[309]

Ni-Based catalysts have also been used as alternative catalysts for NH_3 decomposition due to their substantially lower costs compared to Ru and the higher activity compared to Fe.[310–314] Previously, Ganley *et al.* reported an order of activity as Ru > Ni > Rh > Co > Ir > Fe for NH_3 decomposition.[310] Zhang *et al.* reported a co-precipitation method to prepare a series of supported pre-catalysts by depositing Ni NPs on Al_2O_3.[311] The catalytic activity of Ni/Al_2O_3 increased with increasing Ni loading and reached a maximum at a Ni/Al ratio of 1.2. Interestingly, the conversion of NH_3 was further increased after the addition of a La promoter into the Ni/Al_2O_3 pre-catalyst. For example, when the La/Ni molar ratio increased from 0 to 0.2, the conversion of NH_3 progressively increased from 38.2 to 63.9% at 773 K. The characterization results indicated that the Ni/La–Al_2O_3 pre-catalyst with an appropriate amount of La possessed a more open mesoporous structure and higher dispersion of Ni as compared to Ni/Al_2O_3. Later on, Xu and coworker reported that the addition of CeO_2 obviously improved the catalytic activity and stability of Ni/Al_2O_3 for NH_3 decomposition to CO_x-free H_2.[315] The characterization results showed that the addition of CeO_2 could enlarge the pre-catalyst pores, moderate the interaction between the metal and support, suppress Ni NPs from sintering, and improve the recombinative desorption of N adatoms from the Ni NP surface. After that, the group of Liu has also proved that adding an appropriate amount of Ce and La to Ni/SBA-15 can improve the NH_3 decomposition activity, and the highest activity could be achieved when the Ce(La)/Ni ratio was around 0.3.[316] Rare-earth oxides can not only act as an additive but can also be employed as an efficient support for the synthesis of high performance Ni-based catalysts. Okura and coworkers investigated the catalytic performances over Ni supported on various rare-earth oxides (Y_2O_3, CeO_2, La_2O_3, Sm_2O_3 and Gd_2O_3) for NH_3 decomposition.[317] Among the samples investigated, the Ni/Y_2O_3 pre-catalyst showed the highest catalytic activity. The kinetics studies revealed that most of the rare-earth oxides could effectively alleviate the inhibition of hydrogen in the decomposition reaction. In addition, the desorption behavior of hydrogen showed that the amount of hydrogen atoms adsorbed on the Ni NP surface of Ni/Y_2O_3 was relatively small at high temperatures. Furthermore, this group also found that the catalytic activity of Ni/Y_2O_3 can be remarkably improved by modifying with a small amount of Sr or Ba species, while the addition of Mg and Ca species was not effective.[318] Recently, ceria catalytic structures with a woodpile geometry of micro-channels have been prepared by 3D printing and used as a support to disperse Ni NPs.[319] The obtained 3D-printed Ni/CeO_2 pre-catalyst showed higher catalytic performance than the Ni/CeO_2 powder pre-catalyst and the conventional cordierite honeycomb wash coated with Ni/CeO_2 under the same reaction conditions.

Compared with Fe-based and Ni-based catalysts, Co-based catalysts are less studied in NH_3 decomposition reactions.[320,321] The roles of supports such as carbon materials and mesoporous silica and various promoters were also investigated on Co as well. Zhang *et al.* reported that fresh commercial carbon nanotubes (CNTs) containing residual Co or Fe NPs are highly active for NH_3 decomposition, and the microstructure of the CNTs remained unchanged after the decomposition reaction.[320] After that, Co supported on CNTs was synthesized and studied.[321] The conversion of NH_3 over Co/CNTs was 60.8%, which was higher as compared to 14.8% for Fe/CNTs and 25.4% for Ni/CNTs at 500 °C. Moreover, the effect of metal–support interactions between Co and CNTs was investigated by varying the pretreatment temperatures (230–700 °C) and gas (N_2 and H_2).[322] It is found that the catalytic activity of Co/CNT pre-catalyst treatment in N_2 was higher than that of Co/CNT in H_2, and the pretreatment of Co/CNTs at 600 °C showed the highest NH_3 decomposition activity and the lowest activation energy (68.6 kJ mol^{-1}). Furthermore, Li and coworkers found that the Co@C-700-N sample calcined under limited air atmosphere showed a better activity for NH_3 decomposition as compared to the calcined sample in pure N_2 flow.[323] Podila and coworkers have reported that Co supported on a Mg–La mixed oxide showed high activity for NH_3 decomposition.[324,325] Recently, Jia and coworkers synthesized a high surface area Co–SiO_2 pre-catalyst by a simple two-step procedure with activated carbon as the template for NH_3 decomposition reaction.[326] The presence of SiO_2 can effectively protect active Co species from agglomeration during the calcination and NH_3 decomposition reaction. The obtained Co–SiO_2 exerted superior activity to other reported catalysts.

4.2. Bimetallic catalysts

Bimetallic catalysts with unique structures may achieve excellent catalytic activity in comparison with their individual

monometallic components. To date, a series of bimetallic catalysts, such as Co–Mo,[327–329] Fe–Mo,[330] Fe–Co,[331–334] Fe–Ni[335–337] and Co–Ni,[338] have been prepared and employed as catalysts for NH_3 decomposition. For example, Duan *et al.* reported that the bimetallic Co–Mo/MCM-41 pre-catalyst shows a higher activity in the NH_3 decomposition reaction than a monometallic Co/MCM-41 or Mo/MCM-41 pre-catalyst under the same conditions.[327] In addition, Co–Mo/MCM-41 with a Co/Mo molar ratio of 7/3 shows the highest NH_3 conversion and exhibits good thermal stability. Later on, they studied the effects of Co–Mo precursors on the catalytic activity.[328] The results showed that the CoMo-I/γ-Al_2O_3 pre-catalyst prepared using monocomponent metal amine metallate ($Co(en)_3MoO_4$) as the active phase precursor exhibited higher activity and stability for ammonia decomposition than the CoMo-II/γ-Al_2O_3 pre-catalyst prepared using bicomponent $Co(NO_3)_2$ and $(NH_4)_6Mo_7O_{24}$ as the active phase precursors. Moreover, they found that the textural and chemical properties of the Co–Mo pre-catalyst were significantly affected by the calcination atmosphere (*i.e.*, Ar and Air).[329] The Co–Mo pre-catalyst calcined in air showed higher catalytic activity, and Co_3Mo_3N is suggested as the dominant active phase of Co–Mo. In addition, FeMo-based pre-catalysts were also investigated and they were found to be active in NH_3 decomposition reaction.[330]

Zhang *et al.* successfully encapsulated Fe–Co alloy NPs inside CNTs (FeCo-in-CNTs) on the basis of the capillary phenomenon in the channel of CNTs, which effectively prevented the metal NPs from aggregating even at high temperature.[331] Thus, the resulting FeCo-in-CNT showed remarkable thermal stability in NH_3 decomposition reaction. Recently, 2D ultrathin Co–Fe spinel oxide nanosheets confined in mesoporous silica shells ($Co_xFe_{3-x}O_4$@$mSiO_2$) have been fabricated by Zhang and coworkers.[334] By tuning the chemical stoichiometry of $Co_xFe_{3-x}O_4$ nanosheets, the strength of the M–N bond can reasonably adjust and subsequently greatly optimize the catalytic performance. The optimized $Co_{0.89}Fe_{2.11}O_4$@$mSiO_2$ pre-catalyst attained 88% conversion of NH_3 at 600 °C and a space velocity of 60 000 $cm^3\ g^{-1}\ h^{-1}$, even maintained for 48 h without attenuation. Similarly, Ni–Fe/Al_2O_3,[335,336] Ni–Fe alloys[337] and NiCo/$Ce_{0.6}Zr_{0.3}Y_{0.1}O_2$ solid solutions[338] were found to show higher catalytic performance than the single metal pre-catalyst toward the decomposition of NH_3.

4.3. Metal carbides/nitrides

Transition metal carbides (WC_x, MoC_x FeC_x, VC_x and TaC_x) and nitrides (MoN_x, VN_x and WN_x) have also been investigated for NH_3 decomposition reaction.[339–344] Sourabh and coworkers reported that WC can attain complete decomposition of NH_3 at 550 °C; however, the WC samples need to be pretreated in a gas mixture (H_2/CO) before the decomposition reaction.[339] Subsequently, Shi and coworkers synthesized a mesoporous WC pre-catalyst *via* an impregnation–compaction route, which showed high and stable catalytic activity, and complete NH_3 decomposition was achieved at a low temperature (500 °C).[340] Kraupner and coworkers reported mesoporous Fe_3C with high crystallinity and high surface area by a combination of a hard-templating approach and carbothermal reduction.[341] The obtained Fe_3C pre-catalyst showed good catalytic activity in NH_3 decomposition with conversion above 95% at 700 °C. Choi *et al.* investigated VC and TaC as pre-catalysts for NH_3 decomposition, which showed excellent catalytic performance, higher than that of a Pt/C pre-catalyst.[342,343] Zheng *et al.* synthesized high-surface area Mo_2C from a h-MoO_3 precursor *via* a temperature-programmed reduction–carburization under a flowing atmosphere of H_2 and CH_4.[344] The result showed that Mo_2C undergoes a phase transformation during the NH_3 decomposition reaction, and the active phase is actually MoN.

Mo-Based nitrides for NH_3 decomposition are the most studied among the metal carbides and nitrides due to their low cost and high activity. Li *et al.* reported that MoN_x/α-Al_2O_3 and $NiMoN_y$/α-Al_2O_3 exhibited excellent catalytic properties for NH_3 decomposition with conversions reaching as high as 98.7% and 99.8%, respectively, at 650 °C.[345] Moreover, the increasing nitride phase content of Ni_2Mo_3N up to 37 wt% doubles the NH_3 conversion at 550 °C.[346] Podila *et al.* found that the addition of Co into γ-Mo_2N can further improve the conversion of NH_3 decomposition, which is due to the formation of the Co_3Mo_3N phase in Co-containing samples.[347] After that, Srifa *et al.* synthesized pure phase Co_3Mo_3N from $CoMoO_4$ *via* a temperature-programmed reaction method, which showed almost 100% of NH_3 conversion at 600 °C.[289] The catalytic activity of the Co_3Mo_3N pre-catalyst for NH_3 decomposition can be significantly improved by the addition of a small amount of Cs species.[348] Furthermore, Mo-based nitrides such as Mo_2N, Ni_2Mo_3N, Ni_3Mo_3N and Fe_3Mo_3N also have been suggested as the highly active species for the NH_3 decomposition reaction.[348–350]

5. Hydrous hydrazine

Anhydrous hydrazine (N_2H_4), a colorless flammable liquid at room temperature, has a high hydrogen capacity as high as 12.5 wt%. Hydrogen stored in N_2H_4 can be catalytically decomposed over supported metals, metal carbides, and metal nitrides in two pathways (eqn (5) and eqn (6)).[351–358] The reaction decomposition routes are determined by the catalysts used and the reaction conditions. However, most of the reports on hydrazine decomposition showed that ammonia is present as a product, while reports on the selective decomposition of hydrazine exclusively to hydrogen are rare, and high temperatures (>300 °C) are usually required due to the decomposition of NH_3. Even worse, the anhydrous hydrazine (>98%) is highly toxic and explosive when exposed to metal catalyst surfaces, making it difficult to use it safely.

$$N_2H_4 \rightarrow N_2 + 2H_2 \quad (5)$$

$$3N_2H_4 \rightarrow N_2 + 4NH_3 \quad (6)$$

Hydrous hydrazine, such as hydrazine monohydrate ($N_2H_4{\cdot}H_2O$) which has a hydrogen capacity of 8.0 wt%, is

believed to be relatively safe.[19,20,22,359–361] Notably, $N_2H_4{\cdot}H_2O$ is a liquid over a wide range of temperatures (213–392 K), and therefore it is easy to recharge using the current equipment for liquid fuels. Furthermore, the complete decomposition of N_2H_4 generates only a by-product of N_2 in addition to H_2, which does not need on-board collection for recycling. These merits have made $N_2H_4{\cdot}H_2O$ a promising hydrogen carrier for storage and transportation. Thereby, it is crucial to develop effective and selective catalysts for complete hydrogen generation from $N_2H_4{\cdot}H_2O$.[361–367] Xu and co-workers initially investigated various metal (Rh, Co, Ru, Ir, Cu, Ni, Fe, Pt and Pd) NPs as catalysts for N_2H_4 decomposition.[368] Among all the synthesized metal NPs, Rh showed the highest H_2 selectivity (43.8%) for hydrogen evolution from $N_2H_4{\cdot}H_2O$ decomposition. Other metal NPs, such as Co, Ru, and Ir, exhibited poor H_2 selectivity (7%), and Fe, Cu, Ni, Pd, and Pt were totally inactive under the same reaction conditions. Up to now, Ni,[369–372] Ni–Pt,[373–377] Ni–Rh,[378–383] Ni–Ir,[384,385] Ni–Pd,[386,387] Co–Pt,[388,389] Co–Ir,[390] Rh–Mo,[191] Rh–P,[391] Ni–Fe,[392–394] Ni–Cu,[224,395,396] and Ni–Co[397] have been reported to be efficient in the decomposition of $N_2H_4{\cdot}H_2O$ to H_2. Since noble metals (Pt, Rh, Ir, and Pd) are expensive, noble-metal-free catalysts (Ni, Fe, and Cu) were developed for the economic advantage, which is essential for promoting the potential applications of $N_2H_4{\cdot}H_2O$ as a hydrogen storage material. Herein, we categorize noble-metal-free catalysts into three major groups: (a) Ni-based metal NPs, (b) complex oxide supported catalysts, and (c) other supported catalysts for catalytic decomposition of $N_2H_4{\cdot}H_2O$ to H_2 under various reaction conditions (Table 4).

5.1. Metal NP catalysts

Xu and co-workers synthesized bimetallic Ni–Fe NPs by co-reduction of an aqueous solution of $NiCl_2$ and $FeSO_4$ in the presence of CTAB.[392] Although all the synthesized Ni–Fe NPs are inactive in the decomposition reaction of $N_2H_4{\cdot}H_2O$ at 298 K, a hydrogen selectivity of 81% can be achieved with $Ni_{0.5}Fe_{0.5}$ NPs with elevation of the reaction temperature at 343 K (Fig. 10). Furthermore, it was found that the hydrogen selectivity could be significantly enhanced by the addition of NaOH into the reaction mixture. The $Ni_{0.5}Fe_{0.5}$ NPs released gases in a stoichiometric amount (3.0 equiv.) with 100% H_2 selectivity from the decomposition of $N_2H_4{\cdot}H_2O$ in 190 min with NaOH (0.5 M) at 343 K. However, the addition of a weaker base such as NH_3 and CH_3COONa had no effect on the catalytic performance of the Ni–Fe NPs. The possible reason is that the highly alkaline reaction conditions make the catalyst surface highly basic, which may be unfavorable for the formation of basic NH_3, therefore hindering the decomposition of N_2H_4 to NH_3.

It has been reported that the catalytic activity and H_2 selectivity of Ni–Fe NPs could be improved by introducing a Cu core.[398] The Cu core is not selective for hydrogen evolution from the decomposition of $N_2H_4{\cdot}H_2O$, while the NiFe/Cu NPs exhibited high activity, stability, and ~100% H_2 selectivity for hydrogen evolution at 330–340 K. After that, Zhang and co-workers synthesized core–shell $Cu@Fe_5Ni_5$ NPs *via* an *in situ* seeding-growth approach and investigated their catalytic performances.[399] The core–shell $Cu@Fe_5Ni_5$ NPs have a small size of about 8.5 nm. The core–shell $Cu@Fe_5Ni_5$ pre-catalyst showed high activity and 100% H_2 selectivity within 70 min

Table 4 Catalytic activities for hydrogen evolution from $N_2H_4{\cdot}H_2O$ catalyzed by different catalysts

Catalyst	Temp. (K)	$n_{metal}/n_{N_2H_4{\cdot}H_2O}$	H_2 selectivity (%)	TOF (mol_{H_2} mol_{metal}^{-1} h^{-1})	E_a (kJ mol^{-1})	Ref.
$Ni_{0.5}Fe_{0.5}$ NPs	343	0.1	100	6.3	—	392
NiFe/Cu	343	0.2	100	35.3	44	398
$Cu@Fe_5Ni_5$	353	0.11	100	18.2	79.2	399
NiMoB–$La(OH)_3$	323	0.3	100	13.3	55.1	400
$Ni_{0.6}Fe_{0.4}Mo$	323	0.1	100	28.8	50.7	401
$Cu_{0.4}Ni_{0.6}Mo$	323	0.2	100	38.7	56.6	402
Ni–Al_2O_3-HT	303	0.4	93	2.2	49.3	403
RANEY® Ni	303	—	>99	162	44.4	369
Ni-0.080CeO_2	303	0.45	99	51.6	47	370
Ni/CeO_2	323	0.1	100	34.0	56.2	404
$Ni_{0.5}Cu_{0.5}/CeO_2$	323	0.2	100	111.7	63.0	395
$Ni_{0.5}Cu_{0.5}/CeO_2$	343	0.2	100	371.1	—	395
Ni–CeO_2@SiO_2	343	0.1	100	219.5	59.26	405
2D $Ni_{0.6}Fe_{0.4}/CeO_2$	323	0.1	99	5.76	44.06	406
NiFe/$CeZrO_2$	343	0.1	100	119.2	50.4	407
NiFe–$La(OH)_3$	343	0.2	100	100.6	57.8	408
$Ni_{1.5}Fe_{1.0}/(MgO)_{3.5}$	299	0.21	99	10.3	—	393
$Ni_{0.9}Fe_{0.1}$–Cr_2O_3	343	0.2	100	893.5	86.3	394
NiCo/NiO–CoO_x	298	0.2	99	12.8	45.15	397
Ni_3Fe-$(CeO_x)_{0.15}$/rGO	343	0.1	100	126.2	34.3	409
Ni_3Fe-$(CeO_x)_{0.15}$/rGO	328	0.1	100	56.8	—	409
Ni nanofiber	333	0.5	100	6.9	52.07	371
Ni–CNTs-OH	333	—	100	19.4	51.05	410
Ni@TNTs	333	0.125	100	96	53.2	411
$Ni_{0.5}Cu_{0.5}$/MCNS	333	0.28	100	21.8	—	224
$Ni_{10}Mo$/Ni–Mo–O	323	0.167	100	54.5	—	412
Ni_{250} NPs	343	0.5	100	11.0	56.3	366

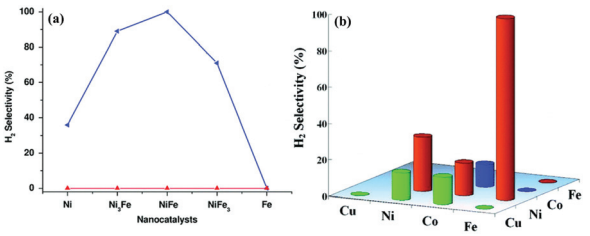

Fig. 10 (a) Comparison of hydrogen selectivity over Ni, Ni_3Fe, NiFe and Fe nanocatalysts (catalyst/N_2H_4 = 0.1) with NaOH (0.5 M) at (red) 298 K and (blue) 343 K. (b) Comparative hydrogen selectivity in the decomposition of $N_2H_4{\cdot}H_2O$ (0.5 M) to hydrogen in the presence of different nanocatalysts. Reprinted with permission from ref. 392. Copyright (2011) American Chemical Society.

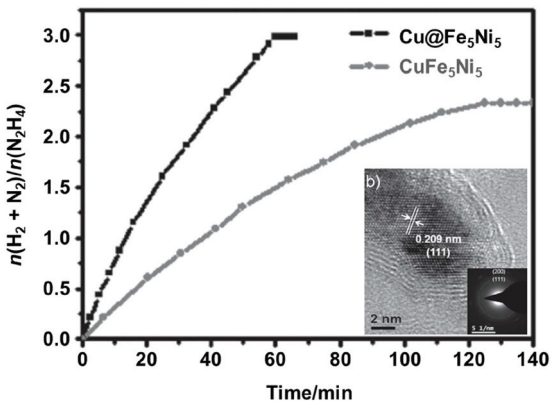

Fig. 11 Time-course plots for the decomposition of $N_2H_4H_2O$ toward H_2 over $Cu@Fe_5Ni_5$ and $CuFe_5Ni_5$NCs in the presence of NaOH at 70 °C. The inset shows an HR-TEM image of the as-synthesized $Cu@Fe_5Ni_5$ NCs. Reprinted with permission from ref. 399. Copyright (2014) Wiley-VCH.

toward the complete decomposition of $N_2H_4{\cdot}H_2O$ in the presence of NaOH at 343 K (Fig. 11). In contrast, for the $CuFe_5Ni_5$ alloy NPs, only 2.3 equivalents of gas (H_2 selectivity = 74%) were generated even after 125 min under the same reaction conditions.

Wang and coworkers found that the NiB NP pre-catalyst showed poor catalytic activity for $N_2H_4{\cdot}H_2O$ decomposition.[400] But upon incorporation of Mo and La elements into NiB NPs, the catalytic properties of the NiMoB–$La(OH)_3$ pre-catalyst was obviously enhanced for both catalytic activity (13.3 h^{-1}) and H_2 selectivity. Later on, noble-metal-free NiFeMo NPs have been synthesized *via* a simple one-step synthetic route at room temperature.[401] The optimized $Ni_{0.6}Fe_{0.4}Mo$ NPs lead to the complete decomposition of $N_2H_4{\cdot}H_2O$ and superior catalytic activity (28.8 h^{-1}) within 15 min at 323 K. Mo acted as an electron donor for Ni and Fe atoms, and it has the potential to endow itself with high catalytic activity for hydrogen generation from the decomposition of $N_2H_4{\cdot}H_2O$. Recently, our group reported the synthesis of a CuNiMo pre-catalyst, which also showed excellent catalytic activity toward $N_2H_4{\cdot}H_2O$ decomposition for hydrogen production.[402]

5.2. Complex oxide supported catalysts

Using a Ni–Al hydrotalcite-like compound (Ni–Al-HT) as the precursor, He *et al.* obtained a highly dispersed Ni–Al_2O_3-HT pre-catalyst after reduction of Ni–Al-HT under a H_2 atmosphere at 773 K.[403] The obtained Ni–Al_2O_3-HT pre-catalyst showed a high catalytic activity and 93% H_2 selectivity towards H_2 for $N_2H_4{\cdot}H_2O$ decomposition within 70 min at 303 K. In contrast, the impregnated counterpart Ni/Al_2O_3–IMP pre-catalyst exhibited a much lower H_2 selectivity (67%) and catalytic activity with a total reaction time of 440 min. The high catalytic performance of Ni–Al_2O_3-HT could be attributed to a much stronger interaction of the Ni component with Al_2O_3 and the strongly basic sites. This is the first report that supported a base metal pre-catalyst showing such high H_2 selectivity towards the decomposition of N_2H_4 aqueous solution. They also found that RANEY® Ni was active and exhibited >99% selectivity towards H_2 for the decomposition of $N_2H_4{\cdot}H_2O$ in the presence of NaOH at 303 K.[369] Compared with RANEY® Ni-40, RANEY® Ni-300 showed higher catalytic and H_2 selectivity in this decomposition reaction, which was probably due to a relatively low content of remaining aluminum. In addition, RANEY® Ni-300 could be easily collected and reused after the catalytic reaction, as RANEY® Ni has excellent magnetic properties. This convenient route provides great potential for industrial applications.

He *et al.* developed a facile coprecipitation approach to synthesize CeO_2-modified Ni RANEY® Ni-300. The obtained Ni–$0.08CeO_2$ pre-catalyst (Fig. 12) showed a 99% H_2 selectivity and a 3-fold higher TOF value than bare Ni NPs and the impregnated counterpart Ni/CeO_2–IMP for $N_2H_4{\cdot}H_2O$ decomposition reaction.[370] This improvement was caused by the modification of Ni with CeO_2 nearby through strong metal–support interactions (*e.g.*, Ni–O–Ce structure). Although the Ni–O–Ce structure itself is inactive for $N_2H_4{\cdot}H_2O$ decomposition, it could alter the chemical properties of surface Ni and make it both active and selective for $N_2H_4{\cdot}H_2O$. Furthermore, this promoting effect could be extended to other oxides which can also form strong metal–support interactions with Ni, such as ZrO_2, MgO, and La_2O_3. Later on, a series of Ni/CeO_2 were prepared by solution combustion synthesis (SCS) in a one-step process and used as efficient catalysts for decomposition of $N_2H_4{\cdot}H_2O$.[404] It was found that the catalytic activity and H_2

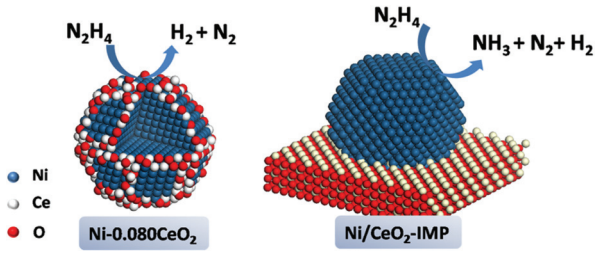

Fig. 12 Structure model of Ni-$0.080CeO_2$ and Ni/CeO_2–IMPcatalysts and the scheme of $N_2H_4{\cdot}H_2O$ decomposition. Reprinted with permission from ref. 370. Copyright (2015) American Chemical Society.

selectivity for hydrogen evolution from $N_2H_4{\cdot}H_2O$ significantly depended on the SCS synthesis parameters (ratio of precursor oxidizers, fuel-to-oxidizer ratio and fuel type). The tailored 6 wt% Ni/CeO_2 pre-catalyst prepared with a fuel-to-oxidizer ratio of 2 and N_2H_4 fuel showed the highest catalytic and 100% hydrogen selectivity, for which the decomposition reaction took 17.7 min for 50% conversion of $N_2H_4{\cdot}H_2O$ in the presence of NaOH, corresponding to a TOF value of 34.0 h^{-1} at 323 K. The characterization results confirmed the interaction between Ni and CeO_2, namely the existence of Ni–O–Ce solid solution. In addition, the oxygen vacancy in the Ni–O–Ce solid solution of the Ni/CeO_2 pre-catalyst modifies the electronic ability of Ni as an electron donor and alters the interaction between Ni and N_2H_4, which promotes N–H bond dissociation rather than N–N bond dissociation and makes the H_2 generation easier. Inspired by this effective method, they also found that the addition of Cu to Ni/CeO_2 exhibited a synergistic effect to enhance the catalytic activity for the reaction.[395]

The above results showed that the catalytic properties of Ni-based catalysts can be significantly enhanced by introducing a certain amount of CeO_2. To further maximize the active interface and the stability of catalysts, our group designed and synthesized ultrafine Ni NPs self-assembled on CeO_2 nanowires embedded in a microporous silica shell ($Ni–CeO_2@SiO_2$) *via* a one-pot facile strategy (Fig. 13).[405] The resulting wormlike core–shell-structured $Ni–CeO_2@SiO_2$ pre-catalyst showed high performance and robust durability with 100% hydrogen selectivity for H_2 production from N_2H_4 aqueous solution. The excellent catalytic properties of $Ni–CeO_2@SiO_2$ can be attributed to the synergistic electronic effect and strong interactions between Ni NPs and CeO_2 NWs with plenty of oxygen vacancies, as well as the unique structure effect.

Wen and co-workers synthesized a two-dimensional $NiFe/CeO_2$ pre-catalyst *via* a dynamics controlling coprecipitation reduction (DCCR) process followed by calcination.[406] Small NiFe NPs (~5 nm) were uniformly anchored on the surface of CeO_2 nanosheets. The optimal $Ni_{0.6}Fe_{0.4}/CeO_2$ pre-catalyst displayed over 99% selectivity towards H_2 evolution from $N_2H_4{\cdot}H_2O$ without using an alkali additive at 323 K. Besides

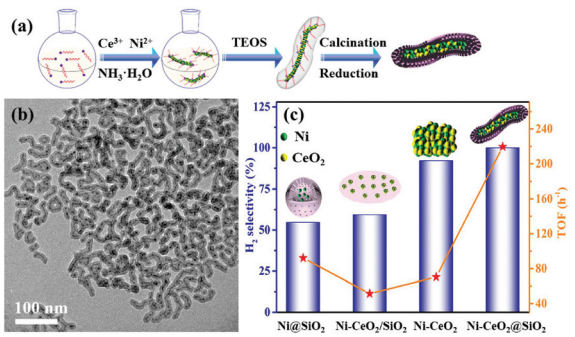

Fig. 13 (a) Synthetic scheme for the preparation of $Ni–CeO_2@SiO_2$. (b) The TEM image of the $Ni–CeO_2@SiO_2$ catalyst. (c) The hydrogen selectivity and TOF value over different catalysts (nNi/nHH = 0.1) for gas generation from $N_2H_4{\cdot}H_2O$ (200 mM, 5 mL) at 343 K. Reprinted with permission from ref. 405. Copyright (2020) American Chemical Society.

CeO_2, recently we adopted nano $CeZrO_2$ solid solution as a support to disperse NiFe NPs well, leading to the complete decomposition of N_2H_4 to H_2.[407] Later, we prepared a NiFe–$La(OH)_3$ pre-catalyst for N_2H_4 dehydrogenation, in which metal NPs were highly dispersed with smaller particle size and low crystallinity.[408] Importantly, 100% hydrogen selectivity from N_2H_4 aqueous solution was achieved in 6.5 min, providing a rather high TOF value of 100.6 h^{-1} at 343 K, which is about 35-fold higher than that of pure NiFe NPs (2.8 h^{-1}).

Using the DCCR method, Wen and co-workers synthesized $NiCo/NiO–CoO_x$ ultrathin layered nanocomposites with NiCo NPs (~4 nm) uniformly anchored on the $NiO–CoO_x$ ultrathin layered nanosheets.[397] The obtained $Ni_{70}Co_{30}/NiO–CoO_x$ pre-catalyst exhibited optimal catalytic performance and 99% hydrogen selectivity for H_2 evolution from the decomposition of $N_2H_4{\cdot}H_2O$ without the assistance of NaOH at 298 K. Wu *et al.* fabricated a bifunctional NiFe/MgO pre-catalyst containing both the NiFe-alloy active center and a solid base *via* a calcination–reduction of a NiFeMg-layered double hydroxide (LDH) precursor.[393] Moreover, the basicity of $Ni_{1.5}Fe_{1.0}/(MgO)_z$ can be easily tuned by changing the amount of the Mg precursor. The optimized $Ni_{1.5}Fe_{1.0}/(MgO)_{3.5}$ pre-catalyst showed a high catalytic performance with 100% conversion and 99% H_2 selectivity for $N_2H_4{\cdot}H_2O$ decomposition at 299 K. Notably, there was no obvious correlation between the catalytic performance and surface area, which further confirms that the basicity of the MgO support has a more pronounced effect on the catalytic behavior. Recently, our group reported the synthesis of a NiFe–Cr_2O_3 pre-catalyst, which displayed an extraordinary catalytic activity (893.5 h^{-1}) for the complete decomposition of $N_2H_4{\cdot}H_2O$ at 343 K.[394]

5.3. Other supported metal catalysts

Various support materials, such as graphene, carbon nanotubes, titanate nanotubes, mesoporous carbons, and so on, have also been used to fabricate well-dispersed noble-metal NPs with controllable size and morphology. Luo and co-workers reported the synthesis of CeO_x-modified NiFe nanodendrites supported on reduced graphene oxide ($NiFe–CeO_x$/rGO).[409] The optimal Ni_3Fe-$(CeO_x)_{0.15}$/rGO exhibited superior catalytic activity toward H_2 evolution from $N_2H_4{\cdot}H_2O$ under alkaline conditions with a TOF value of 126.2 h^{-1} at 343 K. Zhao and coworkers prepared Ni nanofibers *via* an electrospinning and vacuum thermal reduction method.[371] The catalytic performance of the prepared Ni nanofibers significantly depended on the morphologies and Ni grain sizes. The Ni nanofibers with PVP : EC mass ratios of 7 : 3, and having a high specific surface area and small crystal size, showed nearly 100% hydrogen selectivity to H_2 generation and a TOF of 6.9 h^{-1} in NaOH solution at 333 K. Recently, they have grown carbon nanotubes (CNTs) on Ni nanofibers (Ni–CNTs) and then subjected them to a hydroxylation treatment (Ni–CNTs–OH).[410] They found that the introduced CNTs and the hydroxyl groups on the CNTs significantly improved the catalytic performance of the active Ni nanofibers. The Ni–CNTs–OH showed excellent catalytic performance with a TOF of 19.4 h^{-1}

toward the $N_2H_4{\cdot}H_2O$ decomposition reaction in the presence of NaOH at 333 K.

Wang and co-workers successfully confined Ni NPs inside a titanate nanotube (Ni@TNT) channel by using the capillary force under ultrasonic treatment.[411] The obtained Ni@TNT pre-catalyst exhibited high activity and 100% hydrogen selectivity, completing the $N_2H_4{\cdot}H_2O$ decomposition in only 5 min in the presence of NaOH at 333 K, which is higher than that of Ni/TNTs. In addition, owing to the good stability of the Ni@TNT pre-catalyst, no significant decrease in catalytic performance was observed, while the Ni/TNTs showed an obvious decrease during the reuse (Fig. 14). The excellent catalytic performance of the Ni@TNT pre-catalyst is attributed to the small size and high dispersion of Ni NPs after encapsulation in the channel of TNTs. The Kleitz group prepared highly dispersed CuNi alloy NPs supported on mesoporous carbons (CuNi/MCNS) by a simple incipient wetness method.[224] Interestingly, all the bimetallic CuNi/MCNS pre-catalysts showed 100% selectivity to H_2 from the $N_2H_4{\cdot}H_2O$ decomposition and the reaction was complete within 50 min over $Cu_{0.5}Ni_{0.5}$/MCNS in the presence of NaOH at 333 K.

Recently, Wang and coworkers reported the synthesis of $Ni_{10}Mo$ NPs on a Ni–W–O matrix ($Ni_{10}Mo$ NPs/Ni–W–O) through a simple hydrothermal method followed by annealing treatment under a H_2 atmosphere.[412] The obtained nanocomposite enabled the complete decomposition of $N_2H_4{\cdot}H_2O$ in 7 min at 323 K, providing a TOF value of 54.5 h^{-1}. They also synthesized a monolithic $Ni_{10}Mo$/Ni–Mo–O/Ni foam pre-catalyst and showed a high hydrogen generation rate with 98% H_2 selectivity and rapid dynamic response after 5 start/stop cycles.[412] Using a similar method, they also synthesized a series of Ni–W–O-derived nanocomposites.[413] It was found that the catalytic properties of the resulting pre-catalyst depended significantly upon the annealing temperature. On the basis of a combination of experimental and DFT theoretical calculations, the observed changes in catalytic properties are related to the changes in the phase structure and microstructural features with temperature during the reductive annealing process. Specifically, the as-synthesized Ni_4W/WO_2/$NiWO_4$ exhibited remarkably distinct catalytic performance, nearly 100% selectivity, and high stability in catalyzing $N_2H_4{\cdot}H_2O$ decomposition for hydrogen production.

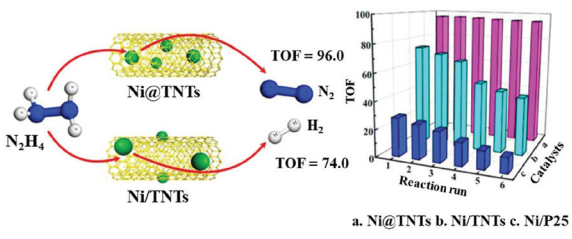

Fig. 14 (Left) Schematic illustration of the formation processes of Ni@TNTs and Ni/TNTs and $N_2H_4{\cdot}H_2O$ decomposition. (Right) The tests of re-usability of (a) Ni@TNTs, (b) Ni/TNTs and (c) Ni/P25 for hydrogen generation from $N_2H_4{\cdot}H_2O$. Reprinted with permission from ref. 411. Copyright (2018) Elsevier.

Furthermore, they also reported a first-principles study of the elementary steps of N_2H_4 decomposition over a Ni pre-catalyst.[372] The calculation results indicated that the decomposition behaviors of N_2H_4 strongly depend on the surface coverage. At a lower coverage, the cleavage of the N–N bond is dominant, resulting in the formation of NH_3. In contrast, at a higher coverage, the cleavage of the N–H bond is in competition with that of the N–N bond, and N_2 and H_2 are finally released.

Overall, Ni and Ni-based noble-metal-free catalysts can efficiently catalyze the complete decomposition of $N_2H_4{\cdot}H_2O$ to produce hydrogen, but the catalytic activity is still not satisfactory at room temperature or without additives (*e.g.* NaOH). Therefore, for the practical use of $N_2H_4{\cdot}H_2O$ as a safe and effective hydrogen storage material, it is necessary to further develop more effective noble-metal-free catalysts for complete conversion of $N_2H_4{\cdot}H_2O$ to H_2 at low temperature without additives.

6. Hydrazine borane

Hydrazine borane ($N_2H_4BH_3$, HB, 15.4 wt%), a derivative of NH_3BH_3 where an N_2H_4 group substituted the NH_3 group, has been regarded as a competitive candidate for chemical hydrogen storage.[22,150,151,414–420] $N_2H_4BH_3$ can be easily synthesized by the reaction of $(N_2H_5)_2SO_4$ with $NaBH_4$ in dioxane at room temperature.[421] The hydrogen in $N_2H_4BH_3$ can be released through either thermolysis or solvolysis.[421–428] The thermal decomposition of $N_2H_4BH_3$ was firstly reported by Goubeau and Ricker.[421] $N_2H_4BH_3$ begins to decompose slowly at around 60 °C. It was found that $N_2H_4BH_3$ released 6.5 wt% H_2 within 16 h at 140 °C, while more than 11 wt% H_2 can be released from $N_2H_4BH_3$ in the presence of LiH at 150 °C in less than an hour.[422]

Like for NH_3BH_3, the BH_3 group in $N_2H_4BH_3$ is readily hydrolyzed in the presence of a suitable catalyst (eqn (7)) at room temperature.[427–432] The hydrolysis of $N_2H_4BH_3$ over noble-metal-free catalysts was firstly reported by Özkar and coworkers.[430] They found that highly dispersed Ni(0) and Co(0) NPs stabilized by poly(4-styrenesulfonic acid-*co*-maleic acid (PSSMA-Ni and PSSMA-Co) could be facilely prepared by *in situ* reduction of $NiCl_2$ and $CoCl_2$ during the hydrolytic dehydrogenation of $N_2H_4BH_3$.[430,431] The *in situ* formed PSSMA-Ni and PSSMA-Co NPs were highly active in the hydrolysis of $N_2H_4BH_3$ with the release of nearly 3 equiv. H_2 per $N_2H_4BH_3$. Moreover, the obtained PSSMA-Co (TOF = 370 h^{-1}) showed much higher catalytic performance than PSSMA-Ni (TOF = 183 h^{-1}) for this hydrolysis reaction at 298 K.[430,431] The Cu@SiO_2 core–shell pre-catalyst developed by our research group also showed excellent catalytic activity (TOF = 454.8 h^{-1}) in the hydrolytic dehydrogenation of $N_2H_4BH_3$.[204] Due to the protection of the porous silica shell, the stability of the pre-catalyst is effectively improved, because of which the Cu@SiO_2 nanospheres preserved 85% of their initial catalytic activity even in the tenth run. Recently, we found that transition metal (Cr, Mo, and W)

modified Ni NPs showed high activity toward hydrogen generation from the hydrolysis of $N_2H_4BH_3$ at 298 K.[187]

$$N_2H_4BH_3 + 2H_2O \rightarrow N_2H_5BO_2 + 3H_2 \quad (7)$$

By the hydrolysis of the BH_3 group of $N_2H_4BH_3$, the liberation of H_2 with good kinetics can be achieved with the catalysts reported above. However, the effective GHSC of the $N_2H_4BH_3{\cdot}3H_2O$ system (6.0 wt%) is not high because H in N_2H_4 is not released. Similar to hydrolysis, 1 mol $N_2H_4BH_3$ can also produce 3 mol of H_2 by methanolysis in a suitable catalyst (eqn (8)).[267,366,425] *In situ* formed bulk Ni and PVP-stabilized Ni NPs were developed by Özkar and co-worker for hydrogen evolution from the methanolysis of $N_2H_4BH_3$.[267,425] Since the weight of methanol is much higher than that of water, the GHSC of an $N_2H_4BH_3{\cdot}4MeOH$ (3.5 wt%) system is much lower than that of an $N_2H_4BH_3{\cdot}2H_2O$ (7.4 wt%) system. However, the methanolysis reaction of $N_2H_4BH_3$ can be initiated even below 0 °C, thereby satisfying the cold start requirements of vehicular and portable applications in cold weather.

$$N_2H_4BH_3 + 4MeOH \rightarrow N_2H_5B(OMe)_4 + 3H_2 \quad (8)$$

Unlike the NH_3 moiety of NH_3BH_3, the N_2H_4 moiety in $N_2H_4BH_3$ can also be dehydrogenated to H_2 and N_2 over a selective catalyst (eqn (5)).[433–442] Theoretically, 1 mol $N_2H_4BH_3$ can be completely dehydrogenated into 5 mol H_2 and 1 mol N_2 (eqn (9)). This corresponds to an effective GHSC of 10.0 wt% for the $N_2H_4BH_3{\cdot}3H_2O$ system, which is much higher than those of $NaBH_4{\cdot}4H_2O$ (7.3 wt%), $NH_3BH_3{\cdot}2H_2O$ (8.9 wt%) and $N_2H_4{\cdot}H_2O$ (8.0 wt%).[22,416] However, the dehydrogenation reaction is in competition with NH_3 release (eqn (10)). In 2014, Demirci and co-worker synthesized a series of Ni-based bimetallic pre-catalysts for the hydrolysis of the BH_3 group and then decomposition of the N_2H_4 group.[443] The optimized $Ni_{0.7}Fe_{0.3}$ NPs can release 3.9 equiv. (H_2 + N_2) per $N_2H_4BH_3$ (21% H_2 selectivity) in 180 min at 323 K, indicating an activity in the decomposition of the N_2H_4 moiety NH_3BH_3. However, the conversion of $N_2H_4BH_3$ is incomplete and the reaction kinetics is slow. Therefore, great efforts were devoted to synthesize a highly selective catalyst that could achieve complete dehydrogenation of NH_3BH_3 to H_2.

$$N_2H_4BH_3 + 3H_2O \rightarrow B(OH)_3 + 5H_2 + N_2 \quad (9)$$

$$N_2H_4BH_3 + 3H_2O \rightarrow B(OH)_3 + (3 + 2\alpha)H_2 + (2\alpha + 1)/3N_2 + 4(1 - \alpha)/3NH_3 \quad (10)$$

In 2018, our group reported highly active and selective noble-metal-free CuNiMo NPs by using a facile chemical reduction approach.[402] Among all the synthesized pre-catalysts, the optimized $Cu_{0.4}Ni_{0.6}Mo$ exhibited the highest catalytic activity and 100% H_2 selectivity toward hydrogen generation from $N_2H_4BH_3$ in an alkaline solution, with which 6 equiv. (H_2 + N_2) per $N_2H_4BH_3$ (Fig. 15) can be released within 13.9 min. To the best of our knowledge, this is the first report that a noble-metal-free pre-catalyst can achieve a complete conversion of $N_2H_4BH_3$ to H_2 (Table 5). Later on, Yan and co-workers reported the synthesis of a boron nitride (BN) supported Ni-MoO_x (Ni-MoO_x/BN) pre-catalyst without the help of a surfactant by a sequential impregnation reduction approach.[444] The resultant Ni-MoO_x/BN showed excellent catalytic performance with 100% H_2 selectivity for hydrogen generation from $N_2H_4BH_3$ alkaline conditions at 323 K, giving a TOF value of 600.0 h^{-1}. They also developed a facile and universal methodology for the synthesis of amorphous/poorly crystallized noble-metal-free NiFe–CeO_x NPs supported on a MOF substrate, and the obtained NiFe–CeO_x/MOF pre-catalyst can also show 100% H_2 selectivity and record good catalytic performance for $N_2H_4BH_3$ decomposition at 343 K.[445]

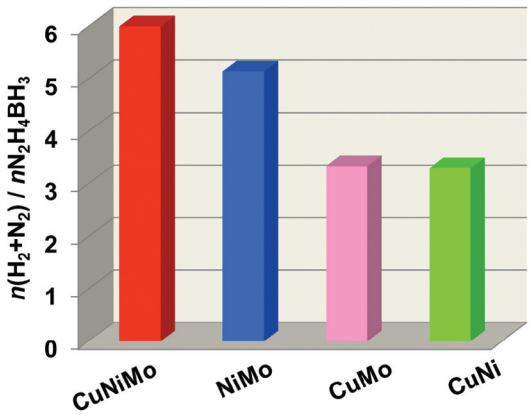

Fig. 15 $n(H_2 + N_2)/n(N_2H_4BH_3)$ for dehydrogenation of $N_2H_4BH_3$ catalyzed by CuNiMo, NiMo, CuMo, and CuNi nanocatalysts in the presence of NaOH (2.0 M) at 323 K. Reprinted with permission from ref. 402. Copyright (2018) Royal Society of Chemistry.

Recently, our group reported a wormlike Ni–CeO_2@SiO_2 core–shell pre-catalyst with high performance (442.5 h^{-1}) and 100% hydrogen selectivity for hydrogen evolution from $N_2H_4BH_3$ aqueous solution at 343 K.[405] In addition, we proposed a plausible mechanism for metal catalyzed dehydrogenation of $N_2H_4BH_3$, which involves the chemisorption of $N_2H_4BH_3$ molecules on the metal active surface and generates the activated intermediate species.[405] Subsequently, the activated intermediate species is attacked by H_2O molecules, leading to the dissociation of the B–N bond in $N_2H_4BH_3$. Then, the BH_3 moiety of $N_2H_4BH_3$ is catalytically hydrolyzed by metal active sites; meanwhile, the resulting N_2H_4 group is decomposed to produce H_2 and N_2.

Despite much progress having been made in recent years, the noble-metal-free catalysts reported above for complete hydrogen evolution from NH_3BH_3 required a relatively high reaction temperature (≥323 K). Therefore, the development of non-noble-metal catalysts for the complete dehydrogenation of $N_2H_4BH_3$ at room temperature is highly desired. We found that the RANEY® Ni pre-catalyst exhibited an outstanding catalytic performance with 6.0 equiv. (H_2 + N_2) per $N_2H_4BH_3$ being released at 298 K, which is the first report of a noble-metal-free pre-catalyst achieving a complete dehydrogenation of $N_2H_4BH_3$ at room temperature (Table 5).[446] The TOF value over RANEY®

Table 5 Catalytic activities for hydrogen evolution from $N_2H_4BH_3$ by different catalysts

Catalyst	Temp. (K)	$n_{metal}/nN_2H_4BH_3$	$n(H_2 + N_2)/nN_2H_4BH_3$	TOF (mol_{H_2} mol_{metal}^{-1} h^{-1})	Ref.
Ni/PSSMA[a]	298	0.01	3	183	430
Co/PSSMA[a]	298	0.01	3	370	431
Cu@SiO_2[a]	298	0.09	3	454.8	204
$Ni_{0.9}Mo_{0.1}$[a]	298	0.05	3	2400	187
Bulk Ni NPs[b]	298	0.006	3	1440	425
PVP-stabilized Ni[b]	298	0.005	3	2136	267
$Ni_{0.7}Fe_{0.3}$ NPs	323	0.35	3.9	3.3	443
$Cu_{0.4}Ni_{0.6}Mo$	323	0.1	6	108	402
Ni-MoO_x/BN	323	0.1	6	600	444
$Ni_{0.5}Fe_{0.5}$-CeO_x/MIL-101	343	0.2	6	351.3	445
$Ni_{0.5}Fe_{0.5}$-CeO_x/ZIF-67	343	0.2	6	361.5	445
Ni–CeO_2@SiO_2	343	0.1	6	442.5	405
NiFe–$La(OH)_3$	343	0.2	6	251.4	408
RANEY® Ni[c]	298	—	6	892	446

[a] Hydrogen release from the hydrolysis of the BH_3 group of HB only. [b] Hydrogen release from the methanolysis of the BH_3 group of HB only. [c] The TOF reported here was calculated based on the surface Ni atoms in the catalyst.

Ni for the complete dehydrogenation of $N_2H_4BH_3$ at room temperature was calculated to be 892 h^{-1} based on surface Ni atoms.

Up to now, preliminary progress has been made in noble-metal-free catalysts for complete hydrogen generation from $N_2H_4BH_3$. However, there are still only a handful of catalysts that can catalyze the complete hydrogen evolution from $N_2H_4BH_3$ (Table 5). Moreover, the kinetics of the N_2H_4 moiety decomposition is much sluggish than that of the BH_3 group hydrolysis. Therefore, the current challenges include finding a catalyst that can catalyze both BH_3 group hydrolysis and N_2H_4 moiety decomposition reactions with similar kinetics.

7. Summary

Safe and efficient storage and delivery of hydrogen are essential for the development of a hydrogen-based energy infrastructure. Boron- and nitrogen-based hydrogen storage materials reviewed above have a relatively high hydrogen content and have tremendous potential to be used as hydrogen sources for portable fuel cells. Overall, each of these materials has its own merits and drawbacks. The catalytic performances for hydrogen evolution from these systems have been greatly improved. Non-noble metal catalysts with low cost and relatively high catalytic activity can make boron- and nitrogen-based hydrides potential candidates for portable fuel cells. However, there is still a certain gap in the catalytic activity between non-noble metal catalysts and noble metal catalysts. In addition, the stability of non-noble metal catalysts is generally low, mainly because of their easy oxidation and agglomeration. Therefore, the development of high-activity and high-stability non-noble metal catalysts still requires further efforts.

Besides, the mechanism of nucleation and growth of metal NPs and the active sites of multi-component catalysts are not clear. Theoretical calculations and modern characterization technologies (*e.g.*, *in situ* X-ray absorption spectroscopy (XAS), transmission electron microscopy (TEM), Raman spectroscopy, *etc.*) could be helpful in understanding the structure–catalysis relationship, thus providing an effective method to guide the design of metal catalysts at the molecular level. Furthermore, some new methods (*e.g.* photocatalysis assisted technology) can be developed to promote the hydrogen generation rate from boron- and nitrogen-based chemical hydrides. Additionally, to maximize the use of metal atoms, highly dispersed catalysts (*e.g.* metal single-atom) can be designed and synthesized for further improving the catalytic activity of the catalyst. We are looking forward to new breakthroughs in noble-metal-free catalysts for hydrogen generation from boron- and nitrogen-based chemical hydrides and their practical applications.

Conflicts of interest

There are no conflicts to declare.

Acknowledgements

This work was financially supported by the National Natural Science Foundation of China (No. 21763012 and 21802056), the Natural Science Foundation of Jiangxi Province of China (No. 20192BAB203009), and the Sponsored Program for Cultivating Youths of Outstanding Ability in Jiangxi Normal University.

References

1 L. Schlapbach and A. Zuttel, Hydrogen-storage materials for mobile applications, *Nature*, 2001, **414**, 353–358.
2 U. Eberle, M. Felderhoff and F. Schueth, Chemical and physical solutions for hydrogen storage, *Angew. Chem., Int. Ed.*, 2009, **48**, 6608–6630.

3 J. H. Shi, F. Qiu, W. B. Yuan, M. M. Guo, C. L. Yuan and Z. H. Lu, Novel electrocatalyst of nanoporous FeP cubes prepared by fast electrodeposition coupling with acid-etching for efficient hydrogen evolution, *Electrochim. Acta*, 2020, **329**, 135185.
4 J. H. Shi, F. Qiu, W. B. Yuan, M. M. Guo and Z. H. Lu, Nitrogen-doped carbon-decorated yolk-shell CoP@FeCoP micro-polyhedra derived from MOF for efficient overall water splitting, *Chem. Eng. J.*, 2021, **403**, 126312.
5 S. I. Orimo, Y. Nakamori, J. R. Eliseo, A. Zuettel and C. M. Jensen, Complex hydrides for hydrogen storage, *Chem. Rev.*, 2007, **107**, 4111–4132.
6 H. M. Cheng, Q. H. Yang and C. Liu, Hydrogen storage in carbon nanotubes, *Carbon*, 2001, **39**, 1447–1454.
7 H. W. Langmi, D. Book, A. Walton, S. R. Johnson, M. M. Al-Mamouri, J. D. Speight, P. P. Edwards, I. R. Harris and P. A. Anderson, Hydrogen storage in ion-exchanged zeolites, *J. Alloys Compd.*, 2005, **404**, 637–642.
8 N. L. Rosi, J. Eckert, M. Eddaoudi, D. T. Vodak, J. Kim, M. O'Keeffe and O. M. Yaghi, Hydrogen storage in microporous metal-organic frameworks, *Science*, 2003, **300**, 1127–1129.
9 Y. G. Wang, N. Shah and G. P. Huffman, Simultaneous production of hydrogen and carbon nanostructures by decomposition of propane and cyclohexane over alumina supported binary catalysts, *Catal. Today*, 2005, **99**, 359–364.
10 P. Makowski, A. Thomas, P. Kuhn and F. Goettmann, Organic materials for hydrogen storage applications: from physisorption on organic solids to chemisorption in organic molecules, *Energy Environ. Sci.*, 2009, **2**, 480–490.
11 U. Eberle, M. Felderhoff and F. Schuth, Chemical and physical solutions for hydrogen storage, *Angew. Chem., Int. Ed.*, 2009, **48**, 6608–6630.
12 J. Chen, Z. H. Lu, Q. L. Yao, G. Feng and Y. Luo, Complete dehydrogenation of $N_2H_4BH_3$ with NiM-Cr_2O_3 (M = Pt, Rh, and Ir) hybrid nanoparticles, *J. Mater. Chem. A*, 2018, **6**, 20746–20752.
13 Z. Zhang, Y. Luo, S. Liu, Q. Yao, S. Qing and Z. H. Lu, A PdAg-CeO_2 nanocomposite anchored on mesoporous carbon: a highly efficient catalyst for hydrogen production from formic acid at room temperature, *J. Mater. Chem. A*, 2019, **7**, 21438–21446.
14 Y. Luo, Q. Yang, W. Nie, Q. L. Yao, Z. Zhang and Z. H. Lu, Anchoring IrPdAu nanoparticles on NH_2-SBA-15 for fast hydrogen production from formic acid at room temperature, *ACS Appl. Mater. Interfaces*, 2020, **12**, 8082–8090.
15 C. W. Hamilton, R. T. Baker, A. Staubitz and I. Manners, B-N compounds for chemical hydrogen storage, *Chem. Soc. Rev.*, 2009, **38**, 279–293.
16 H. L. Jiang, S. K. Singh, J. M. Yan, X. B. Zhang and Q. Xu, Liquid-phase chemical hydrogen storage: catalytic hydrogen generation under ambient conditions, *ChemSusChem*, 2010, **3**, 541–549.
17 T. He, H. Wu, G. Wu, J. Wang, W. Zhou, Z. Xiong, J. Chen, T. Zhang and P. Chen, Borohydride hydrazinates: high hydrogen content materials for hydrogen storage, *Energy Environ. Sci.*, 2012, **5**, 5686–5689.
18 G. Moussa, R. Moury, U. B. Demirci, T. Şener and P. Miele, Boron-based hydrides for chemical hydrogen storage, *Int. J. Energy Res.*, 2013, **37**, 825–842.
19 L. He, B. Liang, Y. Huang and T. Zhang, Design strategies of highly selective nickel catalysts for H_2 production via hydrous hydrazine decomposition: a review, *Natl. Sci. Rev.*, 2018, **5**, 356–364.
20 Y. Cheng, X. Wu and H. Xu, Catalytic decomposition of hydrous hydrazine for hydrogen production, *Sustainable Energy Fuels*, 2019, **3**, 343–365.
21 C. Lang, Y. Jia and X. Yao, Recent advances in liquid-phase chemical hydrogen storage, *Energy Storage Mater.*, 2020, **26**, 290–312.
22 M. Yadav and Q. Xu, Liquid-phase chemical hydrogen storage materials, *Energy Environ. Sci.*, 2012, **5**, 9698–9725.
23 A. K. Singh and Q. Xu, Synergistic Catalysis over Bimetallic Alloy Nanoparticles, *ChemCatChem*, 2013, **5**, 652–676.
24 T. E. Bell and L. Torrente-Murciano, H_2 production via ammonia decomposition using non-noble metal catalysts: A review, *Top. Catal.*, 2016, **59**, 1438–1457.
25 W. W. Zhan, Q. L. Zhu and Q. Xu, Dehydrogenation of ammonia aorane by metal nanoparticle catalysts, *ACS Catal.*, 2016, **6**, 6892–6905.
26 S. Mukherjee, S. V. Devaguptapu, A. Sviripa, C. R. F. Lund and G. Wu, Low-temperature ammonia decomposition catalysts for hydrogen generation, *Appl. Catal., B*, 2018, **226**, 162–181.
27 Y. Hu, Y. Wang, Z. H. Lu, X. Chen and L. Xiong, Core–shell nanospheres Pt@SiO_2 for catalytic hydrogen production, *Appl. Surf. Sci.*, 2015, **341**, 185–189.
28 Q. L. Yao, Z. H. Lu, Y. Jia, X. Chen and X. Liu, In situ facile synthesis of Rh nanoparticles supported on carbon nanotubes as highly active catalysts for H_2 generation from NH_3BH_3 hydrolysis, *Int. J. Hydrogen Energy*, 2015, **40**, 2207–2215.
29 W. Wang, Z. H. Lu, Y. Luo, A. Zou, Q. L. Yao and X. Chen, Mesoporous carbon nitride supported Pd and Pd-Ni nanoparticles as highly efficient catalyst for catalytic hydrolysis of NH_3BH_3, *ChemCatChem*, 2018, **10**, 1620–1626.
30 W. Wang, X. Hong, Q. L. Yao and Z. H. Lu, Bimetallic Ni–Pt nanoparticles immobilized on mesoporous N-doped carbon as a highly efficient catalyst for complete hydrogen evolution from hydrazine, *J. Mater. Chem. A*, 2020, **8**, 13694–13701.
31 U. B. Demirci and P. Miele, Cobalt-based catalysts for the hydrolysis of $NaBH_4$ and NH_3BH_3, *Phys. Chem. Chem. Phys.*, 2014, **16**, 6872–6885.
32 Y. J. Shih, C. C. Su, Y. H. Huang and M. C. Lu, SiO_2-supported ferromagnetic catalysts for hydrogen generation from alkaline $NaBH_4$ (sodium borohydride) solution, *Energy*, 2013, **54**, 263–270.
33 B. H. Liu and Z. P. Li, A review: Hydrogen generation from borohydride hydrolysis reaction, *J. Power Sources*, 2009, **187**, 527–534.

34 U. B. Demirci and P. Miele, Sodium borohydride versus ammonia borane, in hydrogen storage and direct fuel cell applications, *Energy Environ. Sci.*, 2009, **2**, 627–637.
35 L. Lu, H. Zhang, S. Zhang and F. Li, A family of high-efficiency hydrogen-generation catalysts based on ammonium species, *Angew. Chem., Int. Ed.*, 2015, **54**, 9328–9332.
36 J. Wang, Z. Huang, L. Lu, Q. Jia, L. Huang, S. Chang, M. Zhang, Z. Zhang, S. Li, D. He, W. Wu, S. Zhang, N. Toshima and H. Zhang, Colloidal Co single-atom catalyst: a facile synthesis strategy and high catalytic activity for hydrogen generation, *Green Chem.*, 2020, **22**, 1269–1274.
37 O. Sahin, H. Dolas and M. Ozdemir, The effect of various factors on the hydrogen generation by hydrolysis reaction of potassium borohydride, *Int. J. Hydrogen Energy*, 2007, **32**, 2330–2336.
38 D. Xu, H. Wang, Q. Guo and S. Ji, Catalytic behavior of carbon supported Ni–B, Co–B and Co–Ni–B in hydrogen generation by hydrolysis of KBH_4, *Fuel Process. Technol.*, 2011, **92**, 1606–1610.
39 X. Wang, S. Sun, Z. Huang, H. Zhang and S. Zhang, Preparation and catalytic activity of PVP-protected Au/Ni bimetallic nanoparticles for hydrogen generation from hydrolysis of basic $NaBH_4$ solution, *Int. J. Hydrogen Energy*, 2014, **39**, 905–916.
40 X. Wang, Z. Huang, L. Lu, H. Zhang, Y. Cao, Y. Gu, Z. Cheng and S. Zhang, Preparation and catalytic activities of Au/Co bimetallic nanoparticles for hydrogen generation from $NaBH_4$ solution, *J. Nanosci. Nanotechnol.*, 2015, **15**, 2770–2276.
41 L. Wang, L. Huang, C. Jiao, Z. Huang, F. Liang, S. Liu, Y. Wang and H. Zhang, Preparation of Rh/Ni bimetallic nanoparticles and their catalytic activities for hydrogen generation from hydrolysis of KBH_4, *Catalysts*, 2017, **7**, 125.
42 L. Huang, C. Jiao, L. Wang, Z. Huang, F. Liang, S. Liu, Y. Wang, H. Zhang and S. Zhang, Preparation of Rh/Ag bimetallic nanoparticles as effective catalyst for hydrogen generation from hydrolysis of KBH_4, *Nanotechnology*, 2018, **29**, 044002.
43 Y. Pei, L. Wang, L. Huang, Y. Hu, Q. Jia, H. Zhang and S. Zhang, ISOBAM-stabilized Ni^{2+} colloidal catalysts: high catalytic activities for hydrogen generation from hydrolysis of KBH_4, *Nanotechnology*, 2020, **31**, 134003.
44 J. Urgnani, F. J. Torres, M. Palumbo and M. Baricco, Hydrogen release from solid state $NaBH_4$, *Int. J. Hydrogen Energy*, 2008, **33**, 3111–3115.
45 P. Martelli, R. Caputo, A. Remhof, P. Mauron, A. Borgschulte and A. Züttel, Stability and decomposition of $NaBH_4$, *J. Phys. Chem. C*, 2010, **114**, 7173–7177.
46 P. Ngene, R. van den Berg, M. H. W. Verkuijlen, K. P. de Jong and P. E. de Jongh, Reversibility of the hydrogen desorption from $NaBH_4$ by confinement in nanoporous carbon, *Energy Environ. Sci.*, 2011, **4**, 4108–4115.
47 S. S. Muir and X. Yao, Progress in sodium borohydride as a hydrogen storage material: Development of hydrolysis catalysts and reaction systems, *Int. J. Hydrogen Energy*, 2011, **36**, 5983–5997.
48 P. Brack, S. E. Dann and K. G. U. Wijayantha, Heterogeneous and homogenous catalysts for hydrogen generation by hydrolysis of aqueous sodium borohydride ($NaBH_4$) solutions, *Energy Sci. Eng.*, 2015, **3**, 174–188.
49 K. A. Holbrook and P. J. Twist, Hydrolysis of the borohydride ion catalysed by metal-boron alloys, *J. Chem. Soc. A*, 1971, **15**, 890–894.
50 R. Peña-Alonso, A. Sicurelli, E. Callone, G. Carturan and R. Raj, A picoscale catalyst for hydrogen generation from $NaBH_4$ for fuel cells, *J. Power Sources*, 2007, **165**, 315–323.
51 G. Guella, C. Zanchetta, B. Patton and A. Miotello, New insights on the mechanism of palladium-catalyzed hydrolysis of sodium borohydride from 11B NMR measurements, *J. Phys. Chem. B*, 2006, **110**, 17024–17033.
52 G. Guella, B. Patton and A. Miotello, Kinetic features of the platinum catalyzed hydrolysis of sodium borohydride from 11B NMR measurements, *J. Phys. Chem. C*, 2007, **111**, 18744–18750.
53 P. Wang and X. D. Kang, Hydrogen-rich boron-containing materials for hydrogen storage, *Dalton Trans.*, 2008, **40**, 5400–5413.
54 H. I. Schlesinger, H. C. Brown, A. E. Finholt, J. R. Gilbreath, H. R. Hoekstra and E. K. Hyde, Sodium borohydride, its hydrolysis and its use as a reducing agent and in the generation of hydrogen, *J. Am. Chem. Soc.*, 1953, **75**, 215–219.
55 M. Zahmakiran and S. Özkar, Zeolite-confined ruthenium (0) nanoclusters catalyst: record catalytic activity, reusability, and lifetime in hydrogen generation from the hydrolysis of sodium borohydride, *Langmuir*, 2009, **25**, 2667–2678.
56 Y. V. Larichev, O. V. Netskina, O. V. Komova and V. I. Simagina, comparative XPS study of Rh/Al_2O_3 and Rh/TiO_2 as catalysts for $NaBH_4$ hydrolysis, *Int. J. Hydrogen Energy*, 2010, **35**, 6501–6507.
57 D. Xu, H. Zhang and W. Ye, Hydrogen generation from hydrolysis of alkaline sodium borohydride solution using Pt/C catalyst, *Catal. Commun.*, 2007, **8**, 1767–1771.
58 P. Krishnan, T.-H. Yang, W.-Y. Lee and C.-S. Kim, PtRu-$LiCoO_2$—an efficient catalyst for hydrogen generation from sodium borohydride solutions, *J. Power Sources*, 2005, **143**, 17–23.
59 U. B. Demirci and P. Miele, Cobalt in $NaBH_4$ hydrolysis, *Phys. Chem. Chem. Phys.*, 2010, **12**, 14651–14665.
60 N. Patel and A. Miotello, Progress in Co–B related catalyst for hydrogen production by hydrolysis of boron-hydrides: A review and the perspectives to substitute noble metals, *Int. J. Hydrogen Energy*, 2015, **40**, 1429–1464.
61 H. Sun, J. Meng, L. Jiao, F. Cheng and J. Chen, A review of transition-metal boride/phosphide-based materials for catalytic hydrogen generation from hydrolysis of boron-hydrides, *Inorg. Chem. Front.*, 2018, **5**, 760–772.
62 M. Rakap and S. Özkar, Intrazeolite cobalt(0) nanoclusters as low-cost and reusable catalyst for hydrogen generation

from the hydrolysis of sodium borohydride, *Appl. Catal., B*, 2009, **91**, 21–29.

63 J. W. Jaworski, S. Cho, Y. Kim, J. H. Jung, H. S. Jeon, B. K. Min and K. Y. Kwon, Hydroxyapatite supported cobalt catalysts for hydrogen generation, *J. Colloid Interface Sci.*, 2013, **394**, 401–408.

64 S. Bennici, H. Yu, E. Obeid and A. Auroux, Highly active heteropolyanions supported Co catalysts for fast hydrogen generation in $NaBH_4$ hydrolysis, *Int. J. Hydrogen Energy*, 2011, **36**, 7431–7442.

65 D. Xu, P. Dai, X. Liu, C. Cao and Q. Guo, Carbon-supported cobalt catalyst for hydrogen generation from alkaline sodium borohydride solution, *J. Power Sources*, 2008, **182**, 616–620.

66 J. Zhu, R. Li, W. Niu, Y. Wu and X. Gou, Facile hydrogen generation using colloidal carbon supported cobalt to catalyze hydrolysis of sodium borohydride, *J. Power Sources*, 2012, **211**, 33–39.

67 J. Zhu, R. Li, W. Niu, Y. Wu and X. Gou, Fast hydrogen generation from NaBH4 hydrolysis catalyzed by carbon aerogels supported cobalt nanoparticles, *Int. J. Hydrogen Energy*, 2013, **38**, 10864–10870.

68 X. Zhang, X. Sun, D. Xu, X. Tao, P. Dai, Q. Guo and X. Liu, Synthesis of MOF-derived Co@C composites and application for efficient hydrolysis of sodium borohydride, *Appl. Surf. Sci.*, 2019, **469**, 764–769.

69 J. Li, X. Hong, Y. Wang, Y. Luo, P. Huang, B. Li, K. Zhang, Y. Zou, L. Sun, F. Xu, F. Rosei, S. P. Verevkin and A. A. Pimerzin, Encapsulated cobalt nanoparticles as a recoverable catalyst for the hydrolysis of sodium borohydride, *Energy Storage Mater.*, 2020, **27**, 187–197.

70 C. H. Liu, B. H. Chen, C. L. Hsueh, J. R. Ku, F. Tsau and K. J. Hwang, Preparation of magnetic cobalt-based catalyst for hydrogen generation from alkaline $NaBH_4$ solution, *Appl. Catal., B*, 2009, **91**, 368–379.

71 B. Chen, S. Chen, H. A. Bandal, R. Appiah-Ntiamoah, A. R. Jadhav and H. Kim, Cobalt nanoparticles supported on magnetic core-shell structured carbon as a highly efficient catalyst for hydrogen generation from $NaBH_4$ hydrolysis, *Int. J. Hydrogen Energy*, 2018, **43**, 9296–9306.

72 A. F. Baye, M. W. Abebe, R. Appiah-Ntiamoah and H. Kim, Engineered iron-carbon-cobalt (Fe_3O_4@C-Co) core-shell composite with synergistic catalytic properties towards hydrogen generation via NaBH4 hydrolysis, *J. Colloid Interface Sci.*, 2019, **543**, 273–284.

73 F. Seven and N. Sahiner, Enhanced catalytic performance in hydrogen generation from $NaBH_4$ hydrolysis by super porous cryogel supported Co and Ni catalysts, *J. Power Sources*, 2014, **272**, 128–136.

74 J. Lee, H. Shin, K. S. Choi, J. Lee, J.-Y. Choi and H. K. Yu, Carbon layer supported nickel catalyst for sodium borohydride ($NaBH_4$) dehydrogenation, *Int. J. Hydrogen Energy*, 2019, **44**, 2943–2950.

75 R. Barrios-Francisco and J. J. García, Semihydrogenation of alkynes in the presence of Ni(0) catalyst using ammonia-borane and sodium borohydride as hydrogen sources, *Appl. Catal., A*, 2010, **385**, 108–113.

76 S. U. Jeong, R. K. Kim, E. A. Cho, H. J. Kim, S. W. Nam, I. H. Oh, S. A. Hong and S. H. Kim, A study on hydrogen generation from NaBH4 solution using the high-performance Co-B catalyst, *J. Power Sources*, 2005, **144**, 129–134.

77 C. Wu, F. Wu, Y. Bai, B. Yi and H. Zhang, Cobalt boride catalysts for hydrogen generation from alkaline NaBH4 solution, *Mater. Lett.*, 2005, **59**, 1748–1751.

78 N. Patel, G. Guella, A. Kale, A. Miotello, B. Patton, C. Zanchetta, L. Mirenghi and P. Rotolo, Thin films of Co–B prepared by pulsed laser deposition as efficient catalysts in hydrogen producing reactions, *Appl. Catal., A*, 2007, **323**, 18–24.

79 H. Ma, W. Ji, J. Zhao, J. Liang and J. Chen, Preparation, characterization and catalytic $NaBH_4$ hydrolysis of Co-B hollow spheres, *J. Alloys Compd.*, 2009, **474**, 584–589.

80 C. C. Yang, M. S. Chen and Y. W. Chen, Hydrogen generation by hydrolysis of sodium borohydride on CoB/SiO_2 catalyst, *Int. J. Hydrogen Energy*, 2011, **36**, 1418–1423.

81 S. Gupta, N. Patel, R. Fernandes, D. C. Kothari and A. Miotello, Mesoporous Co–B nanocatalyst for efficient hydrogen production by hydrolysis of sodium borohydride, *Int. J. Hydrogen Energy*, 2013, **38**, 14685–14692.

82 S. U. Jeong, E. A. Cho, S. W. Nam, I. H. Oh, U. H. Jung and S. H. Kim, Effect of preparation method on Co–B catalytic activity for hydrogen generation from alkali $NaBH_4$ solution, *Int. J. Hydrogen Energy*, 2007, **32**, 1749–1754.

83 O. Akdim, U. B. Demirci, D. Muller and P. Miele, Cobalt(II) salts, performing materials for generating hydrogen from sodium borohydride, *Int. J. Hydrogen Energy*, 2009, **34**, 2631–2637.

84 X. Shen, M. Dai, M. Gao, B. Zhao and W. Ding, Solvent effects in the synthesis of CoB catalysts on hydrogen generation from hydrolysis of sodium borohydride, *Chin. J. Catal.*, 2013, **34**, 979–985.

85 R. Fernandes, N. Patel and A. Miotello, Hydrogen generation by hydrolysis of alkaline NaBH4 solution with Cr-promoted Co–B amorphous catalyst, *Appl. Catal., B*, 2009, **92**, 68–74.

86 N. Patel, R. Fernandes and A. Miotello, Promoting effect of transition metal-doped Co–B alloy catalysts for hydrogen production by hydrolysis of alkaline $NaBH_4$ solution, *J. Catal.*, 2010, **271**, 315–324.

87 H. B. Dai, Y. Liang and P. Wang, Effect of trapped hydrogen on the induction period of cobalt–tungsten–boron/nickel foam catalyst in catalytic hydrolysis reaction of sodium borohydride, *Catal. Today*, 2011, **170**, 27–32.

88 A. Ekinci, Ö. Şahin, C. Saka and T. Avci, The effects of plasma treatment on electrochemical activity of Co–W–B catalyst for hydrogen production by hydrolysis of $NaBH_4$, *Int. J. Hydrogen Energy*, 2013, **38**, 15295–15301.

89 D. Ke, Y. Tao, Y. Li, X. Zhao, L. Zhang, J. Wang and S. Han, Kinetics study on hydrolytic dehydrogenation of alkaline sodium borohydride catalyzed by Mo-modified

Co–B nanoparticles, *Int. J. Hydrogen Energy*, 2015, **40**, 7308–7317.

90 X. Shen, Q. Wang, S. Guo, B. Liu, Z. Sun, Z. Zhang, Z. Wang, B. Zhao and W. Ding, W-modified CoB supported on Ag-activated TiO 2 for hydrogen generation from alkaline NaBH 4 solution, *Int. J. Hydrogen Energy*, 2015, **40**, 6346–6357.

91 Y. Wei, R. Wang, L. Meng, Y. Wang, G. Li, S. Xin, X. Zhao and K. Zhang, Hydrogen generation from alkaline $NaBH_4$ solution using a dandelion-like Co–Mo–B catalyst supported on carbon cloth, *Int. J. Hydrogen Energy*, 2017, **42**, 9945–9951.

92 X. Yuan, C. Jia, X. L. Ding and Z. F. Ma, Effects of heat-treatment temperature on properties of Cobalt–manganese–Boride as efficient catalyst toward hydrolysis of alkaline sodium borohydride solution, *Int. J. Hydrogen Energy*, 2012, **37**, 995–1001.

93 M. Aydin, A. Hasimoglu and O. K. Ozdemir, Kinetic properties of Cobalt–Titanium–Boride (Co–Ti–B) catalysts for sodium borohydride hydrolysis reaction, *Int. J. Hydrogen Energy*, 2016, **41**, 239–248.

94 Y. Zou, Y. Yin, Y. Gao, C. Xiang, H. Chu, S. Qiu, E. Yan, F. Xu and L. Sun, Chitosan-mediated Co–Ce–B nanoparticles for catalyzing the hydrolysis of sodium borohydride, *Int. J. Hydrogen Energy*, 2018, **43**, 4912–4921.

95 C. Xiang, D. Jiang, Z. She, Y. Zou, H. Chu, S. Qiu, H. Zhang, F. Xu, C. Tang and L. Sun, Hydrogen generation by hydrolysis of alkaline sodium borohydride using a cobalt–zinc–boron/graphene nanocomposite treated with sodium hydroxide, *Int. J. Hydrogen Energy*, 2015, **40**, 4111–4118.

96 J. Zhao, H. Ma and J. Chen, Improved hydrogen generation from alkaline $NaBH_4$ solution using carbon-supported Co–B as catalysts, *Int. J. Hydrogen Energy*, 2007, **32**, 4711–4716.

97 Y. Huang, Y. Wang, R. Zhao, P. Shen and Z. Wei, Accurately measuring the hydrogen generation rate for hydrolysis of sodium borohydride on multiwalled carbon nanotubes/Co–B catalysts, *Int. J. Hydrogen Energy*, 2008, **33**, 7110–7115.

98 F. Li, Q. Li and H. Kim, CoB/open-CNTs catalysts for hydrogen generation from alkaline $NaBH_4$ solution, *Chem. Eng. J.*, 2012, **210**, 316–324.

99 Y. C. Lu, M. S. Chen and Y. W. Chen, Hydrogen generation by sodium borohydride hydrolysis on nanosized CoB catalysts supported on TiO_2, Al_2O_3 and CeO_2, *Int. J. Hydrogen Energy*, 2012, **37**, 4254–4258.

100 J. Cheng, C. Xiang, Y. Zou, H. Chu, S. Qiu, H. Zhang, L. Sun and F. Xu, Highly active nanoporous Co–B–TiO_2 framework for hydrolysis of $NaBH_4$, *Ceram. Int.*, 2015, **41**, 899–905.

101 X. Shen, Q. Wang, Q. Wu, S. Guo, Z. Zhang, Z. Sun, B. Liu, Z. Wang, B. Zhao and W. Ding, CoB supported on Ag-activated TiO_2 as a highly active catalyst for hydrolysis of alkaline $NaBH_4$ solution, *Energy*, 2015, **90**, 464–474.

102 H. B. Dai, Y. Liang, P. Wang and H. M. Cheng, Amorphous cobalt–boron/nickel foam as an effective catalyst for hydrogen generation from alkaline sodium borohydride solution, *J. Power Sources*, 2008, **177**, 17–23.

103 S. Guo, Q. Wu, J. Sun, T. Chen, M. Feng, Q. Wang, Z. Wang, B. Zhao and W. Ding, Highly stable and controllable CoB/Ni-foam catalysts for hydrogen generation from alkaline NaBH4 solution, *Int. J. Hydrogen Energy*, 2017, **42**, 21063–21072.

104 Y. Chen and H. Kim, Use of a nickel-boride–silica nanocomposite catalyst prepared by *in situ* reduction for hydrogen production from hydrolysis of sodium borohydride, *Fuel Process. Technol.*, 2008, **89**, 966–972.

105 J. K. Lee, H. H. Ann, Y. Yi, K. W. Lee, S. Uhm and J. Lee, A stable Ni–B catalyst in hydrogen generation via NaBH4 hydrolysis, *Catal. Commun.*, 2011, **16**, 120–123.

106 J. Zhang, C. Li, L. Li, X. Du, B. Song and H. Xu, Multi-shaped amorphous alloy Ni-B: Ultrasonically aided complexing-reduction preparation, catalytic ability for $NaBH_4$ hydrolysis yielding H_2 gas, *Z. Anorg. Allg. Chem.*, 2014, **640**, 456–461.

107 Z. Liang, Q. Li, F. Li, S. Zhao and X. Xia, Hydrogen generation from hydrolysis of NaBH4 based on high stable NiB/$NiFe_2O_4$ catalyst, *Int. J. Hydrogen Energy*, 2017, **42**, 3971–3980.

108 T. N. Tuan, Y. Yi, J. K. Lee and J. Lee, Fe–B catalyst fabricated by hybrid capacitive adsorption–chemical reduction method and its application for hydrogen production from $NaBH_4$ solution, *Catal. Today*, 2013, **216**, 240–245.

109 J. D. Ocon, T. N. Tuan, Y. Yi, R. L. de Leon, J. K. Lee and J. Lee, Ultrafast and stable hydrogen generation from sodium borohydride in methanol and water over Fe–B nanoparticles, *J. Power Sources*, 2013, **243**, 444–450.

110 M. Bekirogullari, Catalytic activities of non-noble metal catalysts (Cu-B, Fe-B, and Ni-B) with C.Vulgaris microalgal strain support modified by using phosphoric acid for hydrogen generation from sodium borohydride methanolysis, *Int. J. Hydrogen Energy*, 2019, **44**, 14981–14991.

111 K. W. Cho and H. S. Kwon, Effects of electrodeposited Co and Co–P catalysts on the hydrogen generation properties from hydrolysis of alkaline sodium borohydride solution, *Catal. Today*, 2007, **120**, 298–304.

112 K. Eom, K. Cho and H. Kwon, Effects of electroless deposition conditions on microstructures of cobalt–phosphorous catalysts and their hydrogen generation properties in alkaline sodium borohydride solution, *J. Power Sources*, 2008, **180**, 484–490.

113 X. Zhang, J. Zhao, F. Cheng, J. Liang, Z. Tao and J. Chen, Electroless-deposited Co–P catalysts for hydrogen generation from alkaline $NaBH_4$ solution, *Int. J. Hydrogen Energy*, 2010, **35**, 8363–8369.

114 Y. Wang, Y. Shen, K. Qi, Z. Cao, K. Zhang and S. Wu, Nanostructured cobalt–phosphorous catalysts for hydrogen generation from hydrolysis of sodium borohydride solution, *Renewable Energy*, 2016, **89**, 285–294.

115 T. Liu, K. Wang, G. Du, A. M. Asiri and X. Sun, Self-supported CoP nanosheet arrays: a non-precious metal catalyst for efficient hydrogen generation from alkaline $NaBH_4$ solution, *J. Mater. Chem. A*, 2016, **4**, 13053–13057.

116 L. Cui, Y. Xu, L. Niu, W. Yang and J. Liu, Monolithically integrated CoP nanowire array: An on/off switch for effective on-demand hydrogen generation via hydrolysis of $NaBH_4$ and NH_3BH_3, *Nano Res.*, 2016, **10**, 595–604.

117 Y. Guo, Z. Dong, Z. Cui, X. Zhang and J. Ma, Promoting effect of W doped in electrodeposited Co–P catalysts for hydrogen generation from alkaline $NaBH_4$ solution, *Int. J. Hydrogen Energy*, 2012, **37**, 1577–1583.

118 L. Wang, Z. Li, X. Liu, P. Zhang and G. Xie, Hydrogen generation from alkaline NaBH 4 solution using electroless-deposited Co–W–P supported on γ-Al_2O_3, *Int. J. Hydrogen Energy*, 2015, **40**, 7965–7973.

119 Y. Wei, X. Huang, J. Wang, H. Yu, X. Zhao and D. Cheng, Synthesis of bifunctional non-noble monolithic catalyst Co-W-P/carbon cloth for sodium borohydride hydrolysis and reduction of 4-nitrophenol, *Int. J. Hydrogen Energy*, 2017, **42**, 25860–25868.

120 D. R. Kim, K. W. Cho, Y. I. Choi and C. J. Park, Fabrication of porous Co–Ni–P catalysts by electrodeposition and their catalytic characteristics for the generation of hydrogen from an alkaline $NaBH_4$ solution, *Int. J. Hydrogen Energy*, 2009, **34**, 2622–2630.

121 Y. Wang, G. Li, S. Wu, Y. Wei, W. Meng, Y. Xie, Y. Cui, X. Lian, Y. Chen and X. Zhang, Hydrogen generation from alkaline $NaBH_4$ solution using nanostructured Co–Ni–P catalysts, *Int. J. Hydrogen Energy*, 2017, **42**, 16529–16537.

122 Z. Li, L. Wang, Y. Zhang and G. Xie, Properties of Cu Co P/γ-Al_2O_3 catalysts for efficient hydrogen generation by hydrolysis of alkaline $NaBH_4$ solution, *Int. J. Hydrogen Energy*, 2017, **42**, 5749–5757.

123 C. Tang, R. Zhang, W. Lu, L. He, X. Jiang, A. M. Asiri and X. Sun, Fe-Doped CoP nanoarray: A monolithic multifunctional catalyst for highly efficient hydrogen generation, *Adv. Mater.*, 2017, **29**, 1602441.

124 S. Carenco, D. Portehault, C. Boissiere, N. Mezailles and C. Sanchez, Nanoscaled metal borides and phosphides: Recent developments and perspectives, *Chem. Rev.*, 2013, **113**, 7981–8065.

125 A. Staubitz, A. P. Robertson and I. Manners, Ammonia-borane and related compounds as dihydrogen sources, *Chem. Rev.*, 2010, **110**, 4079–4124.

126 M. Chandra and Q. Xu, A high-performance hydrogen generation system: Transition metal-catalyzed dissociation and hydrolysis of ammonia–borane, *J. Power Sources*, 2006, **156**, 190–194.

127 H. L. Jiang and Q. Xu, Catalytic hydrolysis of ammonia borane for chemical hydrogen storage, *Catal. Today*, 2011, **170**, 56–63.

128 O. T. Summerscales and J. C. Gordon, Regeneration of ammonia borane from spent fuel materials, *Dalton Trans.*, 2013, **42**, 10075–10084.

129 H. L. Jiang, T. Umegaki, T. Akita, X. B. Zhang, M. Haruta and Q. Xu, Bimetallic Au-Ni nanoparticles embedded in SiO_2 nanospheres: Synergetic catalysis in hydrolytic dehydrogenation of ammonia borane, *Chem. – Eur. J.*, 2010, **16**, 3132–3137.

130 Y. Z. Chen, L. Liang, Q. Yang, M. Hong, Q. Xu, S. H. Yu and H. L. Jiang, A seed-mediated approach to the general and mild synthesis of non-noble metal nanoparticles stabilized by a metal–organic framework for highly efficient catalysis, *Mater. Horiz.*, 2015, **2**, 606–612.

131 Q. Yang, Y. Z. Chen, Z. U. Wang, Q. Xu and H. L. Jiang, One-pot tandem catalysis over Pd@MIL-101: boosting the efficiency of nitro compound hydrogenation by coupling with ammonia borane dehydrogenation, *Chem. Commun.*, 2015, **51**, 10419–10422.

132 X. Ma, Y. X. Zhou, H. Liu, Y. Li and H. L. Jiang, A MOF-derived Co-CoO@N-doped porous carbon for efficient tandem catalysis: dehydrogenation of ammonia borane and hydrogenation of nitro compounds, *Chem. Commun.*, 2016, **52**, 7719–7722.

133 Y. H. Zhou, Q. Yang, Y. Z. Chen and H. L. Jiang, Low-cost CuNi@MIL-101 as an excellent catalyst toward cascade reaction: integration of ammonia borane dehydrogenation with nitroarene hydrogenation, *Chem. Commun.*, 2017, **53**, 12361–12364.

134 A. Boddien, B. Loges, F. Gartner, C. Torborg, K. Fumino, H. Junge, R. Ludwig and M. Beller, Iron-catalyzed hydrogen production from formic acid, *J. Am. Chem. Soc.*, 2010, **132**, 8924–8934.

135 M. C. Denney, V. Pons, T. J. Hebden, D. M. Heinekey and K. I. Goldberg, Efficient catalysis of ammonia borane dehydrogenation, *J. Am. Chem. Soc.*, 2006, **128**, 12048–12049.

136 A. Paul and C. B. Musgrave, Catalyzed dehydrogenation of ammonia-borane by iridium dihydrogen pincer complex differs from ethane dehydrogenation, *Angew. Chem., Int. Ed.*, 2007, **46**, 8153–8156.

137 N. Blaquiere, S. Diallo-Garcia, S. I. Gorelsky, D. A. Black and K. Fagnou, Ruthenium-catalyzed dehydrogenation of ammonia boranes, *J. Am. Chem. Soc.*, 2008, **130**, 14034–14035.

138 P. V. Ramachandran and P. D. Gagare, Preparation of ammonia borane in high yield and purity, methanolysis, and regeneration, *Inorg. Chem.*, 2007, **46**, 7810–7817.

139 A. Gutowska, L. Y. Li, Y. S. Shin, C. M. M. Wang, X. H. S. Li, J. C. Linehan, R. S. Smith, B. D. Kay, B. Schmid, W. Shaw, M. Gutowski and T. Autrey, Nanoscaffold mediates hydrogen release and the reactivity of ammonia borane, *Angew. Chem., Int. Ed.*, 2005, **44**, 3578–3582.

140 M. E. Bluhm, M. G. Bradley, R. Butterick III, U. Kusari and L. G. Sneddon, Amineborane-based chemical hydrogen storage: Enhanced ammonia borane dehydrogenation in ionic liquids, *J. Am. Chem. Soc.*, 2006, **128**, 7748–7749.

141 L. Li, X. Yao, C. Sun, A. Du, L. Cheng, Z. Zhu, C. Yu, J. Zou, S. C. Smith, P. Wang, H. M. Cheng, R. L. Frost and

G. Q. Lu, Lithium-catalyzed dehydrogenation of ammonia borane within mesoporous carbon framework for chemical hydrogen storage, *Adv. Funct. Mater.*, 2009, **19**, 265–271.

142 J. Huang, F. Zhu, W. He, F. Zhang, W. Wang and H. Li, Periodic mesoporous organometallic silicas with unary or binary organometals inside the channel walls as active and reusable catalysts in aqueous organic reactions, *J. Am. Chem. Soc.*, 2010, **132**, 1492–1493.

143 L. Wang, H. Li, W. Zhang, X. Zhao, J. Qiu, A. Li, X. Zheng, Z. Hu, R. Si and J. Zeng, Supported rhodium catalysts for ammonia-borane hydrolysis: Dependence of the catalytic activity on the highest occupied state of the single rhodium atoms, *Angew. Chem., Int. Ed.*, 2017, **56**, 4712–4718.

144 H. Yan, Y. Lin, H. Wu, W. Zhang, Z. Sun, H. Cheng, W. Liu, C. Wang, J. Li, X. Huang, T. Yao, J. Yang, S. Wei and J. Lu, Bottom-up precise synthesis of stable platinum dimers on graphene, *Nat. Commun.*, 2017, **8**, 1070.

145 Q. Sun, N. Wang, T. Zhang, R. Bai, A. Mayoral, P. Zhang, Q. Zhang, O. Terasaki and J. Yu, Zeolite-encaged single-atom rhodium catalysts: Highly-efficient hydrogen generation and shape-selective tandem hydrogenation of nitroarenes, *Angew. Chem., Int. Ed.*, 2019, **58**, 18570–18576.

146 Q. L. Yao, W. Shi, G. Feng, Z. H. Lu, X. Zhang, D. Tao, D. Kong and X. Chen, Ultrafine Ru nanoparticles embedded in SiO_2 nanospheres: Highly efficient catalysts for hydrolytic dehydrogenation of ammonia borane, *J. Power Sources*, 2014, **257**, 293–299.

147 Q. L. Yao, Z. H. Lu, Y. Hu and X. Chen, Core–shell Co@SiO_2 nanosphere immobilized Ag nanoparticles for hydrogen evolution from ammonia borane, *RSC Adv.*, 2016, **6**, 89450–89456.

148 Q. L. Yao, Y. Shi, X. Zhang, X. Chen and Z. H. Lu, Facile Synthesis of Platinum-cerium(IV) oxide hybrids arched on reduced graphene oxide catalyst in reverse micelles with high activity and durability for hydrolysis of ammonia borane, *Chem. – Asian J.*, 2016, **11**, 3251–3257.

149 Q. L. Zhu and Q. Xu, Liquid organic and inorganic chemical hydrides for high-capacity hydrogen storage, *Energy Environ. Sci.*, 2015, **8**, 478–512.

150 Z. H. Lu, Q. L. Yao, Z. Zhang, Y. Yang and X. Chen, Nanocatalysts for hydrogen generation from ammonia borane and hydrazine borane, *J. Nanomater.*, 2014, 729027.

151 Q. L. Yao, X. Chen and Z. H. Lu, Catalytic dehydrogenation of NH_3BH_3, N_2H_4, and $N_2H_4BH_3$ for chemical hydrogen storage, *Energy Environ. Focus*, 2014, **3**, 236–245.

152 C. Y. Alpaydın, S. K. Gülbay and C. O. Colpan, A review on the catalysts used for hydrogen production from ammonia borane, *Int. J. Hydrogen Energy*, 2020, **45**, 3414–3434.

153 M. Zahmakiran and S. Özkar, Transition Metal nanoparticles in catalysis for the hydrogen generation from the hydrolysis of ammonia-borane, *Top. Catal.*, 2013, **56**, 1171–1183.

154 Q. Xu and M. Chandra, Catalytic activities of non-noble metals for hydrogen generation from aqueous ammonia–borane at room temperature, *J. Power Sources*, 2006, **163**, 364–370.

155 J. M. Yan, X. B. Zhang, S. Han, H. Shioyama and Q. Xu, Iron-nanoparticle-catalyzed hydrolytic dehydrogenation of ammonia borane for chemical hydrogen storage, *Angew. Chem., Int. Ed.*, 2008, **47**, 2287–2289.

156 J. M. Yan, X. B. Zhang, H. Shioyama and Q. Xu, Room temperature hydrolytic dehydrogenation of ammonia borane catalyzed by Co nanoparticles, *J. Power Sources*, 2010, **195**, 1091–1094.

157 T. Umegaki, J. M. Yan, X. B. Zhang, H. Shioyama, N. Kuriyama and Q. Xu, Preparation and catalysis of poly (N-vinyl-2-pyrrolidone) (PVP) stabilized nickel catalyst for hydrolytic dehydrogenation of ammonia borane, *Int. J. Hydrogen Energy*, 2009, **34**, 3816–3822.

158 K. Aranishi, Q. L. Zhu and Q. Xu, Dendrimer-encapsulated cobalt nanoparticles as high-performance catalysts for the hydrolysis of ammonia aorane, *ChemCatChem*, 2014, **6**, 1375–1379.

159 S. Duan, G. Han, Y. Su, X. Zhang, Y. Liu, X. Wu and B. Li, Magnetic Co@g-C_3N_4 Core-shells on rGO sheets for momentum transfer with catalytic activity toward continuous-flow hydrogen generation, *Langmuir*, 2016, **32**, 6272–6281.

160 J. Hu, Z. Chen, M. Li, X. Zhou and H. Lu, Amine-capped Co nanoparticles for highly efficient dehydrogenation of ammonia borane, *ACS Appl. Mater. Interfaces*, 2014, **6**, 13191–13200.

161 Y. Men, J. Su, C. Huang, L. Liang, P. Cai, G. Cheng and W. Luo, Three-dimensional nitrogen-doped graphene hydrogel supported Co-CeO_x nanoclusters as efficient catalysts for hydrogen generation from hydrolysis of ammonia borane, *Chin. Chem. Lett.*, 2018, **29**, 1671–1674.

162 M. Chen, R. Xiong, X. Cui, Q. Wang and X. Liu, SiO_2-encompassed Co@N-doped porous carbon assemblies as recyclable catalysts for efficient hydrolysis of ammonia borane, *Langmuir*, 2019, **35**, 671–677.

163 S. L. Zacho, J. Mielby and S. Kegnaes, Hydrolytic dehydrogenation of ammonia borane over ZIF-67 derived Co nanoparticle catalysts, *Catal. Sci. Technol.*, 2018, **8**, 4741–4746.

164 X. Zhao, D. Ke, S. Han, Y. Li, H. Zhang and Y. Cai, Reduced graphene oxide sheets supported waxberry-like Co catalysts for improved hydrolytic dehydrogenation of ammonia borane, *ChemistrySelect*, 2019, **4**, 2513–2518.

165 Y. W. Yang, G. Feng, Z. H. Lu, H. Na, F. Zhang and X. S. Chen, In situ synthesis of reduced graphene oxide supported Co nanoparticles as efficient catalysts for hydrogen generation from NH_3BH_3, *Acta Phys. – Chim. Sin.*, 2014, **30**, 1180–1186.

166 A. Aijaz, A. Karkamkar, Y. J. Choi, N. Tsumori, E. Ronnebro, T. Autrey, H. Shioyama and Q. Xu, Immobilizing highly catalytically active Pt nanoparticles inside the pores of metal-organic framework: a double sol-

vents approach, *J. Am. Chem. Soc.*, 2012, **134**, 13926–13929.

167 P. Liu, X. Gu, K. Kang, H. Zhang, J. Cheng and H. Su, Highly efficient catalytic hydrogen evolution from ammonia borane using the synergistic effect of crystallinity and size of noble-metal-free nanoparticles supported by porous metal-organic frameworks, *ACS Appl. Mater. Interfaces*, 2017, **9**, 10759–10767.

168 Y. Z. Chen, Q. Xu, S. H. Yu and H. L. Jiang, Tiny Pd@Co core-shell nanoparticles confined inside a metal-organic framework for highly efficient catalysis, *Small*, 2015, **11**, 71–76.

169 Z. Li, T. He, L. Liu, W. Chen, M. Zhang, G. Wu and P. Chen, Covalent triazine framework supported non-noble metal nanoparticles with superior activity for catalytic hydrolysis of ammonia borane: from mechanistic study to catalyst design, *Chem. Sci.*, 2017, **8**, 781–788.

170 Y. Fang, Z. Xiao, J. Li, C. Lollar, L. Liu, X. Lian, S. Yuan, S. Banerjee, P. Zhang and H. C. Zhou, Formation of a highly reactive cobalt nanocluster crystal within a highly negatively charged porous coordination cage, *Angew. Chem., Int. Ed.*, 2018, **57**, 5283–5287.

171 H. Wang, Y. Zhao, F. Cheng, Z. Tao and J. Chen, Cobalt nanoparticles embedded in porous N-doped carbon as long-life catalysts for hydrolysis of ammonia borane, *Catal. Sci. Technol.*, 2016, **6**, 3443–3448.

172 L. Zhou, J. Meng, P. Li, Z. Tao, L. Mai and J. Chen, Ultrasmall cobalt nanoparticles supported on nitrogen-doped porous carbon nanowires for hydrogen evolution from ammonia borane, *Mater. Horiz.*, 2017, **4**, 268–273.

173 F. Zhang, C. Ma, Y. Zhang, H. Li, D. Fu, X. Du and X.-M. Zhang, N-doped mesoporous carbon embedded Co nanoparticles for highly efficient and stable H2 generation from hydrolysis of ammonia borane, *J. Power Sources*, 2018, **399**, 89–97.

174 X. L. Zhang, D. X. Zhang, G. G. Chang, X. C. Ma, J. Wu, Y. Wang, H. Z. Yu, G. Tian, J. Chen and X. Y. Yang, Bimetallic (Zn/Co) MOFs-derived highly dispersed metallic Co/HPC for completely hydrolytic dehydrogenation of ammonia–borane, *Ind. Eng. Chem. Res.*, 2019, **58**, 7209–7216.

175 Ö. Metin, V. Mazumder, S. Özkar and S. Sun, Monodisperse nickel nanoparticles and their catalysis in hydrolytic dehydrogenation of ammonia borane, *J. Am. Chem. Soc.*, 2010, **132**, 1468–1469.

176 Y. Li, L. Xie, Y. Li, J. Zheng and X. Li, Metal-organic-framework-based catalyst for highly efficient H_2 generation from aqueous NH_3BH_3 solution, *Chemistry*, 2009, **15**, 8951–8954.

177 A. Nozaki, Y. Tanihara, Y. Kuwahara, T. Ohmichi, K. Mori, T. Nagase, H. Y. Yasuda and H. Yamashita, Skeletal Ni catalysts prepared from amorphous Ni-Zr alloys: Enhanced catalytic performance for hydrogen generation from ammonia borane, *ChemPhysChem*, 2016, **17**, 412–417.

178 J. Manna, S. Akbayrak and S. Özkar, Nickel(0) nanoparticles supported on bare or coated cobalt ferrite as highly active, magnetically isolable and reusable catalyst for hydrolytic dehydrogenation of ammonia borane, *J. Colloid Interface Sci.*, 2017, **508**, 359–368.

179 K. Guo, H. Li and Z. Yu, Size-dependent catalytic activity of monodispersed nickel nanoparticles for the hydrolytic dehydrogenation of ammonia borane, *ACS Appl. Mater. Interfaces*, 2018, **10**, 517–525.

180 Ö. Metin, S. Özkar and S. Sun, Monodisperse nickel nanoparticles supported on SiO_2 as an effective catalyst for the hydrolysis of ammonia-borane, *Nano Res.*, 2010, **3**, 676–684.

181 P. Z. Li, A. Aijaz and Q. Xu, Highly dispersed surfactant-free nickel nanoparticles and their remarkable catalytic activity in the hydrolysis of ammonia borane for hydrogen generation, *Angew. Chem., Int. Ed.*, 2012, **51**, 6753–6756.

182 P. Z. Li, K. Aranishi and Q. Xu, ZIF-8 immobilized nickel nanoparticles: highly effective catalysts for hydrogen generation from hydrolysis of ammonia borane, *Chem. Commun.*, 2012, **48**, 3173–3175.

183 C. Wang, J. Tuninetti, Z. Wang, C. Zhang, R. Ciganda, L. Salmon, S. Moya, J. Ruiz and D. Astruc, Hydrolysis of Ammonia-borane over Ni/ZIF-8 nanocatalyst: High efficiency, mechanism, and controlled hydrogen release, *J. Am. Chem. Soc.*, 2017, **139**, 11610–11615.

184 G. Zhao, J. Zhong, J. Wang, T. K. Sham, X. Sun and S. T. Lee, Revealing the synergetic effects in Ni nanoparticle-carbon nanotube hybrids by scanning transmission X-ray microscopy and their application in the hydrolysis of ammonia borane, *Nanoscale*, 2015, **7**, 9715–9722.

185 J. Zhang, C. Chen, W. Yan, F. Duan, B. Zhang, Z. Gao and Y. Qin, Ni nanoparticles supported on CNTs with excellent activity produced by atomic layer deposition for hydrogen generation from the hydrolysis of ammonia borane, *Catal. Sci. Technol.*, 2016, **6**, 2112–2119.

186 M. Mahyari and A. Shaabani, Nickel nanoparticles immobilized on three-dimensional nitrogen-doped graphene as a superb catalyst for the generation of hydrogen from the hydrolysis of ammonia borane, *J. Mater. Chem. A*, 2014, **2**, 16652–16659.

187 K. Yang, Q. L. Yao, W. Huang, X. Chen and Z. H. Lu, Enhanced catalytic activity of NiM (M=Cr, Mo, W) nanoparticles for hydrogen evolution from ammonia borane and hydrazine borane, *Int. J. Hydrogen Energy*, 2017, **42**, 6840–6850.

188 Q. L. Yao, Z. H. Lu, W. Huang, X. Chen and J. Zhu, High Pt-like activity of the Ni–Mo/graphene catalyst for hydrogen evolution from hydrolysis of ammonia borane, *J. Mater. Chem. A*, 2016, **4**, 8579–8583.

189 K. Yang, Q. L. Yao, Z. H. Lu, Z. B. Kang and X. S. Chen, Facile synthesis of CuMo nanoparticles as highly active and cost-effective catalysts for the hydrolysis of ammonia borane, *Acta Phys. – Chim. Sin.*, 2017, **33**, 993–1000.

190 Q. L. Yao, K. Yang, X. Hong, X. Chen and Z. H. Lu, Base-promoted hydrolytic dehydrogenation of ammonia borane

catalyzed by noble-metal-free nanoparticles, *Catal. Sci. Technol.*, 2018, **8**, 870–877.

191 Q. L. Yao, M. He, X. Hong, X. Chen, G. Feng and Z. H. Lu, Hydrogen production via selective dehydrogenation of hydrazine borane and hydrous hydrazine over MoO_x-promoted Rh catalyst, *Int. J. Hydrogen Energy*, 2019, **44**, 28430–28440.

192 Q. L. Yao, M. He, X. Hong, X. Zhang and Z. H. Lu, MoO_x-modified bimetallic alloy nanoparticles for highly efficient hydrogen production from hydrous hydrazine, *Inorg. Chem. Front.*, 2019, **6**, 1546–1552.

193 Q. L. Yao, K. Yang, W. Nie, Y. Li and Z. H. Lu, Highly efficient hydrogen generation from hydrazine borane via a MoO_x-promoted NiPd nanocatalyst, *Renewable Energy*, 2020, **147**, 2024–2031.

194 Q. L. Yao, Z. H. Lu, Y. Yang, Y. Chen, X. Chen and H. L. Jiang, Facile synthesis of graphene-supported Ni-CeO_x nanocomposites as highly efficient catalysts for hydrolytic dehydrogenation of ammonia borane, *Nano Res.*, 2018, **11**, 4412–4422.

195 Y. H. Zhou, S. Wang, Y. Wan, J. Liang, Y. Chen, S. Luo and C. Yong, Low-cost CuNi-CeO_2/rGO as an efficient catalyst for hydrolysis of ammonia borane and tandem reduction of 4-nitrophenol, *J. Alloys Compd.*, 2017, **728**, 902–909.

196 Y. W. Yang, Z. H. Lu and X. S. Chen, Cu-based nanocatalysts for hydrogen generation via hydrolysis and methanolysis of ammonia borane, *Mater. Technol.*, 2015, **30**, A89–A93.

197 O. Ozay, E. Inger, N. Aktas and N. Sahiner, Hydrogen production from ammonia borane via hydrogel template synthesized Cu, Ni, Co composites, *Int. J. Hydrogen Energy*, 2011, **36**, 8209–8216.

198 S. B. Kalidindi, U. Sanyal and B. R. Jagirdar, Nanostructured Cu and Cu@Cu_2O core shell catalysts for hydrogen generation from ammonia-borane, *Phys. Chem. Chem. Phys.*, 2008, **10**, 5870–5874.

199 Y. Yamada, K. Yano, Q. Xu and S. Fukuzumi, Cu/Co_3O_4 nanoparticles as catalysts for hydrogen evolution from ammonia borane by hydrolysis, *J. Phys. Chem. C*, 2010, **114**, 16456–16462.

200 Y. Yamada, K. Yano and S. Fukuzumi, Catalytic application of shape-controlled Cu_2O particles protected by Co_3O_4 nanoparticles for hydrogen evolution from ammonia borane, *Energy Environ. Sci.*, 2012, **5**, 5356–5363.

201 M. Zahmakıran, F. Durap and S. Özkar, Zeolite confined copper(0) nanoclusters as cost-effective and reusable catalyst in hydrogen generation from the hydrolysis of ammonia-borane, *Int. J. Hydrogen Energy*, 2010, **35**, 187–197.

202 M. Kaya, M. Zahmakiran, S. Özkar and M. Volkan, Copper (0) nanoparticles supported on silica-coated cobalt ferrite magnetic particles: cost effective catalyst in the hydrolysis of ammonia-borane with an exceptional reusability performance, *ACS Appl. Mater. Interfaces*, 2012, **4**, 3866–3873.

203 Y. Yang, Z. H. Lu, Y. Hu, Z. Zhang, W. Shi, X. Chen and T. Wang, Facile in situ synthesis of copper nanoparticles supported on reduced graphene oxide for hydrolytic dehydrogenation of ammonia borane, *RSC Adv.*, 2014, **4**, 13749–13752.

204 Q. L. Yao, Z. H. Lu, Z. Zhang, X. Chen and Y. Lan, One-pot synthesis of core-shell Cu@SiO_2 nanospheres and their catalysis for hydrolytic dehydrogenation of ammonia borane and hydrazine borane, *Sci. Rep.*, 2014, **4**, 7597.

205 J. Zhang, Y. Wang, Y. Zhu, G. Mi, X. Du and Y. Dong, Shape-selective fabrication of Cu nanostructures: Contrastive study of catalytic ability for hydrolytically releasing H_2 from ammonia borane, *Renewable Energy*, 2018, **118**, 146–151.

206 J. X. Kang, T. W. Chen, D. F. Zhang and L. Guo, PtNiAu trimetallic nanoalloys enabled by a digestive-assisted process as highly efficient catalyst for hydrogen generation, *Nano Energy*, 2016, **23**, 145–152.

207 K. Yang, L. Zhou, X. Xiong, M. Ye, L. Li and Q. Xia, RuCuCo nanoparticles supported on MIL-101 as a novel highly efficient catalysts for the hydrolysis of ammonia borane, *Microporous Mesoporous Mater.*, 2016, **225**, 1–8.

208 D. Ke, Y. Li, J. Wang, L. Zhang, J. Wang, X. Zhao, S. Yang and S. Han, Facile fabrication of poly(amidoamine) (PAMAM) dendrimers-encapsulated Ag–Co bimetallic nanoparticles for highly efficient dehydrogenation of ammonia borane, *Int. J. Hydrogen Energy*, 2016, **41**, 2564–2574.

209 Q. Wang, F. Fu, S. Yang, M. M. Moro, M. d. l. A. Ramirez, S. Moya, L. Salmon, J. Ruiz and D. Astruc, Dramatic synergy in CoPt nanocatalysts stabilized by "Click" dendrimers for evolution of hydrogen from hydrolysis of ammonia borane, *ACS Catal.*, 2018, **9**, 1110–1119.

210 J. M. Yan, X. B. Zhang, S. Han, H. Shioyama and Q. Xu, Magnetically recyclable Fe–Ni alloy catalyzed dehydrogenation of ammonia borane in aqueous solution under ambient atmosphere, *J. Power Sources*, 2009, **194**, 478–481.

211 X. Zhou, Z. Chen, D. Yan and H. Lu, Deposition of Fe–Ni nanoparticles on polyethyleneimine-decorated graphene oxide and application in catalytic dehydrogenation of ammonia borane, *J. Mater. Chem.*, 2012, **22**, 13506–13516.

212 S. W. Lai, H. L. Lin, Y. P. Lin and T. L. Yu, Hydrolysis of ammonia–borane catalyzed by an iron–nickel alloy on an SBA-15 support, *Int. J. Hydrogen Energy*, 2013, **38**, 4636–4647.

213 C. Cui, Y. Liu, S. Mehdi, H. Wen, B. Zhou, J. Li and B. Li, Enhancing effect of Fe-doping on the activity of nano Ni catalyst towards hydrogen evolution from NH_3BH_3, *Appl. Catal., B*, 2020, **265**, 118612.

214 F. Qiu, L. Li, G. Liu, Y. Wang, C. An, C. Xu, Y. Xu, Y. Wang, L. Jiao and H. Yuan, Synthesis of $Fe_{0.3}Co_{0.7}$/rGO nanoparticles as a high performance catalyst for the hydrolytic dehydrogenation of ammonia borane, *Int. J. Hydrogen Energy*, 2013, **38**, 7291–7297.

215 F. Qiu, L. Li, G. Liu, Y. Wang, Y. Wang, C. An, Y. Xu, C. Xu, Y. Wang, L. Jiao and H. Yuan, In situ synthesized Fe–Co/C nano-alloys as catalysts for the hydrolysis of ammonia borane, *Int. J. Hydrogen Energy*, 2013, **38**, 3241–3249.

216 F. Y. Qiu, Y. J. Wang, Y. P. Wang, L. Li, G. Liu, C. Yan, L. F. Jiao and H. T. Yuan, Dehydrogenation of ammonia borane catalyzed by in situ synthesized Fe–Co nano-alloy in aqueous solution, *Catal. Today*, 2011, **170**, 64–68.

217 S. Zhou, M. Wen, N. Wang, Q. Wu, Q. Wu and L. Cheng, Highly active NiCo alloy hexagonal nanoplates with crystal plane selective dehydrogenation and visible-light photocatalysis, *J. Mater. Chem.*, 2012, **22**, 16858–16864.

218 Q. Wang, Z. Zhang, J. Liu, R. Liu and T. Liu, Bimetallic non-noble CoNi nanoparticles monodispersed on multi-wall carbon nanotubes: Highly efficient hydrolysis of ammonia borane, *Mater. Chem. Phys.*, 2018, **204**, 58–61.

219 Z. H. Lu, J. Li, A. Zhu, Q. L. Yao, W. Huang, R. Zhou, R. Zhou and X. Chen, Catalytic hydrolysis of ammonia borane via magnetically recyclable copper iron nanoparticles for chemical hydrogen storage, *Int. J. Hydrogen Energy*, 2013, **38**, 5330–5337.

220 J. M. Yan, Z. L. Wang, H. L. Wang and Q. Jiang, Rapid and energy-efficient synthesis of a graphene–CuCo hybrid as a high performance catalyst, *J. Mater. Chem.*, 2012, **22**, 10990–10993.

221 F. Z. Song, Q. L. Zhu, X. C. Yang and Q. Xu, Monodispersed CuCo Nanoparticles supported on diamine-functionalized graphene as a non-noble metal catalyst for hydrolytic dehydrogenation of ammonia borane, *ChemNanoMat*, 2016, **2**, 942–945.

222 Y. Liu, J. Zhang, H. Guan, Y. Zhao, J. H. Yang and B. Zhang, Preparation of bimetallic Cu-Co nanocatalysts on poly (diallyldimethylammonium chloride) functionalized halloysite nanotubes for hydrolytic dehydrogenation of ammonia borane, *Appl. Surf. Sci.*, 2018, **427**, 106–113.

223 A. Bulut, M. Yurderi, İ. E. Ertas, M. Celebi, M. Kaya and M. Zahmakiran, Carbon dispersed copper-cobalt alloy nanoparticles: A cost-effective heterogeneous catalyst with exceptional performance in the hydrolytic dehydrogenation of ammonia-borane, *Appl. Catal., B*, 2016, **180**, 121–129.

224 H. Yen, Y. Seo, S. Kaliaguine and F. Kleitz, Role of Metal–support interactions, particle size, and metal–metal synergy in CuNi nanocatalysts for H_2 generation, *ACS Catal.*, 2015, **5**, 5505–5511.

225 X. Meng, S. Li, B. Xia, L. Yang, N. Cao, J. Su, M. He, W. Luo and G. Cheng, Decoration of graphene with tetrametallic Cu@FeCoNi core–shell nanoparticles for catalytic hydrolysis of amine boranes, *RSC Adv.*, 2014, **4**, 32817–32825.

226 D. Gao, Y. Zhang, L. Zhou and K. Yang, CuNi NPs supported on MIL-101 as highly active catalysts for the hydrolysis of ammonia borane, *Appl. Surf. Sci.*, 2018, **427**, 114–122.

227 S. J. Li, H. L. Wang, J. M. Yan and Q. Jiang, Oleylamine-stabilized $Cu_{0.9}Ni_{0.1}$ nanoparticles as efficient catalyst for ammonia borane dehydrogenation, *Int. J. Hydrogen Energy*, 2017, **42**, 25251–25257.

228 Z. H. Lu, J. Li, G. Feng, Q. L. Yao, F. Zhang, R. Zhou, D. Tao, X. Chen and Z. Yu, Synergistic catalysis of MCM-41 immobilized Cu–Ni nanoparticles in hydrolytic dehydrogeneration of ammonia borane, *Int. J. Hydrogen Energy*, 2014, **39**, 13389–13395.

229 K. Guo, Y. Ding, J. Luo, M. Gu and Z. Yu, NiCu Bimetallic Nanoparticles on silica support for catalytic hydrolysis of ammonia borane: Composition-dependent activity and support size effect, *ACS Appl. Energy Mater.*, 2019, **2**, 5851–5861.

230 Q. L. Yao, Z. H. Lu, Y. Wang, X. Chen and G. Feng, Synergetic catalysis of Non-noble bimetallic Cu–Co nanoparticles embedded in SiO_2 nanospheres in hydrolytic dehydrogenation of ammonia borane, *J. Phys. Chem. C*, 2015, **119**, 14167–14174.

231 J. Li, Q. L. Zhu and Q. Xu, Non-noble bimetallic CuCo nanoparticles encapsulated in the pores of metal–organic frameworks: synergetic catalysis in the hydrolysis of ammonia borane for hydrogen generation, *Catal. Sci. Technol.*, 2015, **5**, 525–530.

232 J. M. Yan, X. B. Zhang, T. Akita, M. Haruta and Q. Xu, One-step seeding growth of magnetically recyclable Au@Co core-shell nanoparticles: highly efficient catalyst for hydrolytic dehydrogenation of ammonia borane, *J. Am. Chem. Soc.*, 2010, **132**, 5326–5327.

233 H. L. Jiang, T. Akita and Q. Xu, A one-pot protocol for synthesis of non-noble metal-based core-shell nanoparticles under ambient conditions: toward highly active and cost-effective catalysts for hydrolytic dehydrogenation of NH_3BH_3, *Chem. Commun.*, 2011, **47**, 10999–11001.

234 Y. Du, N. Cao, L. Yang, W. Luo and G. Cheng, One-step synthesis of magnetically recyclable rGO supported Cu@Co core–shell nanoparticles: highly efficient catalysts for hydrolytic dehydrogenation of ammonia borane and methylamine borane, *New J. Chem.*, 2013, **37**, 3035–3042.

235 J. Zhang, H. Li, H. Zhang, Y. Zhu and G. Mi, Porously hierarchical Cu@Ni cubic-cage microstructure: Very active and durable catalyst for hydrolytically liberating H_2 gas from ammonia borane, *Renewable Energy*, 2016, **99**, 1038–1045.

236 H. L. Wang, J. M. Yan, Z. L. Wang and Q. Jiang, One-step synthesis of Cu@FeNi core–shell nanoparticles: Highly active catalyst for hydrolytic dehydrogenation of ammonia borane, *Int. J. Hydrogen Energy*, 2012, **37**, 10229–10235.

237 F. Qiu, Y. Dai, L. Li, C. Xu, Y. Huang, C. Chen, Y. Wang, L. Jiao and H. Yuan, Synthesis of Cu@FeCo core–shell nanoparticles for the catalytic hydrolysis of ammonia borane, *Int. J. Hydrogen Energy*, 2014, **39**, 436–441.

238 X. Meng, L. Yang, N. Cao, C. Du, K. Hu, J. Su, W. Luo and G. Cheng, Graphene-supported trimetallic core-shell Cu@CoNi nanoparticles for catalytic hydrolysis of amine borane, *ChemPlusChem*, 2014, **79**, 325–332.

239 H. Zhang, X. Wang, C. Chen, C. An, Y. Xu, Y. Huang, Q. Zhang, Y. Wang, L. Jiao and H. Yuan, Facile synthesis of Cu@CoNi core-shell nanoparticles composites for the catalytic hydrolysis of ammonia borane, *Int. J. Hydrogen Energy*, 2015, **40**, 12253–12261.

240 C. Wang, H. Wang, Z. Wang, X. Li, Y. Chi, M. Wang, D. Gao and Z. Zhao, Mo remarkably enhances catalytic activity of Cu@MoCo core-shell nanoparticles for hydrolytic dehydrogenation of ammonia borane, *Int. J. Hydrogen Energy*, 2018, **43**, 7347–7355.

241 Q. Liu, S. Zhang, J. Liao, K. Feng, Y. Zheng, B. G. Pollet and H. Li, $CuCo_2O_4$ nanoplate film as a low-cost, highly active and durable catalyst towards the hydrolytic dehydrogenation of ammonia borane for hydrogen production, *J. Power Sources*, 2017, **355**, 191–198.

242 J. Liao, H. Li, X. Zhang, K. Feng and Y. Yao, Fabrication of a Ti-supported $NiCo_2O_4$ nanosheet array and its superior catalytic performance in the hydrolysis of ammonia borane for hydrogen generation, *Catal. Sci. Technol.*, 2016, **6**, 3893–3899.

243 K. Feng, J. Zhong, B. Zhao, H. Zhang, L. Xu, X. Sun and S. T. Lee, $Cu_xCo_{1-x}O$ nanoparticles on graphene oxide as a aynergistic catalyst for high-efficiency hydrolysis of ammonia-borane, *Angew. Chem., Int. Ed.*, 2016, **55**, 11950–11954.

244 J. Li, X. Ren, H. Lv, Y. Wang, Y. Li and B. Liu, Highly efficient hydrogen production from hydrolysis of ammonia borane over nanostructured $Cu@CuCoO_x$ supported on graphene oxide, *J. Hazard. Mater.*, 2020, **391**, 122199.

245 Q. Liu, S. Zhang, J. Liao, X. Huang, Y. Zheng and H. Li, $MnCo_2O_4$ film composed of nanoplates: synthesis, characterization and its superior catalytic performance in the hydrolytic dehydrogenation of ammonia borane, *Catal. Sci. Technol.*, 2017, **7**, 3573–3579.

246 J. Liao, D. Lu, G. Diao, X. Zhang, M. Zhao and H. Li, $Co_{0.8}Cu_{0.2}MoO_4$ microspheres composed of nanoplatelets as a robust catalyst for the hydrolysis of ammonia borane, *ACS Sustainable Chem. Eng.*, 2018, **6**, 5843–5851.

247 D. Lu, J. Liao, Y. Leng, S. Zhong, J. He, H. Wang, R. Wang and H. Li, Mo-doped $Cu_{0.5}Ni_{0.5}Co_2O_4$ nanowires, a strong substitute for noble-metal-based catalysts towards the hydrolysis of ammonia borane for hydrogen production, *Catal. Commun.*, 2018, **114**, 89–92.

248 D. Lu, J. Liao, H. Li, S. Ji and B. G. Pollet, $Co_3O_4/CuMoO_4$ hybrid microflowers composed of nanorods with rich particle boundaries as a highly active catalyst for ammonia borane Hydrolysis, *ACS Sustainable Chem. Eng.*, 2019, **7**, 16474–16482.

249 J. Liao, Y. Feng, W. Lin, X. Su, S. Ji, L. Li, W. Zhang, B. G. Pollet and H. Li, $CuO–NiO/Co_3O_4$ hybrid nanoplates as highly active catalyst for ammonia borane hydrolysis, *Int. J. Hydrogen Energy*, 2020, **45**, 8168–8176.

250 D. Lu, J. Li, C. Lin, J. Liao, Y. Feng, Z. Ding, Z. Li, Q. Liu and H. Li, A Simple and scalable route to synthesize $Co_xCu_{1-x}Co_2O_4@Co_yCu_{1-y}Co_2O_4$ yolk-shell microspheres, A high-performance catalyst to hydrolyze ammonia borane for hydrogen production, *Small*, 2019, **15**, e1805460.

251 R. Fernandes, N. Patel, A. Miotello, R. Jaiswal and D. C. Kothari, Dehydrogenation of ammonia borane with transition metal-doped Co–B alloy catalysts, *Int. J. Hydrogen Energy*, 2012, **37**, 2397–2406.

252 A. K. Figen and B. Coşkuner, A novel perspective for hydrogen generation from ammonia borane (NH_3BH_3) with Co–B catalysts: "Ultrasonic hydrolysis", *Int. J. Hydrogen Energy*, 2013, **38**, 2824–2835.

253 K. Eom, K. Cho and H. Kwon, Hydrogen generation from hydrolysis of NH_3BH_3 by an electroplated Co–P catalyst, *Int. J. Hydrogen Energy*, 2010, **35**, 181–186.

254 C. Y. Peng, L. Kang, S. Cao, Y. Chen, Z. S. Lin and W. F. Fu, Nanostructured Ni_2P as a robust catalyst for the hydrolytic dehydrogenation of ammonia-borane, *Angew. Chem., Int. Ed.*, 2015, **54**, 15725–15729.

255 C. Tang, L. Xie, K. Wang, G. Du, A. M. Asiri, Y. Luo and X. Sun, A Ni2P nanosheet array integrated on 3D Ni foam: an efficient, robust and reusable monolithic catalyst for the hydrolytic dehydrogenation of ammonia borane toward on-demand hydrogen generation, *J. Mater. Chem. A*, 2016, **4**, 12407–12410.

256 C. Tang, F. Qu, A. M. Asiri, Y. Luo and X. Sun, CoP nanoarray: a robust non-noble-metal hydrogen-generating catalyst toward effective hydrolysis of ammonia borane, *Inorg. Chem. Front.*, 2017, **4**, 659–662.

257 X. Qu, R. Jiang, Q. Li, F. Zeng, X. Zheng, Z. Xu, C. Chen and J. Peng, The hydrolysis of ammonia borane catalyzed by NiCoP/OPC-300 nanocatalysts: high selectivity and efficiency, and mechanism, *Green Chem.*, 2019, **21**, 850–860.

258 N. Patel, R. Fernandes, G. Guella and A. Miotello, Nanoparticle-assembled Co-B thin film for the hydrolysis of ammonia borane: A highly active catalyst for hydrogen production, *Appl. Catal., B*, 2010, **95**, 137–143.

259 N. Patel, R. Fernandes, S. Gupta, R. Edla, D. C. Kothari and A. Miotello, Co-B catalyst supported over mesoporous silica for hydrogen production by catalytic hydrolysis of Ammonia Borane: A study on influence of pore structure, *Appl. Catal., B*, 2013, **140–141**, 125–132.

260 Y. Zou, J. Cheng, Q. Wang, C. Xiang, H. Chu, S. Qiu, H. Zhang, F. Xu, S. Liu, C. Tang and L. Sun, Cobalt–boron/nickel–boron nanocomposite with improved catalytic performance for the hydrolysis of ammonia borane, *Int. J. Hydrogen Energy*, 2015, **40**, 13423–13430.

261 H. Wang, D. Gao, L. Wang, Y. Chi, M. Wang, Y. Gu, C. Wang and Z. Zhao, Highly dispersed surfactant-free amorphous NiCoB nanoparticles and their remarkable catalytic activity for hydrogen generation from ammonia borane dehydrogenation, *Catal. Lett.*, 2018, **148**, 1739–1749.

262 Z. C. Fu, Y. Xu, S. L. Chan, W. W. Wang, F. Li, F. Liang, Y. Chen, Z. S. Lin, W. F. Fu and C. M. Che, Highly efficient hydrolysis of ammonia borane by anion OH^-, F^-, Cl^--tuned interactions between reactant molecules and CoP nanoparticles, *Chem. Commun.*, 2017, **53**, 705–708.

263 C. C. Hou, Q. Li, C. J. Wang, C. Y. Peng, Q. Q. Chen, H. F. Ye, W. F. Fu, C. M. Che, N. López and Y. Chen, Ternary Ni–Co–P nanoparticles as noble-metal-free cata-

lysts to boost the hydrolytic dehydrogenation of ammonia-borane, *Energy Environ. Sci.*, 2017, **10**, 1770–1776.

264 X. Yang, F. Cheng, Z. Tao and J. Chen, Hydrolytic dehydrogenation of ammonia borane catalyzed by carbon supported Co core–Pt shell nanoparticles, *J. Power Sources*, 2011, **196**, 2785–2789.

265 W. Y. Chen, D. L. Li, Z. J. Wang, G. Qian, Z. J. Sui, X. Z. Duan, X. G. Zhou, I. Yeboah and D. Chen, Reaction mechanism and kinetics for hydrolytic dehydrogenation of ammonia borane on a Pt/CNT catalyst, *AIChE J.*, 2017, **63**, 60–65.

266 D. Sun, V. Mazumder, Ö. Metin and S. Sun, Methanolysis of ammonia baorane by CoPd nanoparticles, *ACS Catal.*, 2012, **2**, 1290–1295.

267 D. Özhava, N. Z. Kılıçaslan and S. Özkar, PVP-stabilized nickel(0) nanoparticles as catalyst in hydrogen generation from the methanolysis of hydrazine borane or ammonia borane, *Appl. Catal., B*, 2015, **162**, 573–582.

268 D. Özhava and S. Özkar, Rhodium(0) nanoparticles supported on nanosilica: Highly active and long lived catalyst in hydrogen generation from the methanolysis of ammonia borane, *Appl. Catal., B*, 2016, **181**, 716–726.

269 Y. Fang, J. Li, T. Togo, F. Jin, Z. Xiao, L. Liu, H. Drake, X. Lian and H. C. Zhou, Ultra-small face-centered-cubic Ru nanoparticles confined within a porous coordination cage for dehydrogenation, *Chem*, 2018, **4**, 555–563.

270 A. K. Figen, Improved catalytic performance of metal oxide catalysts fabricated with electrospinning in ammonia borane methanolysis for hydrogen production, *Int. J. Hydrogen Energy*, 2019, **44**, 28451–28462.

271 E. G. Sogut, H. Acidereli, E. Kuyuldar, Y. Karatas, M. Gulcan and F. Sen, Single-walled carbon nanotube supported Pt-Ru bimetallic superb nanocatalyst for the hydrogen generation from the methanolysis of methylamine-borane at mild conditions, *Sci. Rep.*, 2019, **9**, 15724.

272 S. E. Korkut, H. Kucukkececi and Ö. Metin, Mesoporous graphitic carbon nitride/black phosphorus/AgPd alloy nanoparticles ternary nanocomposite: A highly efficient catalyst for the methanolysis of ammonia borane, *ACS Appl. Mater. Interfaces*, 2020, **12**, 8130–8139.

273 X. Li, C. Zhang, M. Luo, Q. L. Yao and Z. H. Lu, Ultrafine Rh nanoparticles confined by nitrogen-rich covalent organic frameworks for methanolysis of ammonia borane, *Inorg. Chem. Front.*, 2020, **7**, 1298–1306.

274 K. O. Amoo, E. N. Onyeozili, E. E. Kalu, J. A. Omoleye and V. E. Efeovbokhan, Activity of varying compositions of Co–Ni–P catalysts for the methanolysis of ammonia borane, *Int. J. Hydrogen Energy*, 2016, **41**, 21221–21235.

275 J. Zhang, Y. Duan, Y. Zhu, Y. Wang, H. Yao and G. Mi, Evenly dispersed microspherical amorphous alloy Co x B 1-x : Robust and magnetically recyclable catalyst for alcoholyzing ammonia borane to release H_2, *Mater. Chem. Phys.*, 2017, **201**, 297–301.

276 S. B. Kalidindi, A. A. Vernekar and B. R. Jagirdar, Co-Co_2B, Ni-Ni_3B and Co-Ni-B nanocomposites catalyzed ammonia-borane methanolysis for hydrogen generation, *Phys. Chem. Chem. Phys.*, 2009, **11**, 770–775.

277 Q. L. Yao, M. Huang, Z. H. Lu, Y. Yang, Y. Zhang, X. Chen and Z. Yang, Methanolysis of ammonia borane by shape-controlled mesoporous copper nanostructures for hydrogen generation, *Dalton Trans.*, 2015, **44**, 1070–1076.

278 M. Yurderi, A. Bulut, I. E. Ertas, M. Zahmakiran and M. Kaya, Supported copper-copper oxide nanoparticles as active, stable and low-cost catalyst in the methanolysis of ammonia-borane for chemical hydrogen storage, *Appl. Catal., B*, 2015, **165**, 169–175.

279 L. Cui, X. Cao, X. Sun, W. Yang and J. Liu, A Bunch-like copper oxide nanowire array as an efficient, durable, and economical catalyst for the methanolysis of ammonia borane, *ChemCatChem*, 2018, **10**, 710–715.

280 C. Yu, J. Fu, M. Muzzio, T. Shen, D. Su, J. Zhu and S. Sun, CuNi nanoparticles assembled on graphene for catalytic methanolysis of ammonia borane and hydrogenation of nitro/nitrile compounds, *Chem. Mater.*, 2017, **29**, 1413–1418.

281 Q. Q. Chen, Q. Li, C. C. Hou, C. J. Wang, C. Y. Peng, N. López and Y. Chen, Enhancing electrostatic interactions to activate polar molecules: ammonia borane methanolysis on a Cu/$Co(OH)_2$ nanohybrid, *Catal. Sci. Technol.*, 2019, **9**, 2828–2835.

282 "Nitrogen (Fixed)–Ammonia", U.S. Geological Survey, Mineral Commodity Summaries, 2017.

283 L. Greenjr, An ammonia energy vector for the hydrogen economy, *Int. J. Hydrogen Energy*, 1982, **7**, 355–359.

284 S. F. Yin, B. Q. Xu, X. P. Zhou and C. T. Au, A mini-review on ammonia decomposition catalysts for on-site generation of hydrogen for fuel cell applications, *Appl. Catal., A*, 2004, **277**, 1–9.

285 A. Klerke, C. H. Christensen, J. K. Nørskov and T. Vegge, Ammonia for hydrogen storage: challenges and opportunities, *J. Mater. Chem.*, 2008, **18**, 2304–2310.

286 F. Schüth, R. Palkovits, R. Schlögl and D. S. Su, Ammonia as a possible element in an energy infrastructure: catalysts for ammonia decomposition, *Energy Environ. Sci.*, 2012, **5**, 6278–6289.

287 C. H. Christensen, T. Johannessen, R. Z. Sørensen and J. K. Nørskov, Towards an ammonia-mediated hydrogen economy?, *Catal. Today*, 2006, **111**, 140–144.

288 D. A. Hansgen, D. G. Vlachos and J. G. Chen, Using first principles to predict bimetallic catalysts for the ammonia decomposition reaction, *Nat. Chem.*, 2010, **2**, 484–489.

289 A. Srifa, K. Okura, T. Okanishi, H. Muroyama, T. Matsui and K. Eguchi, COx-free hydrogen production via ammonia decomposition over molybdenum nitride-based catalysts, *Catal. Sci. Technol.*, 2016, **6**, 7495–7504.

290 T. Umegaki, J. M. Yan, X. B. Zhang, H. Shioyama, N. Kuriyama and Q. Xu, Boron- and nitrogen-based chemical hydrogen storage materials, *Int. J. Hydrogen Energy*, 2009, **34**, 2303–2311.

291 K. Hashimoto and N. Toukai, Decomposition of ammonia over a catalyst consisting of ruthenium metal and cerium

oxides supported on Y-form zeolite, *J. Mol. Catal. A: Chem.*, 2000, **161**, 171–178.

292 A. Boisen, S. Dahl, J. Norskov and C. Christensen, Why the optimal ammonia synthesis catalyst is not the optimal ammonia decomposition catalyst, *J. Catal.*, 2005, **230**, 309–312.

293 C. J. Jacobsen, S. Dahl, B. S. Clausen, S. Bahn, A. Logadottir and J. K. Norskov, Catalyst design by interpolation in the periodic table: Bimetallic ammonia synthesis catalysts, *J. Am. Chem. Soc.*, 2001, **123**, 8404–8405.

294 W. Raróg-Pilecka, Ammonia decomposition over the carbon-based ruthenium catalyst promoted with barium or cesium, *J. Catal.*, 2003, **218**, 465–469.

295 S. F. Yin, B. Q. Xu, C. F. Ng and C. T. Au, Nano Ru/CNTs: a highly active and stable catalyst for the generation of CO -free hydrogen in ammonia decomposition, *Appl. Catal., B*, 2004, **48**, 237–241.

296 L. Li, Z. H. Zhu, Z. F. Yan, G. Q. Lu and L. Rintoul, Catalytic ammonia decomposition over Ru/carbon catalysts: The importance of the structure of carbon support, *Appl. Catal., A*, 2007, **320**, 166–172.

297 Z. Wang, Z. Cai and Z. Wei, Highly Active Ruthenium catalyst supported on barium hexaaluminate for ammonia decomposition to CO_x-free hydrogen, *ACS Sustainable Chem. Eng.*, 2019, **7**, 8226–8235.

298 X. C. Hu, X. P. Fu, W. W. Wang, X. Wang, K. Wu, R. Si, C. Ma, C. J. Jia and C. H. Yan, Ceria-supported ruthenium clusters transforming from isolated single atoms for hydrogen production via decomposition of ammonia, *Appl. Catal., B*, 2020, **268**, 118424.

299 Z. Kowalczyk, J. Sentek, S. Jodzis, M. Muhler and O. Hinrichsen, Effect of potassium on the kinetics of ammonia synthesis and decomposition over fused iron catalyst at atmospheric pressure, *J. Catal.*, 1997, **169**, 407–414.

300 X. Duan, J. Ji, G. Qian, C. Fan, Y. Zhu, X. Zhou, D. Chen and W. Yuan, Ammonia decomposition on Fe(110), Co (111) and Ni(111) surfaces: A density functional theory study, *J. Mol. Catal. A: Chem.*, 2012, **357**, 81–86.

301 D. Rein, K. F. Ortega, C. Weidenthaler, E. Bill and M. Behrens, The roles of Co-precipitation pH, phase-purity and alloy formation for the ammonia decomposition activity of Ga-promoted Fe/MgO catalysts, *Appl. Catal., A*, 2017, **548**, 52–61.

302 Z. P. Hu, L. Chen, C. Chen and Z. Y. Yuan, Fe/ZSM-5 catalysts for ammonia decomposition to CO_x-free hydrogen: effect of SiO_2/Al_2O_3 ratio, *Mol. Catal.*, 2018, **455**, 14–22.

303 Z. P. Hu, L. Chen, C. C. Weng and Z. Y. Yuan, Fe nanocatalysts supported on dealuminated ZSM-5 for efficient decomposition of ammonia to CO_x-free Hydrogen, *ChemistrySelect*, 2018, **3**, 4439–4447.

304 Y. Q. Gu, Z. Jin, H. Zhang, R. J. Xu, M. J. Zheng, Y. M. Guo, Q. S. Song and C. J. Jia, Transition metal nanoparticles dispersed in an alumina matrix as active and stable catalysts for COx-free hydrogen production from ammonia, *J. Mater. Chem. A*, 2015, **3**, 17172–17180.

305 X. Duan, G. Qian, X. Zhou, Z. Sui, D. Chen and W. Yuan, Tuning the size and shape of Fe nanoparticles on carbon nanofibers for catalytic ammonia decomposition, *Appl. Catal., B*, 2011, **101**, 189–196.

306 Z. P. Hu, C. C. Weng, C. Chen and Z. Y. Yuan, Two-dimensional mica nanosheets supported Fe nanoparticles for NH3 decomposition to hydrogen, *Mol. Catal.*, 2018, **448**, 162–170.

307 A. H. Lu, J. J. Nitz, M. Comotti, C. Weidenthaler, K. Schlichte, C. W. Lehmann, O. Terasaki and F. Schuth, Spatially and size selective synthesis of Fe-based nanoparticles on ordered mesoporous supports as highly active and stable catalysts for ammonia decomposition, *J. Am. Chem. Soc.*, 2010, **132**, 14152–14162.

308 Y. Li, S. Liu, L. Yao, W. Ji and C. T. Au, Core-shell structured iron nanoparticles for the generation of CO_x-free hydrogen via ammonia decomposition, *Catal. Commun.*, 2010, **11**, 368–372.

309 D. Varisli, C. Korkusuz and T. Dogu, Microwave-assisted ammonia decomposition reaction over iron incorporated mesoporous carbon catalysts, *Appl. Catal., B*, 2017, **201**, 370–380.

310 J. C. Ganley, F. S. Thomas, E. G. Seebauer and R. I. Masel, A priori catalytic activity correlations: the difficult case of hydrogen production from ammonia, *Catal. Lett.*, 2004, **96**, 117–122.

311 J. Zhang, H. Xu, X. Jin, Q. Ge and W. Li, Characterizations and activities of the nano-sized Ni/Al_2O_3 and $Ni/La–Al_2O_3$ catalysts for NH_3 decomposition, *Appl. Catal., A*, 2005, **290**, 87–96.

312 Z. P. Hu, C. C. Weng, C. Chen and Z. Y. Yuan, Catalytic decomposition of ammonia to CO_x-free hydrogen over Ni/ZSM-5 catalysts: A comparative study of the preparation methods, *Appl. Catal., A*, 2018, **562**, 49–57.

313 D. Sima, H. Wu, K. Tian, S. Xie, J. J. Foo, S. Li, D. Wang, Y. Ye, Z. Zheng and Y.-Q. Liu, Enhanced low temperature catalytic activity of $Ni/Al–Ce_{0.8}Zr_{0.2}O_2$ for hydrogen production from ammonia decomposition, *Int. J. Hydrogen Energy*, 2020, **45**, 9342–9352.

314 Y. Yu, Y.-M. Gan, C. Huang, Z. H. Lu, X. Wang, R. Zhang and G. Feng, Ni/La_2O_3 and $Ni/MgO–La_2O_3$ catalysts for the decomposition of NH_3 into hydrogen, *Int. J. Hydrogen Energy*, 2020, **45**, 16528–16539.

315 W. Zheng, J. Zhang, Q. Ge, H. Xu and W. Li, Effects of CeO_2 addition on Ni/Al_2O_3 catalysts for the reaction of ammonia decomposition to hydrogen, *Appl. Catal., B*, 2008, **80**, 98–105.

316 H. Liu, H. Wang, J. Shen, Y. Sun and Z. Liu, Promotion effect of cerium and lanthanum oxides on Ni/SBA-15 catalyst for ammonia decomposition, *Catal. Today*, 2008, **131**, 444–449.

317 K. Okura, T. Okanishi, H. Muroyama, T. Matsui and K. Eguchi, Ammonia decomposition over nickel catalysts supported on rare-earth oxides for the on-site generation of hydrogen, *ChemCatChem*, 2016, **8**, 2988–2995.

318 K. Okura, T. Okanishi, H. Muroyama, T. Matsui and K. Eguchi, Additive effect of alkaline earth metals on ammonia decomposition reaction over Ni/Y_2O_3 catalysts, *RSC Adv.*, 2016, **6**, 85142–85148.

319 I. Lucentini, I. Serrano, L. Soler, N. J. Divins and J. Llorca, Ammonia decomposition over 3D-printed CeO_2 structures loaded with Ni, *Appl. Catal., A*, 2020, **591**, 117382.

320 J. Zhang, M. Comotti, F. Schüth, R. Schlögl and D. S. Su, Commercial Fe- or Co-containing carbon nanotubes as catalysts for NH_3 decomposition, *Chem. Commun.*, 2007, 1916–1918.

321 H. Zhang, Y. A. Alhamed, Y. Kojima, A. A. Al-Zahrani and L. A. Petrov, Cobalt supported on carbon nanotubes. An efficient catalyst for ammonia decomposition, *C. R. Acad. Bulg. Sci.*, 2013, **66**, 519–524.

322 H. Zhang, Y. A. Alhamed, W. Chu, Z. Ye, A. AlZahrani and L. Petrov, Controlling Co-support interaction in Co/MWCNTs catalysts and catalytic performance for hydrogen production via NH_3 decomposition, *Appl. Catal., A*, 2013, **464–465**, 156–164.

323 L. Li, R. Jiang, W. Chu, H. Cang, H. Chen and J. Yan, Cobalt nanoparticles embedded in a porous carbon matrix as an efficient catalyst for ammonia decomposition, *Catal. Sci. Technol.*, 2017, **7**, 1363–1371.

324 S. Podila, Y. A. Alhamed, A. A. AlZahrani and L. A. Petrov, Hydrogen production by ammonia decomposition using Co catalyst supported on Mg mixed oxide systems, *Int. J. Hydrogen Energy*, 2015, **40**, 15411–15422.

325 S. Podila, H. Driss, S. F. Zaman, A. M. Ali, A. A. Al-Zahrani, M. A. Daous and L. A. Petrov, Effect of preparation methods on the catalyst performance of Co/Mg La mixed oxide catalyst for CO_x-free hydrogen production by ammonia decomposition, *Int. J. Hydrogen Energy*, 2017, **42**, 24213–24221.

326 X. C. Hu, W. W. Wang, Y. Q. Gu, Z. Jin, Q. S. Song and C. J. Jia, Ammonia decomposition for CO_x-free hydrogen production over $Co\text{-}SiO_2$ nanocomposite catalysts, *ChemPlusChem*, 2017, **82**, 368–375.

327 X. Duan, G. Qian, X. Zhou, D. Chen and W. Yuan, MCM-41 supported CoMo bimetallic catalysts for enhanced hydrogen production by ammonia decomposition, *Chem. Eng. J.*, 2012, **207–208**, 103–108.

328 J. Ji, X. Duan, G. Qian, X. Zhou, G. Tong and W. Yuan, Towards an efficient $CoMo/\gamma\text{-}Al_2O_3$ catalyst using metal amine metallate as an active phase precursor: Enhanced hydrogen production by ammonia decomposition, *Int. J. Hydrogen Energy*, 2014, **39**, 12490–12498.

329 X. Duan, J. Ji, X. Yan, G. Qian, D. Chen and X. Zhou, Understanding Co-Mo catalyzed ammonia decomposition: influence of calcination atmosphere and identification of active phase, *ChemCatChem*, 2016, **8**, 938–945.

330 B. Lorenzut, T. Montini, M. Bevilacqua and P. Fornasiero, FeMo-based catalysts for H_2 production by NH_3 decomposition, *Appl. Catal., B*, 2012, **125**, 409–417.

331 J. Zhang, J. O. Muller, W. Zheng, D. Wang, D. Su and R. Schlogl, Individual Fe-Co alloy nanoparticles on carbon nanotubes: structural and catalytic properties, *Nano Lett.*, 2008, **8**, 2738–2743.

332 Z. Lendzion-Bieluń and W. Arabczyk, Fused FeCo catalysts for hydrogen production by means of the ammonia decomposition reaction, *Catal. Today*, 2013, **212**, 215–219.

333 Z. Lendzion-Bieluń, R. Pelka and Ł. Czekajło, Characterization of FeCo based catalyst for ammonia decomposition. The effect of potassium oxide, *Pol. J. Chem. Technol.*, 2014, **16**, 111–116.

334 L. Huo, B. Liu, H. Li, B. Cao, X. C. Hu, X. P. Fu, C. Jia and J. Zhang, Component synergy and armor protection induced superior catalytic activity and stability of ultrathin Co-Fe spinel nanosheets confined in mesoporous silica shells for ammonia decomposition reaction, *Appl. Catal., B*, 2019, **253**, 121–130.

335 S. B. Simonsen, D. Chakraborty, I. Chorkendorff and S. Dahl, Alloyed Ni-Fe nanoparticles as catalysts for NH_3 decomposition, *Appl. Catal., A*, 2012, **447–448**, 22–31.

336 H. Silva, M. G. Nielsen, E. M. Fiordaliso, C. D. Damsgaard, C. Gundlach, T. Kasama, I. B. Chorkendorff and D. Chakraborty, Synthesis and characterization of Fe–Ni/É£-Al_2O_3 egg-shell catalyst for H2 generation by ammonia decomposition, *Appl. Catal., A*, 2015, **505**, 548–556.

337 Y. Yi, L. Wang, Y. Guo, S. Sun and H. Guo, Plasma–assisted ammonia decomposition over Fe–Ni alloy catalysts for CO_x–free hydrogen, *AIChE J.*, 2019, **65**, 691–701.

338 C. Huang, H. Li, J. Yang, C. Wang, F. Hu, X. Wang, Z. H. Lu, G. Feng and R. Zhang, $Ce_{0.6}Zr_{0.3}Y_{0.1}O_2$ solid solutions-supported Ni Co bimetal nanocatalysts for NH_3 decomposition, *Appl. Surf. Sci.*, 2019, **478**, 708–716.

339 S. S. Pansare, W. Torres and J. G. Goodwin, Ammonia decomposition on tungsten carbide, *Catal. Commun.*, 2007, **8**, 649–654.

340 X. Cui, H. Li, L. Guo, D. He, H. Chen and J. Shi, Synthesis of mesoporous tungsten carbide by an impregnation-compaction route, and its NH_3 decomposition catalytic activity, *Dalton Trans.*, 2008, 6435–6440.

341 A. Kraupner, A. Markus, R. Palkovits, K. Schlicht and C. Giordano, Mesoporous Fe_3C sponges as magnetic supports and as heterogeneous catalyst, *J. Mater. Chem.*, 2010, **20**, 6019–6022.

342 J. C. Ingersoll, N. Mani, J. C. Thenmozhiyal and A. Muthaiah, Catalytic hydrolysis of sodium borohydride by a novel nickel–cobalt–boride catalyst, *J. Power Sources*, 2007, **173**, 450–457.

343 J. G. Choi, Synthesis and catalytic properties of porous Ta carbide crystallites for hydrogen production from the decomposition of ammonia, *J. Porous Mater.*, 2013, **20**, 1059–1068.

344 W. Zheng, T. P. Cotter, P. Kaghazchi, T. Jacob, B. Frank, K. Schlichte, W. Zhang, D. S. Su, F. Schuth and R. Schlogl, Experimental and theoretical investigation of molybdenum carbide and nitride as catalysts for ammonia decomposition, *J. Am. Chem. Soc.*, 2013, **135**, 3458–3464.

345 C. Liang, W. Li, Z. Wei, Q. Xin and C. Li, Catalytic Decomposition of ammonia over nitrided $MoN_x/\alpha\text{-}Al_2O_3$

and $NiMoN_y/\alpha$-Al_2O_3 catalysts, *Ind. Eng. Chem. Res.*, 2000, **39**, 3694–3697.

346 D. V. Leybo, A. N. Baiguzhina, D. S. Muratov, D. I. Arkhipov, E. A. Kolesnikov, V. V. Levina, N. I. Kosova and D. V. Kuznetsov, Effects of composition and production route on structure and catalytic activity for ammonia decomposition reaction of ternary Ni–Mo nitride catalysts, *Int. J. Hydrogen Energy*, 2016, **41**, 3854–3860.

347 S. Podila, S. F. Zaman, H. Driss, A. A. Al-Zahrani, M. A. Daous and L. A. Petrov, High performance of bulk Mo_2N and Co_3Mo_3N catalysts for hydrogen production from ammonia: Role of citric acid to Mo molar ratio in preparation of high surface area nitride catalysts, *Int. J. Hydrogen Energy*, 2017, **42**, 8006–8020.

348 A. Srifa, K. Okura, T. Okanishi, H. Muroyama, T. Matsui and K. Eguchi, Hydrogen production by ammonia decomposition over Cs-modified Co_3Mo_3N catalysts, *Appl. Catal., B*, 2017, **218**, 1–8.

349 L. A. Jolaoso, S. F. Zaman, S. Podila, H. Driss, A. A. Al-Zahrani, M. A. Daous and L. Petrov, Ammonia decomposition over citric acid induced γ-Mo_2N and Co_3Mo_3N catalysts, *Int. J. Hydrogen Energy*, 2018, **43**, 4839–4844.

350 S. F. Zaman, L. A. Jolaoso, S. Podila, A. A. Al-Zahrani, Y. A. Alhamed, H. Driss, M. M. Daous and L. Petrov, Ammonia decomposition over citric acid chelated γ-Mo_2N and Ni_2Mo_3N catalysts, *Int. J. Hydrogen Energy*, 2018, **43**, 17252–17258.

351 P. X. Zhang, Y. G. Wang, Y. Q. Huang, T. Zhang, G. S. Wu and J. Li, Density functional theory investigations on the catalytic mechanisms of hydrazine decompositions on Ir (111), *Catal. Today*, 2011, **165**, 80–88.

352 H. Gu, R. Ran, W. Zhou, Z. Shao, W. Jin, N. Xu and J. Ahn, Solid-oxide fuel cell operated on in situ catalytic decomposition products of liquid hydrazine, *J. Power Sources*, 2008, **177**, 323–329.

353 M. Zheng, X. Chen, R. Cheng, N. Li, J. Sun, X. Wang and T. Zhang, Catalytic decomposition of hydrazine on iron nitride catalysts, *Catal. Commun.*, 2006, **7**, 187–191.

354 M. Zheng, R. Cheng, X. Chen, N. Li, L. Li, X. Wang and T. Zhang, A novel approach for CO-free H production via catalytic decomposition of hydrazine, *Int. J. Hydrogen Energy*, 2005, **30**, 1081–1089.

355 J. Santos, Catalytic Decomposition of hydrazine on tungsten carbide: The Influence of adsorbed oxygen, *J. Catal.*, 2002, **210**, 1–6.

356 X. Chen, T. Zhang, P. Ying, M. Zheng, W. Wu, L. Xia, T. Li, X. Wang and C. Li, A novel catalyst for hydrazine decomposition: molybdenum carbide support on γ-Al_2O_3, *Chem. Commun.*, 2002, 288–289.

357 X. W. Chen, T. Zhang, L. G. Xia, T. Li, M. Y. Zheng, Z. L. Wu, X. D. Wang, Z. B. Wei, Q. Xin and C. Li, Catalytic decomposition of hydrazine over supported molybdenum nitride catalysts in a monopropellant thruster, *Catal. Lett.*, 2002, **79**, 21–25.

358 L. Ding, Y. Shu, A. Wang, M. Zheng, L. Li, X. Wang and T. Zhang, Preparation and catalytic performances of ternary phosphides NiCoP for hydrazine decomposition, *Appl. Catal., A*, 2010, **385**, 232–237.

359 S. K. Singh and Q. Xu, Nanocatalysts for hydrogen generation from hydrazine, *Catal. Sci. Technol.*, 2013, **3**, 1889.

360 D. Bhattacharjee and S. Dasgupta, Trimetallic NiFePd nanoalloy catalysed hydrogen generation from alkaline hydrous hydrazine and sodium borohydride at room temperature, *J. Mater. Chem. A*, 2015, **3**, 24371–24378.

361 Y. P. Qiu, Q. Shi, L. L. Zhou, M. H. Chen, C. Chen, P. P. Tang, G. S. Walker and P. Wang, NiPt nanoparticles anchored onto hierarchical nanoporous N-doped carbon as an efficient catalyst for hydrogen generation from hydrazine monohydrate, *ACS Appl. Mater. Interfaces*, 2020, **12**, 18617–18624.

362 A. Kumar, X. Yang and Q. Xu, Ultrafine bimetallic Pt–Ni nanoparticles immobilized on 3-dimensional N-doped graphene networks: a highly efficient catalyst for dehydrogenation of hydrous hydrazine, *J. Mater. Chem. A*, 2019, **7**, 112–115.

363 F. Z. Song, X. Yang and Q. Xu, Ultrafine bimetallic Pt–Ni nanoparticles achieved by metal–organic framework templated zirconia/porous carbon/reduced graphene oxide: remarkable catalytic activity in dehydrogenation of hydrous hydrazine, *Small Methods*, 2019, **4**, 1900707.

364 H. L. Wang, J. M. Yan, Z. L. Wang, O. Song-Il and Q. Jiang, Highly efficient hydrogen generation from hydrous hydrazine over amorphous $Ni_{0.9}Pt_{0.1}/Ce_2O_3$ nanocatalyst at room temperature, *J. Mater. Chem. A*, 2013, **1**, 14957–14962.

365 X. Lu, S. Francis, D. Motta, N. Dimitratos and A. Roldan, Mechanistic study of hydrazine decomposition on Ir(111), *Phys. Chem. Chem. Phys.*, 2020, **22**, 3883–3896.

366 H. Wang, L. Wu, Y. Wang, X. Li and Y. Wang, Facile synthesis of Ni nanoparticles from triangular $Ni(HCO_3)_2$ nanosheets as catalysts for hydrogen generation from hydrous hydrazine, *Catal. Commun.*, 2017, **100**, 33–37.

367 T. Liu, J. Yu, H. Bie and Z. Hao, Highly efficient hydrogen generation from hydrous hydrazine using a reduced graphene oxide-supported NiPtP nanoparticle catalyst, *J. Alloys Compd.*, 2017, **690**, 783–790.

368 S. K. Singh, X. B. Zhang and Q. Xu, Room-temperature hydrogen generation from hydrous hydrazine for chemical hydrogen storage, *J. Am. Chem. Soc.*, 2009, **131**, 9894–9895.

369 L. He, Y. Huang, A. Wang, X. Wang and T. Zhang, H_2 production by selective decomposition of hydrous hydrazine over Raney Ni catalyst under ambient conditions, *AIChE J.*, 2013, **59**, 4297–4302.

370 L. He, B. Liang, L. Li, X. Yang, Y. Huang, A. Wang, X. Wang and T. Zhang, Cerium-oxide-modified nickel as a non-noble metal catalyst for selective decomposition of hydrous hydrazine to hydrogen, *ACS Catal.*, 2015, **5**, 1623–1628.

371 Q. Fu, P. Yang, J. Wang, H. Wang, L. Yang and X. Zhao, In situ synthesis of Ni nanofibers via vacuum thermal

reduction and their efficient catalytic properties for hydrogen generation, *J. Mater. Chem. A*, 2018, **6**, 11370–11376.

372 H. Yin, Y. P. Qiu, H. Dai, L. Y. Gan, H. B. Dai and P. Wang, Understanding of selective H_2 generation from hydrazine decomposition on Ni(111) surface, *J. Phys. Chem. C*, 2018, **122**, 5443–5451.

373 N. Cao, L. Yang, C. Du, J. Su, W. Luo and G. Cheng, Highly efficient dehydrogenation of hydrazine over graphene supported flower-like Ni–Pt nanoclusters at room temperature, *J. Mater. Chem. A*, 2014, **2**, 14344–14347.

374 H. Ma, H. Wang and C. Na, Microwave-assisted optimization of platinum-nickel nanoalloys for catalytic water treatment, *Appl. Catal., B*, 2015, **163**, 198–204.

375 C. Wan, L. Sun, L. Xu, D. G. Cheng, F. Chen, X. Zhan and Y. Yang, Novel NiPt alloy nanoparticle decorated 2D layered g-C_3N_4 nanosheets: a highly efficient catalyst for hydrogen generation from hydrous hydrazine, *J. Mater. Chem. A*, 2019, **7**, 8798–8804.

376 M. Zhang, L. Liu, S. Lu, L. Xu, Y. An and C. Wan, Facile fabrication of NiPt/CNTs as an efficient catalyst for hydrogen production from hydrous hydrazine, *ChemistrySelect*, 2019, **4**, 10494–10500.

377 F. Guo, H. Zou, Q. L. Yao, B. Huang and Z. H. Lu, Monodispersed bimetallic nanoparticles anchored on TiO_2-decorated titanium carbide MXene for efficient hydrogen production from hydrazine in aqueous solution, *Renewable Energy*, 2020, **155**, 1293–1301.

378 J. Wang, X. B. Zhang, Z. L. Wang, L. M. Wang and Y. Zhang, Rhodium–nickel nanoparticles grown on graphene as highly efficient catalyst for complete decomposition of hydrous hydrazine at room temperature for chemical hydrogen storage, *Energy Environ. Sci.*, 2012, **5**, 6885–6888.

379 J. Wang, W. Li, Y. Wen, L. Gu and Y. Zhang, Rh-Ni-B Nanoparticles as highly efficient catalysts for hydrogen generation from hydrous hydrazine, *Adv. Energy Mater.*, 2015, **5**, 1401879.

380 J. B. Yoo, H. S. Kim, S. H. Kang, B. Lee and N. H. Hur, Hollow nickel-coated silica microspheres containing rhodium nanoparticles for highly selective production of hydrogen from hydrous hydrazine, *J. Mater. Chem. A*, 2014, **2**, 18929–18937.

381 P. Zhao, N. Cao, W. Luo and G. Cheng, Nanoscale MIL-101 supported RhNi nanoparticles: an efficient catalyst for hydrogen generation from hydrous hydrazine, *J. Mater. Chem. A*, 2015, **3**, 12468–12475.

382 J. Chen, Q. L. Yao, J. Zhu, X. Chen and Z. H. Lu, Rh–Ni nanoparticles immobilized on $Ce(OH)CO_3$ nanorods as highly efficient catalysts for hydrogen generation from alkaline solution of hydrazine, *Int. J. Hydrogen Energy*, 2016, **41**, 3946–3954.

383 R. Jiang, X. Qu, F. Zeng, Q. Li, X. Zheng, Z. Xu and J. Peng, MOF-74-immobilized ternary Rh-Ni-P nanoparticles as highly efficient hydrous hydrazine dehydrogenation catalysts in alkaline solutions, *Int. J. Hydrogen Energy*, 2019, **44**, 6383–6391.

384 L. He, Y. Huang, X. Y. Liu, L. Li, A. Wang, X. Wang, C.-Y. Mou and T. Zhang, Structural and catalytic properties of supported Ni–Ir alloy catalysts for H_2 generation via hydrous hydrazine decomposition, *Appl. Catal., B*, 2014, **147**, 779–788.

385 Y. P. Qiu, H. Yin, H. Dai, L. Y. Gan, H. B. Dai and P. Wang, Tuning the surface composition of Ni/meso-CeO_2 with iridium as an efficient catalyst for hydrogen generation from hydrous hydrazine, *Chemistry*, 2018, **24**, 4902–4908.

386 D. Bhattacharjee, K. Mandal and S. Dasgupta, High performance nickel–palladium nanocatalyst for hydrogen generation from alkaline hydrous hydrazine at room temperature, *J. Power Sources*, 2015, **287**, 96–99.

387 Y. Chen, L. Wang, Y. Zhai, H. Chen, Y. Dou, J. Li, H. Zheng and R. Cao, Pd–Ni nanoparticles supported on reduced graphene oxides as catalysts for hydrogen generation from hydrazine, *RSC Adv.*, 2017, **7**, 32310–32315.

388 O. Song-Il, J. M. Yan, H. L. Wang, Z. L. Wang and Q. Jiang, High catalytic kinetic performance of amorphous CoPt NPs induced on CeO_x for H_2 generation from hydrous hydrazine, *Int. J. Hydrogen Energy*, 2014, **39**, 3755–3761.

389 K. Wang, Q. L. Yao, S. Qing and Z. H. Lu, $La(OH)_3$ nanosheet-supported CoPt nanoparticles: a highly efficient and magnetically recyclable catalyst for hydrogen production from hydrazine in aqueous solution, *J. Mater. Chem. A*, 2019, **7**, 9903–9911.

390 N. Firdous, N. K. Janjua, I. Qazi and M. H. S. Wattoo, Optimal Co–Ir bimetallic catalysts supported on γ-Al_2O_3 for hydrogen generation from hydrous hydrazine, *Int. J. Hydrogen Energy*, 2016, **41**, 984–995.

391 X. Du, P. Cai, W. Luo and G. Cheng, Facile synthesis of P-doped Rh nanoparticles with superior catalytic activity toward dehydrogenation of hydrous hydrazine, *Int. J. Hydrogen Energy*, 2017, **42**, 6137–6143.

392 S. K. Singh, A. K. Singh, K. Aranishi and Q. Xu, Noble-metal-free bimetallic nanoparticle-catalyzed selective hydrogen generation from hydrous hydrazine for chemical hydrogen storage, *J. Am. Chem. Soc.*, 2011, **133**, 19638–19641.

393 W. Gao, C. Li, H. Chen, M. Wu, S. He, M. Wei, D. G. Evans and X. Duan, Supported nickel–iron nanocomposites as a bifunctional catalyst towards hydrogen generation from $N_2H_4{\cdot}H_2O$, *Green Chem.*, 2014, **16**, 1560–1568.

394 J. Chen, H. Zou, Q. L. Yao, M. Luo, X. Li and Z. H. Lu, Cr_2O_3-modified NiFe nanoparticles as a noble-metal-free catalyst for complete dehydrogenation of hydrazine in aqueous solution, *Appl. Surf. Sci.*, 2020, **501**, 144247.

395 W. Kang, H. Guo and A. Varma, Noble-metal-free NiCu/CeO_2 catalysts for H_2 generation from hydrous hydrazine, *Appl. Catal., B*, 2019, **249**, 54–62.

396 H. Wang, Q. Fu, G. Zhang and Y. Sun, The synthesis of Ni–Cu alloy nanofibers via vacuum thermal Co-reduction toward hydrogen generation from hydrazine decomposition, *Catal. Lett.*, 2018, **149**, 77–83.

397 D. Wu, M. Wen, X. Lin, Q. Wu, C. Gu and H. Chen, A NiCo/NiO–CoO_x ultrathin layered catalyst with strong

basic sites for high-performance H_2 generation from hydrous hydrazine, *J. Mater. Chem. A*, 2016, **4**, 6595–6602.

398 K. V. Manukyan, A. Cross, S. Rouvimov, J. Miller, A. S. Mukasyan and E. E. Wolf, Low temperature decomposition of hydrous hydrazine over FeNi/Cu nanoparticles, *Appl. Catal., A*, 2014, **476**, 47–53.

399 J. Wang, Y. Li and Y. Zhang, Precious-metal-free nanocatalysts for highly efficient hydrogen production from hydrous hydrazine, *Adv. Funct. Mater.*, 2014, **24**, 7073–7077.

400 J. Zhang, Q. Kang, Z. Yang, H. Dai, D. Zhuang and P. Wang, A cost-effective NiMoB–$La(OH)_3$ catalyst for hydrogen generation from decomposition of alkaline hydrous hydrazine solution, *J. Mater. Chem. A*, 2013, **1**, 11623–11628.

401 H. L. Wang, J. M. Yan, S. J. Li, X. W. Zhang and Q. Jiang, Noble-metal-free NiFeMo nanocatalyst for hydrogen generation from the decomposition of hydrous hydrazine, *J. Mater. Chem. A*, 2015, **3**, 121–124.

402 Q. L. Yao, Z. H. Lu, R. Zhang, S. Zhang, X. Chen and H. L. Jiang, A noble-metal-free nanocatalyst for highly efficient and complete hydrogen evolution from $N_2H_4BH_3$, *J. Mater. Chem. A*, 2018, **6**, 4386–4393.

403 L. He, Y. Huang, A. Wang, X. Wang, X. Chen, J. J. Delgado and T. Zhang, A noble-metal-free catalyst derived from Ni-Al hydrotalcite for hydrogen generation from $N_2H_4{\cdot}H_2O$ decomposition, *Angew. Chem., Int. Ed.*, 2012, **51**, 6191–6194.

404 W. Kang and A. Varma, Hydrogen generation from hydrous hydrazine over Ni/CeO_2 catalysts prepared by solution combustion synthesis, *Appl. Catal., B*, 2018, **220**, 409–416.

405 M. Huang, Q. L. Yao, G. Feng, H. Zou and Z. H. Lu, Nickel-ceria nanowires embedded in microporous silica: controllable synthesis, formation mechanism, and catalytic applications, *Inorg. Chem.*, 2020, **59**, 5781–5790.

406 D. Wu, M. Wen, C. Gu and Q. Wu, 2D $NiFe/CeO_2$ basic-site-enhanced catalyst via *in situ* topotactic reduction for selectively catalyzing the H_2 generation from $N_2H_4{\cdot}H_2O$, *ACS Appl. Mater. Interfaces*, 2017, **9**, 16103–16108.

407 H. Zou, Q. L. Yao, M. Huang, M. Zhu, F. Zhang and Z. H. Lu, Noble-metal-free NiFe nanoparticles immobilized on nano $CeZrO_2$ solid solutions for highly efficient hydrogen production from hydrous hydrazine, *Sustainable Energy Fuels*, 2019, **3**, 3071–3077.

408 H. Zou, F. Guo, M. Luo, Q. L. Yao and Z. H. Lu, $La(OH)_3$-decorated NiFe nanoparticles as efficient catalyst for hydrogen evolution from hydrous hydrazine and hydrazine borane, *Int. J. Hydrogen Energy*, 2020, **45**, 11641–11650.

409 Y. Men, X. Du, G. Cheng and W. Luo, CeO_x-modified NiFe nanodendrits grown on rGO for efficient catalytic hydrogen generation from alkaline solution of hydrazine, *Int. J. Hydrogen Energy*, 2017, **42**, 27165–27173.

410 P. Yang, L. Yang, Q. Gao, Q. Luo, X. Zhao, X. Mai, Q. Fu, M. Dong, J. Wang, Y. Hao, R. Yang, X. Lai, S. Wu, Q. Shao, T. Ding, J. Lin and Z. Guo, Anchoring carbon nanotubes and post-hydroxylation treatment enhanced Ni nanofiber catalysts towards efficient hydrous hydrazine decomposition for effective hydrogen generation, *Chem. Commun.*, 2019, **55**, 9011–9014.

411 H. Wang, L. Wu, A. Jia, X. Li, Z. Shi, M. Duan and Y. Wang, Ni nanoparticles encapsulated in the channel of titanate nanotubes: Efficient noble-metal-free catalysts for selective hydrogen generation from hydrous hydrazine, *Chem. Eng. J.*, 2018, **332**, 637–646.

412 Y. P. Qiu, G. X. Cao, H. Wen, Q. Shi, H. Dai and P. Wang, High-capacity hydrogen generation from hydrazine monohydrate using a noble-metal-free $Ni_{10}Mo$/Ni–Mo–O nanocatalyst, *Int. J. Hydrogen Energy*, 2019, **44**, 15110–15117.

413 Q. Shi, D. X. Zhang, H. Yin, Y. P. Qiu, L. L. Zhou, C. Chen, H. Wu and P. Wang, Noble-metal-free Ni–W–O-derived catalysts for high-capacity hydrogen production from hydrazine monohydrate, *ACS Sustainable Chem. Eng.*, 2020, **8**, 5595–5603.

414 R. Moury and U. Demirci, Hydrazine borane and Hydrazinidoboranes as chemical hydrogen storage materials, *Energies*, 2015, **8**, 3118–3141.

415 Y. Zhu and N. S. Hosmane, Nanocatalysis: Recent advances and applications in boron chemistry, *Coord. Chem. Rev.*, 2015, **293–294**, 357–367.

416 S. Zhang, Q. L. Yao and Z. H. Lu, Synthesis and dehydrogenation of hydrazine borane, *Prog. Chem.*, 2017, **29**, 426–434.

417 J. Chen, Z. H. Lu, W. Huang, Z. Kang and X. Chen, Galvanic replacement synthesis of NiPt/graphene as highly efficient catalysts for hydrogen release from hydrazine and hydrazine borane, *J. Alloys Compd.*, 2017, **695**, 3036–3043.

418 Z. Zhang, S. Zhang, Q. L. Yao, X. Chen and Z. H. Lu, Controlled synthesis of MOF-encapsulated NiPt nanoparticles toward efficient and complete hydrogen evolution from hydrazine borane and hydrazine, *Inorg. Chem.*, 2017, **56**, 11938–11945.

419 K. Yang, K. Yang, S. Zhang, Y. Luo, Q. L. Yao and Z. H. Lu, Complete dehydrogenation of hydrazine borane and hydrazine catalyzed by MIL-101 supported NiFePd nanoparticles, *J. Alloys Compd.*, 2018, **732**, 363–371.

420 Z. Zhang, S. Zhang, Q. L. Yao, G. Feng, M. Zhu and Z. H. Lu, Metal–organic framework immobilized RhNi alloy nanoparticles for complete H_2 evolution from hydrazine borane and hydrous hydrazine, *Inorg. Chem. Front.*, 2018, **5**, 370–377.

421 J. Goubeau and E. Ricker, Borinhydrazin und seine Pyrolyseprodukte, *Z. Anorg. Allg. Chem.*, 1961, **310**, 123–142.

422 T. Hugle, M. F. Kuhnel and D. Lentz, Hydrazine borane: a promising hydrogen storage material, *J. Am. Chem. Soc.*, 2009, **131**, 7444–7446.

423 Y. S. Chua, Q. Pei, X. Ju, W. Zhou, T. J. Udovic, G. Wu, Z. Xiong, P. Chen and H. Wu, Alkali metal hydride modifi-

cation on hydrazine borane for improved dehydrogenation, *J. Phys. Chem. C*, 2014, **118**, 11244–11251.

424 R. Moury, K. Robeyns, Y. Filinchuk, P. Miele and U. B. Demirci, In situ thermodiffraction to monitor synthesis and thermolysis of hydrazine borane-based materials, *J. Alloys Compd.*, 2016, **659**, 210–216.

425 S. Karahan, M. Zahmakiran and S. Özkar, Catalytic methanolysis of hydrazine borane: a new and efficient hydrogen generation system under mild conditions, *Dalton Trans.*, 2012, **41**, 4912–4918.

426 Y. Karatas, M. Gülcan and F. Sen, Catalytic methanolysis and hydrolysis of hydrazine-borane with monodisperse Ru NPs@nano-CeO_2 catalyst for hydrogen generation at room temperature, *Int. J. Hydrogen Energy*, 2019, **44**, 13432–13442.

427 D. Çelik, S. Karahan, M. Zahmakıran and S. Özkar, Hydrogen generation from the hydrolysis of hydrazine-borane catalyzed by rhodium(0) nanoparticles supported on hydroxyapatite, *Int. J. Hydrogen Energy*, 2012, **37**, 5143–5151.

428 Q. L. Yao, Z. H. Lu, K. Yang, X. Chen and M. Zhu, Ruthenium nanoparticles confined in SBA-15 as highly efficient catalyst for hydrolytic dehydrogenation of ammonia borane and hydrazine borane, *Sci. Rep.*, 2015, **5**, 15186.

429 S. Karahan, M. Zahmakıran and S. Özkar, Catalytic hydrolysis of hydrazine borane for chemical hydrogen storage: Highly efficient and fast hydrogen generation system at room temperature, *Int. J. Hydrogen Energy*, 2011, **36**, 4958–4966.

430 S. Şencanlı, S. Karahan and S. Özkar, Poly(4-styrenesulfonic acid-co-maleic acid) stabilized nickel(0) nanoparticles: Highly active and cost effective catalyst in hydrogen generation from the hydrolysis of hydrazine borane, *Int. J. Hydrogen Energy*, 2013, **38**, 14693–14703.

431 S. Karahan and S. Özkar, Poly(4-styrenesulfonic acid-co-maleic acid) stabilized cobalt(0) nanoparticles: A cost-effective and magnetically recoverable catalyst in hydrogen generation from the hydrolysis of hydrazine borane, *Int. J. Hydrogen Energy*, 2015, **40**, 2255–2265.

432 N. Tunç, B. Abay and M. Rakap, Hydrogen generation from hydrolytic dehydrogenation of hydrazine borane by poly(N-vinyl-2-pyrrolidone)-stabilized palladium nanoparticles, *J. Power Sources*, 2015, **299**, 403–407.

433 J. Hannauer, O. Akdim, U. B. Demirci, C. Geantet, J. M. Herrmann, P. Miele and Q. Xu, High-extent dehydrogenation of hydrazine borane $N_2H_4BH_3$ by hydrolysis of BH_3 and decomposition of N_2H_4, *Energy Environ. Sci.*, 2011, **4**, 3355–3358.

434 Ç. Çakanyıldırım, U. B. Demirci, T. Şener, Q. Xu and P. Miele, Nickel-based bimetallic nanocatalysts in high-extent dehydrogenation of hydrazine borane, *Int. J. Hydrogen Energy*, 2012, **37**, 9722–9729.

435 J. Hannauer, U. B. Demirci, C. Geantet, J. M. Herrmann and P. Miele, Transition metal-catalyzed dehydrogenation of hydrazine borane $N_2H_4BH_3$ via the hydrolysis of BH_3 and the decomposition of N_2H_4, *Int. J. Hydrogen Energy*, 2012, **37**, 10758–10767.

436 D. C. Zhong, K. Aranishi, A. K. Singh, U. B. Demirci and Q. Xu, The synergistic effect of Rh-Ni catalysts on the highly-efficient dehydrogenation of aqueous hydrazine borane for chemical hydrogen storage, *Chem. Commun.*, 2012, **48**, 11945–11947.

437 C. Li, Y. Dou, J. Liu, Y. Chen, S. He, M. Wei, D. G. Evans and X. Duan, Synthesis of supported Ni@(RhNi-alloy) nanocomposites as an efficient catalyst towards hydrogen generation from $N_2H_4BH_3$, *Chem. Commun.*, 2013, **49**, 9992–9994.

438 Q. L. Zhu, D. C. Zhong, U. B. Demirci and Q. Xu, Controlled synthesis of ultrafine surfactant-free NiPt nanocatalysts toward efficient and complete hydrogen generation from hydrazine borane at room temperature, *ACS Catal.*, 2014, **4**, 4261–4268.

439 Z. Zhang, Z. H. Lu and X. Chen, Ultrafine Ni–Pt alloy nanoparticles grown on graphene as highly efficient catalyst for complete hydrogen generation from hydrazine borane, *ACS Sustainable Chem. Eng.*, 2015, **3**, 1255–1261.

440 Z. Zhang, Z. H. Lu, H. Tan, X. Chen and Q. L. Yao, CeO_x-modified RhNi nanoparticles grown on rGO as highly efficient catalysts for complete hydrogen generation from hydrazine borane and hydrazine, *J. Mater. Chem. A*, 2015, **3**, 23520–23529.

441 Z. Zhang, Y. Wang, X. Chen and Z. H. Lu, Facile synthesis of NiPt–CeO_2 nanocomposite as an efficient catalyst for hydrogen generation from hydrazine borane, *J. Power Sources*, 2015, **291**, 14–19.

442 X. Hong, Q. L. Yao, M. Huang, H. Du and Z. H. Lu, Bimetallic NiIr nanoparticles supported on lanthanum oxy-carbonate as highly efficient catalysts for hydrogen evolution from hydrazine borane and hydrazine, *Inorg. Chem. Front.*, 2019, **6**, 2271–2278.

443 W. Ben Aziza, J. F. Petit, U. B. Demirci, Q. Xu and P. Miele, Bimetallic nickel-based nanocatalysts for hydrogen generation from aqueous hydrazine borane: Investigation of iron, cobalt and palladium as the second metal, *Int. J. Hydrogen Energy*, 2014, **39**, 16919–16926.

444 S. J. Li, X. Kang, B. R. Wulan, X. L. Qu, K. Zheng, X. D. Han and J. M. Yan, Noble–metal–free Ni–MoO_x nanoparticles supported on BN as a highly efficient catalyst toward complete decomposition of Hydrazine Borane, *Small Methods*, 2018, **2**, 1800250.

445 S. J. Li, H. L. Wang, B. R. Wulan, X. B. Zhang, J. M. Yan and Q. Jiang, Complete dehydrogenation of $N_2H_4BH_3$ over noble-metal-free $Ni_{0.5}Fe_{0.5}$-CeO_x/MIL-101 with high activity and 100% H_2 selectivity, *Adv. Energy Mater.*, 2018, **8**, 1800625.

446 S. Zhang, Q. L. Yao, Q. Li, G. Feng and Z. H. Lu, Complete hydrogen production from hydrazine Bborane over raney Ni catalyst at room temperature, *Energy Technol.*, 2019, **7**, 1800533.

